

TALLINN UNIVERSITY OF TECHNOLOGY
DOCTORAL THESIS
55/2020

**Performance of Ceramic-Metal
Composites as Tool Materials for Friction
Stir Welding**

MART KOLNES



TALLINN UNIVERSITY OF TECHNOLOGY

School of Engineering

Department of Mechanical and Industrial Engineering

This dissertation was accepted for the defence of the degree 22/11/2020

Supervisor:

Prof. Jakob Kübarsepp
School of Engineering
Tallinn University of Technology
Tallinn, Estonia

Co-supervisor:

Prof. Fjodor Sergejev
School of Engineering
Tallinn University of Technology
Tallinn, Estonia

Opponents:

Associate Professor Pedro Vilaça
School of Engineering
Aalto University
Aalto, Finland

PhD Madis Umalas
Hanza Mechanics Tartu AS
Tartu, Estonia

Defence of the thesis: 21/12/2020, Tallinn

Declaration:

Hereby I declare that this doctoral thesis, my original investigation and achievement, submitted for the doctoral degree at Tallinn University of Technology has not been submitted for doctoral or equivalent academic degree.

Mart Kolnes

signature



European Union
European Regional
Development Fund



Investing
in your future

Copyright: Mart Kolnes, 2020

ISSN 2585-6898 (publication)

ISBN 978-9949-83-643-7 (publication)

ISSN 2585-6901 (PDF)

ISBN 978-9949-83-644-4 (PDF)

Printed by Koopia Niini & Rauam

TALLINNA TEHNIKAÜLIKOOL
DOKTORITÖÖ
55/2020

Keraamilis-metalsed komposiidid otshõõrdkeevituse tööriista materjalidena

MART KOLNES



Contents

List of Publications	7
Author's Contribution to the Publications	8
Introduction	9
Abbreviations	10
Symbols	11
1 Review of literature.....	12
1.1 Friction stir welding: process and applications	12
1.1.1 FSW process	12
1.1.2 Tool geometry and welding regimes.....	13
1.1.3 FSW applications.....	14
1.2 The wear of the FSW tools and their materials.....	14
1.2.1 Requirements for FSW tool materials.....	14
1.2.2 FSW of Al and Al alloys	16
1.2.3 FSW of Cu	17
1.2.4 FSW of stainless steel.....	18
1.3 Aim of the study and objectives.....	20
2 Materials and experimental methods.....	22
2.1 Materials	22
2.1.1 Tool materials	22
2.1.2 Workpiece materials	24
2.2 Experimental details.....	25
2.2.1 Model wear tests	25
2.2.2 Diffusion testing.....	27
2.2.3 FSW feasibility studies	28
2.2.4 Material characterization methods.....	29
3 Performance of cermets and hardmetals as tool materials for FSW of low- and high- melting point metals	30
3.1 FSW of aluminium alloy	31
3.1.1 Model wear tests	31
3.1.2 Diffusion tests	33
3.1.3 Friction stir welding trials.....	36
3.1.4 Summary	36
3.2 FSW of copper	37
3.2.1 Model wear tests	37
3.2.2 Diffusion tests	38
3.2.3 Friction stir welding trials.....	41
3.2.4 Summary	41
3.3 FSW of stainless steel.....	42
3.3.1 Model wear tests	42
3.3.2 Diffusion tests	43
3.3.3 Friction stir welding trials.....	46
3.3.4 Summary	47
4 Conclusions	48

References	50
Abstract.....	57
Lühikokkuvõte.....	59
Appendix	61
Curriculum vitae.....	124
Elulookirjeldus.....	125

List of Publications

The list of author's publications, on the basis of which the thesis has been prepared:

- I **Kolnes, M.**, Kübarsepp, J., Sergejev, F., Kolnes, M. Comparative study of adhesive wear for CoCr, TiC-NiMo, WC-Co as potential FSW tool materials. In: R. Bendikienė, K. Juzėnas (Ed.). *Materials Engineering 2017* (224–228).10.10.2017 Trans Tech Publications Ltd. (Solid State Phenomena; 267), 2017.
- II **Kolnes, M.**, Kübarsepp, J., Sergejev, F., Kolnes, M. Adhesive wear of WC- and TiC-based friction stir welding tool materials for aluminium alloy welding. *Euro PM2018 proceedings*, 2018, 1-8.
- III **Kolnes, M.**, Kübarsepp, J., Sergejev, F., Kolnes, M. Wear of potential tool materials for aluminium alloys friction stir welding at weld temperatures. *Proceedings of the Estonian Academy of Sciences*, 2019, 68 (2), 198-206
- IV **Kolnes, M.**, Kübarsepp, J., Sergejev, F., Kolnes, M., Tarraste, M., Mikli, V. Wear behaviour of ceramic metal composites as tool materials for FSW of stainless steel. In: J. Padgurskas (Ed.). *Proceedings of BALTRIB'2019* (107–112). Vytautas Magnus University, 2019.
- V **Kolnes, M.**, Kübarsepp, J., Sergejev, F., Kolnes, M., Tarraste, M., Viljus, M. Performance of ceramic-metal composites as potential tool materials for friction stir welding of aluminium, copper and stainless steel. *Materials*, 2020, 13 (8): 1994, 1-18.
- VI **Kolnes, M.**, Kübarsepp, J., Sergejev, F., Kolnes, M., Tarraste, M., Viljus, M. Wear behaviour of ceramic-metal composites as tool material for FSW of copper. In: *Materials Engineering 2020* Trans Tech Publications Ltd. (Solid State Phenomena). (accepted for publication: September, 2020).

Author's Contribution to the Publications

Author's work/contribution to the publications in this thesis is:

- I First and corresponding author. Production of the specimens. Preparation and conduction of experiments, analysis of the results. Manuscript preparation.
- II First and corresponding author. Production of the specimens. Preparation and conduction of experiments, analysis of the results. Manuscript preparation.
- III First and corresponding author. Production of the specimens. Development of the test methodology. Preparation and conduction of experiments. Interpreting results. Manuscript preparation.
- IV First and corresponding author. Production of the specimens. Development of the test methodology. Preparation and conduction of experiments. Interpreting results. Manuscript preparation.
- V First and corresponding author. Production of the specimens. Development of the test methodology. Preparation and conduction of experiments. Interpreting results. Manuscript preparation.
- VI First and corresponding author. Production of the specimens. Development of the test methodology. Preparation and conduction of experiments. Results interpretation. Manuscript preparation.

Introduction

The demand for better use of resources, energy efficiency as well as environmental friendliness are the major demands for industrial success in the 21st century. These demands can be satisfied among other things through advanced materials, in particular wear resistant materials. The losses resulting from corrosion and wear in life cycle costs of equipment may be tremendous in some industries (metallurgy, mining, etc.). Therefore, the challenge is to develop advanced cost-effective and reliable (durable) wear resistant materials and industrial applications.

Technological and commercial importance of welding derives from providing a permanent joint. Welding is usually the most economical way for joining components in terms of fabrication costs and material usage. Oxyfuel gas welding and arc welding were among the first processes developed at the end of the 19th century. Joining technology advanced fast during the 20th century. Among several advancements, invention of friction stir welding (FSW) in 1991 (Thomas, 1991) is important. This solid-state welding technique, in comparison with other welding methods, consumes considerably less energy, has low environmental impact and ensures high quality of joints welding difficult-to-weld metals (e.g., stainless steel, aluminium, copper etc.) in the conditions of proper welding regimes. FSW application is widening in the transport industries (in particular shipbuilding), automotive, aerospace and other industries.

Tool materials and their properties are critical for a high quality of FSW joints and process efficiency. Tool material to be used depends on the workpiece metal, tool geometry and processing parameters. However, studies on the tool degradation (wear) and degradation mechanism during the FSW of different metals are scarce. According to author's, no fundamental studies have been performed to investigate the performance and wear mechanism of ceramic-metal composites (WC- and TiC-based) as potential tool materials for FSW of metals with substantially different welding temperatures. Therefore, the motivation of the present study was to develop, select and use reliable, durable and cost-effective tool materials for the FSW of low melting point (aluminium) as well as high melting point (copper, stainless steel) metals.

The objectives of the research were development of the model testing methodology for assessment of tool degradation for ceramic-metal composites as potential tool materials for FSW of low- and high melting point metals. Improvement of understanding of the wear mechanism and proving welding feasibility studies using FSW tool prototypes.

The model wear test specimens and FSW tool prototypes were produced using the conventional PM technology of hardmetals and cermets. A comparative study for investigation of ceramic-metal composites as tool materials for the FSW of various metals (aluminium alloy, copper, stainless steel) as well as a study of wear mechanism of ceramic-metal tools during the developed model wear tests and FSW tests were performed. The feasibility studies, using prototypes of FSW tools from ceramic-metal composites, were conducted.

The main novel outcomes of the research were: (1) development and application of the model wear testing method for assessment of tools wear during working at regular FSW temperatures; (2) comparative study of performance of TiC-based cermets and WC-based hardmetals during the working of metals with different melting and working temperatures; (3) revealing the effect of composition and characteristics of workpiece materials and ceramic metal composites (cermets, hardmetals) on the tools degradation mechanism; (4) production of FSW tools prototypes and FSW feasibility studies.

Abbreviations

AISI	American Iron and Steel Institute
AMC	Aluminium matrix composite
APS	Atmospheric plasma spray
CBN	Cubic boron nitride
EDS	Energy dispersive X-ray spectroscopy
FSP	Friction stir processing
FSW	Friction stir welding
GMAW	Gas metal arc welding
GTAW	Gas tungsten arc welding
HAZ	Heat affected zone
HSS	High speed steel
LPS	Liquid phase sintering
MIG welding	Metal inert gas welding
PCBN	Polycrystalline cubic boron nitride
PM	Powder metallurgy
PTA	Plasma transferred arc
PVD	Physical vapour deposition
rpm	Rotations per minute
SEM	Scanning electron microscopy
SPS	Spark plasma sintering
SS	Stainless steel
TiC	Titanium carbide
TiCN; Ti(C,N)	Titanium carbonitride
TIG welding	Tungsten inert gas welding
Vol.%	Volume percentage
WC	Tungsten carbide
Wt.%	Weight percentage
XRD	X-ray diffraction

Symbols

μ	Friction coefficient
D_{50}	Median diameter of powder particle size, μm
HV30	Vickers hardness, load 298 N
K_{1C}	Fracture toughness, $\text{MPa}\cdot\text{m}^{1/2}$
p	Normal force, kN
q	Heat input, $\text{kJ}\cdot\text{mm}^{-2}$
R_s	FSW tool shoulder radius, m
s	Traverse speed, $\text{mm}\cdot\text{s}^{-2}$
T	Temperature, $^{\circ}\text{C}$
η	Efficiency coefficient

1 Review of literature

Until the end of the 19th century (Lohwasser, 2010), the only welding process was forge welding, which blacksmiths had used for thousands of years to join iron and steel by heating and forging. Arc welding and oxyfuel gas welding were among the first processes developed late in the 19th century (Lohwasser, 2010), and electric resistance welding followed soon after. Welding technology advanced quickly during the early 20th century as world wars drove the demand for reliable and inexpensive joining methods. The invention of many welding processes during the last century culminated with the invention of friction stir welding (FSW) in 1991 (Thomas, 1991). Similar to the first welding process, forge welding FSW does not involve melting of the materials being joined.

1.1 Friction stir welding: process and applications

1.1.1 FSW process

Friction stir welding (FSW) was invented at the Welding Institute (TWI) of the United Kingdom in 1991 as a solid-state joining technique, initially applied to aluminium alloys (Thomas, 1991). FSW is a solid-state joining process that uses a specially designed non-consumable rotating tool to join materials without melting them (Murr, 1998). Heating is created within the workpiece by friction between the welded material and the rotating tool (Schneider, 2007). The localized heating softens the material around the tool and while the tool is traversed along the joint line, it mechanically intermixes the two welded materials (see Figure 1). To avoid defects and welding tool fracture, the process temperature should be approximately 0.7 times of the melting temperature of the workpiece material (Tang, 1998; Publication V).

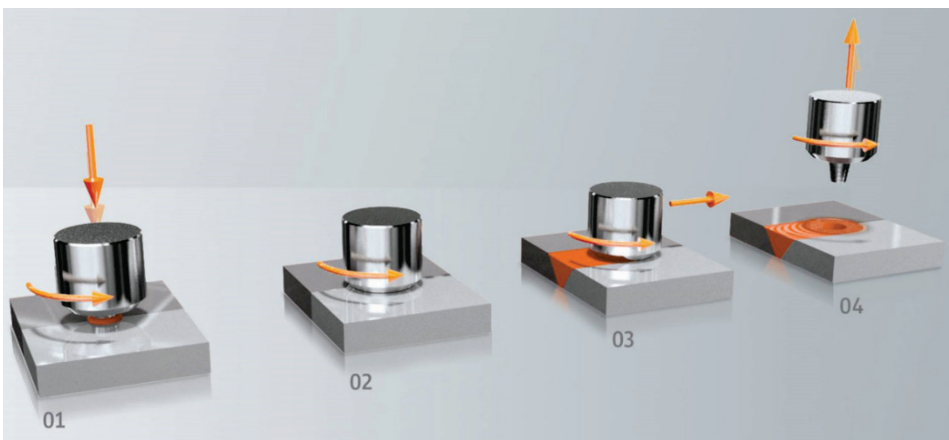


Figure 1. FSW process steps: (1) approach and plunge; (2) dwell for heating; (3) welding; (4) end of welding (Publication V).

Marked superiorities over traditional fusion welding methods arise from the solid-state nature of FSW. Firstly, the fully recrystallized, fine-grained microstructure created in the weld by the deformation at welding temperatures. In addition, there appears no conduction problems connected with cooling to the solid phase, such as porosity, liquation cracking, solidification cracking and alloying element loss (Kah, 2015). Additionally, FSW is an arising “green technology” because of its energy efficiency and

environmental friendliness (Kumar, 2014). In comparison with other welding methods, FSW consumes considerably less energy, no fumes, no arc-related emissions and no protective gas are present - FSW has low environmental impact. Also, no filler materials are needed, which gives a further advantage that formation of unwanted phases in the weld microstructure due to the mixing of the parent metal and filler material can be avoided.

1.1.2 Tool geometry and welding regimes

The welding tool design, including both its geometry and the material from which it is made, is critical to the successful use of the process. In FSW, the parameters that influence the quality of the welded joint can be categorized into primary and secondary parameters. The primary parameters are traverse speed, rotational speed, and tool geometry. Meanwhile, the secondary parameters are thickness of the workpiece, workpiece material, welding tool material, and pin profile (Emamian, 2017). Figure 2 shows the schematic of the most commonly used pin profiles.

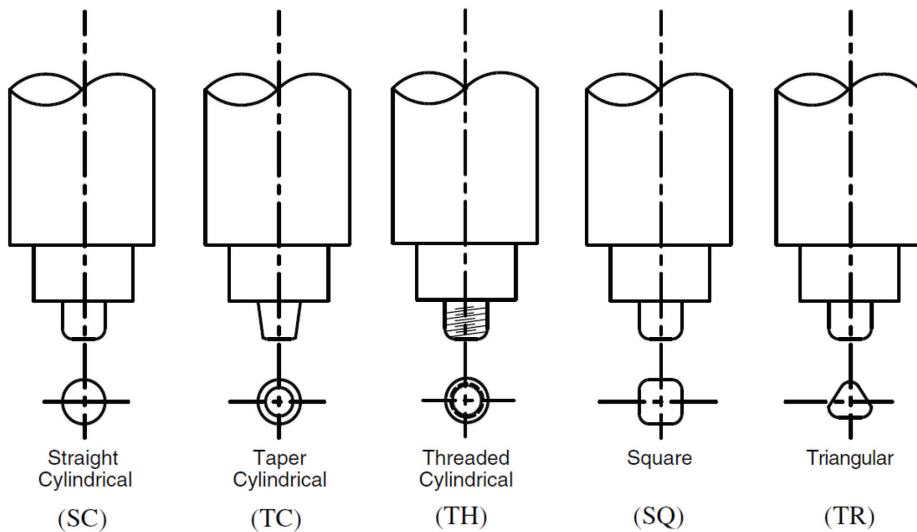


Figure 2. FSW tool pin profiles (Elangovan, 2008).

Tool rotational speed, welding speed (traverse speed) and tilt angle of the tool are important influencing process parameters on the tensile strength and the hardness of the weld. The traversing force and the side force are not considered as process parameters and are only used for monitoring the process. Friction stir welding parameters have been selected based on acceptable mechanical, microstructural, fatigue and corrosion properties requirement to obtain efficient, defect free friction stir welded joints (Boopathi, 2017). In FSW heat is caused by rubbing of the tool faces against the workpiece, and by viscoelastic dissipation of mechanical energy at high strain rates developed through interactions with the tool (Mall, 2017). During welding, the material along the joint is heated to a softened condition transferred around the periphery of the tool and subsequently recoalesced along the back surface of the pin to produce weld. In case of FSW process the heat input (q , KJ/mm) is given by the equation as follows (Kumar, 2014):

$$q = \frac{2\pi}{3s} \times \mu \times p \times \omega \times R_s \times \eta,$$

where s is traverse speed (mm/s); μ is the coefficient of friction; p is the normal force (kN); ω is the rotational speed (rev/s); R_s is the shoulder radius (m); η is the efficiency coefficient.

Depending on the material of the tool, only one parameter affects the heat input – the coefficient of friction. Consequently, in case of the tool material selection coefficient of friction between the tool and the workpiece material have to be taken into account (Yi, 2016). Table 1 presents the widely used welding parameters used for FSW of low- and high melting point metals.

Table 1. Welding parameters used for FSW of low- and high melting point materials (Rai, 2011).

Welding parameters	Low melting point materials	High melting point materials
ω , (rev/s)	600...2000	100...1250
s , (mm/min)	10...2000	25...200

1.1.3 FSW applications

Forces and torque during FSW require that the structures/parts to be welded, are quite rigidly clamped and tool rigidly positioned. The precision of positioning also needs to be high. Thus, from an engineering point of view, it is reasonable to suggest that the application of FSW is more suited to fabrication environments (Lohwasser, 2010). As it has turned out, during the last 15 years, FSW has actually enabled many manufacturing processes to become significantly more efficient or enabled new and efficient manufacturing routes to be developed. Mostly long and straight FSW welds are used in the transport industries, including shipbuilding, offshore, rail, automotive, and aerospace. In addition to the previous applications, three-dimensional and non-linear FSW welds are performed in other industry sectors (Lohwasser, 2010).

1.2 The wear of the FSW tools and their materials

Tools have to withstand severe wear conditions during the FSW process. The degradation (wear) mechanism is complicated and depends on the interaction between the workpiece and the tool material, welding parameters and tool geometry (Fuller, 2007). However, studies on the tool wear mechanism in FSW are scarce; at the same time, adhesion, abrasion and diffusion-controlled wear are the expected wear mechanisms (Publication V). Wear through abrasion is especially important in the presence of a hard phase in the welded material such as in aluminium matrix composites (Liu, 2005).

According to the author's knowledge, no comparative studies have been conducted addressing the performance and degradation mechanism of ceramic-metal composites as potential tool materials for the FSW of different metals with substantially different welding temperatures (Publication V).

1.2.1 Requirements for FSW tool materials

In spite of the fact that FSW was invented for aluminium alloys, nowadays FSW is used to weld a various metals – copper-, magnesium-, titanium alloys, stainless steels, and polymers (Strand, 2003). In this work, focus was on the FSW of aluminium alloy, copper and stainless steel because of their quite poor weldability as compared to the liquid

phase welding of low-carbon steels (ASM Handbook, 1993; Olsan, 1993), and high interest from the industrial application site, especially in Republic of Estonia.

Tool material properties are critical for high quality FSW joints. The tool material to be used depends on the workpiece material and the desired tool life. Primary characteristics that have to be considered in selecting the tool material for FSW/FSP of any metal are (Zhang, 2012; Meilinger, 2013; Cui, 2018):

- resistance to (abrasive, adhesive and diffusion) wear,
- good strength, dimensional stability,
- good thermal fatigue strength to resist repeated heating and cooling,
- good fracture toughness to resist the deformation during plunging and dwelling,
- high compressive yield strength at elevated temperatures,
- no harmful reactions with the workpiece material,
- low coefficient of thermal expansion to reduce the thermal stresses,
- good machinability to ease manufacture of complex features of the shoulder and probe of a tool,
- low or affordable cost.

In addition to tool material, tool degradation and tool life in FSW depend on a number of parameters, such as tool geometry and processing parameters, rotational speed, traverse speed and travel distance.

As a solid-phase welding, FSW prevents the welding defects connected with fusion welding processes (Liu, 2005). Every metal to be welded needs special attention for selecting the relevant tool material as well as welding regimes. Tool wear and weld quality are two essential aspects in the selection of FSW instrument material. Rai et al. presented an excellent understanding of the tool materials used for aluminium alloys and Cui et al. for steels FSW (Rai, 2011; Cui, 2018). Chromium-molybdenum hot work air hardening tool steel X40CrMoV (AISI H13) and polycrystalline cubic boron nitride (PCBN) are the most widely used tool materials for aluminium alloys and stainless steels, respectively (Publication V). Arulmoni et al. introduced a complete review of the tool materials used for FSW of copper (Arulmoni, 2015). Tool steel AISI H13 is the most widely used for the FSW of copper. Table 2 and 3 present the tool materials widely used to weld low- and high melting point metals, respectively.

Table 2. Common tool materials used for FSW of low melting point metals (Rai, 2011, Johnson, 2003).

Low melting point materials	Aluminium alloys	Magnesium alloys	Aluminium matrix composites
Tool materials	Tool steel (AISI H13), high carbon steel, high speed steel (HSS)	Tool steel (AISI H13), tungsten carbide, HSS	PCBN, tungsten alloy, tungsten carbide, Ir alloys

Table 3. Common tool materials used for FSW of high melting point metals (Rai, 2011; Jeganathan Arulmoni, 2015; Cui, 2018).

High melting point materials	Titanium alloys	Copper alloys	Ferrous alloys
Tool materials	PCBN, high speed steel (HSS), tungsten alloy, tungsten carbide	Tool steel (AISI H13), tungsten carbide, high speed steel (HSS)	PCBN, tungsten alloy, tungsten carbide, Ir alloys

1.2.2 FSW of Al and Al alloys

The FSW process is carried out at much lower temperatures than conventional fusion welding. As a result, it offers significant benefits over conventional joining processes of Al and Al-alloys, such as gas tungsten arc welding (GTAW) or TIG-welding (tungsten inert gas welding) and gas metal arc welding (GMAW) or MIG-welding (metal inert gas welding). It has been demonstrated by several researchers that FSW joints have comparatively excellent structure and mechanical properties when compared to GTAW (TIG-welding) and GMAW (MIG-welding) joints (Jannet, 2013; Kaur, 2016, Kumar, 2014). Joining aluminium with the FSW process is widely used in numerous applications and by many companies worldwide. Due to their low softening temperature and stresses, aluminium alloys are conveniently welded by using tools made of various types of tool steels, which is reviewed by Rai et al. (Rai, 2011). However, studies on the wear mechanisms of tool materials in the FSW of aluminium are scarce. Adhesion, diffusion and abrasion (expectedly during the tool plunge phase) are the wear mechanisms expected (Rai, 2011, Tarasov, 2014). Prevailing wear mechanism depends on both the material to be welded and the tool material.

AISI H13 tool steel

Most widely used FSW tool material for aluminium welding is chromium–molybdenum hot worked air hardening tool steel AISI H13 (X40CrMoV5-1) (Rai, 2011) and high-speed steels. Despite the fact that H13 is the most common tool material, studies of its wear and reaction with the welded material are rare. This may be due to the fact that the tool made from tool steel lasts for quite a long time. However, it should be underlined that the wear of the FSW tools reduces the stirring efficiency and increases the probability of generating defects in the weld also during the FSW of aluminium and aluminium alloys.

Tarasov et al. studied the FSW tool wear from a standpoint of tribological layer generation and interaction of this layer with the tool's metal (Tarasov, 2014). The FSW tool is commonly coated by a layer of weldable material, in particular an aluminium alloy. The generation of the tribological layer on the tool's surface creates conditions for diffusion of elements into the tool's metal and thus may cause its intensive wear (Publication V). These layers are very inhomogeneous by composition and consist of a mixture of aluminium alloy particles, silicides and oxides. In the vicinity of the tool's surface, there is a layer of FeAl₃ intermetallic compound of both continuous and spiked morphologies. The generation of the tribological layer on the tool surface creates conditions for the diffusion of elements into the tool metal. A rationale behind the tool wear in the FSW of aluminium alloys could be strong adhesion of the aluminium alloy to a steel tool and the following reaction diffusion of the tool material into aluminium due to high temperatures during welding (Tarasov, 2014).

Coated tools

Instead of using expensive wear-resistant materials for tools, tool life can be also extended by using anti-wear tribological coatings on tool steels. Wieckowski and others studied the surface thickness and morphology and resistance to the wear of commercial anti-wear coatings such as TiAlN, TiN, TiCN and AlCrN deposited on hot work steel AISI H13 as a base material during the FSW of aluminium alloy 7075-T6 to improve tool life (Wieckowski, 2019). The aim of their study was to choose a coating for further wear tests of FSW tools with deposited protective coating using several well-known tribological

tests. Based on their laboratory study, they suggested that the AlCrN coating was the best use in further industrial tests to weld 7075-T6 aluminium alloy.

The durability of the coating in the case of aluminium alloy welding has also been further studied in the FSW tests carried out by Adesina et al. They presented the results of the examinations of the wear of 4140 grade alloy steel tool with AlCrN coating in the process of FSW welding of 6 mm thick aluminium alloy 6061-T6. The researchers demonstrated the usefulness of the coating, which both limited tool wear and helped obtain the joint without many substantial defects (Adesina et al., 2017).

FSW of aluminium matrix composites

FSW is the most preferred joining method used in aluminium matrix composites (AMC-s). FSW is done below the melting point of the workpiece material, preventing the formation of the theta phase, which produces stronger joints as compared to any of the fusion welding processes (Bist, 2016). While relatively few studies have addressed tool wear in aluminium FSW, significantly more studies of tool wear mechanisms have been conducted for the FSW of AMCs. Tool wear is a key issue for the FSW of AMCs, especially when the volume fraction of reinforcing particulates is relatively high (Liu, 2005). Various tool materials have been used for the FSW of AMC, such as tool steels, high-speed steels (Bozkurt, 2018) and WC-Co hardmetals (Liu, 2005). Also, significant improvement in the wear resistance of the FSW tool has been reported when the tool was physical vapor deposition (PVD) coated in comparison to an uncoated AISI H13 tool. Dominant wear mechanisms on the AlCrN and TiAlN coated tools were abrasive erosion and chipping off from the coating surface by sharp hard SiC particles while severe striation and oxidation was found to characterize the wear mechanism of the uncoated tool (Adesina, 2018). Domination of abrasive wear in the case of AMC FSW is also confirmed by Prado et al. (Padro, 2001). There was essentially zero tool wear performing weld of a commercial 6061 aluminium alloy without hard solid particles. In the case of AMC welding, it has become clear that tool wear is not just a bad indicator because using the worn tool geometry, it is possible to predict the optimal shape of the tool. They suggested that shape-related solid-state flow control is an essential feature of FSW and especially in assuring limited tool wear and an optimum long tool life (Padro, 2003). Additionally, self-optimized tools have another beneficial phenomenon – the welds are more homogeneous and there is very little hard particle comminution (Fernandez, 2004).

1.2.3 FSW of Cu

Copper is widely used in many industrial fields for its high electrical and thermal conductivity, excellent resistance to corrosion. However, it is difficult to join pure Cu by fusion welding because of its high thermal conductivity and high oxidation rate at welding temperatures (Welding Handbook, Vol. 5, 2015). FSW as a solid-state welding process can be used to produce defect-free joints from Cu and its alloys successfully (Shen, 2010; Hwang, 2010; Miličić, 2016; Park, 2008; Sun, 2010; Savolainen, 2004). However, FSW of Cu and its alloys as comparatively high-melting point metals have not been studied extensively as compared to the FSW of low-melting point metals such as Al and Mg. Primary attention has been paid to the study of the effect of welding regimes [Shen, 2010 etc.] and also tool geometry (Miličić, 2016; Khodaverdizadeh, 2013) on the structure and mechanical characteristics as well as the quality of FSW welds.

Although in addition to shorter tool life, FSW tool wear leads to unexpected weld properties (structure, mechanical properties), only few studies have addressed the tool

wear mechanism and tool materials selection of Cu and Cu alloys (Savolainen, 2004; Nakata, 2005; Sahlot, 2017; Sahlot, 2019).

Sahlot et al. present a quantitative wear analysis of H13 hot work steel during the FSW of CuCrZr (0.8 Cr, 0.1 Zr) alloy. Severe tool wear was observed for H13 steel tool due to high stresses at elevated welding temperatures. Macroscopic surface investigation showed that Cu alloy gets stuck at localized locations over the tool surface due to diffusion bonding. Scratches and grooves were also observed, proving also abrasive wear due to interaction of flowing workpiece material with a rotating tool. Higher tool wear was observed for faster tool rotational speeds and slower traverse speeds during initial stages of tool travel (~300 mm). With further tool travels, the wear rate decreases significantly and is not affected much by the process parameters (Sahlot, 2017; Sahlot, 2019).

Savolainen et al. (Savolainen, 2004) investigated the factors affecting friction stir weldability of pure copper and its alloys and addressed correct welding parameters and performance of tool materials. Studied tool materials were H13-type hot-work steel, Ni-based superalloy, TiC-NiMo and TiC-NiW cermets, pure tungsten, and poly-crystalline cubic boron nitride (PCBN). PCBN demonstrated the best performance as it was the only tool material able to produce welds in all the base materials – pure copper, aluminium bronze CuAl5Zn5Sn and copper-nickel CuNi25. The use of sintered TiC-NiW and TiC-NiMo cermets was not recommended as they demonstrated poor mechanical properties (were too brittle). However, authors comment that with optimal manufacturing parameters, these composites may prove to be successful as FSW tool material (Savolainen, 2004).

1.2.4 FSW of stainless steel

FSW of Al and Al alloys has been successfully applied in several industries such as aerospace, automotive, railways and shipbuilding industries. FSW of steels, in particular stainless steels, has not attained so far similar levels of application. The reasons are: FSW of steel is more difficult than FSW of aluminium, owing to the demands on the tooling and consequently, the potential advantages of FSW have not been fully realised. Special tools that can survive at high temperature, stress and wear need to be used for FSW of steels. Increased research investments are needed to develop more affordable and reliable tool materials (Liu, 2018; Cam, 2017).

Numerous studies were conducted on the FSW of steels in the last two decades (Reynolds, 2003; Park, 2005; Fujii, 2011; Li, 2015). There are several reasons for this. Firstly, lower heat inputs are involved in FSW as compared to fusion welding processes, resulting in less metallurgical changes in the heat-affected zone (HAZ). Secondly, this process has potential to join some difficult-to-fusion-weld steels. Thirdly, hydrogen cracking is not an issue in FSW. Finally, the temperatures experienced in the FSW of steels are 1000–1200 °C (Darvazi, 2014), which is much lower than those during conventional fusion welding (Cam, 2017).

Stainless steel requires high temperature to soften and at the same time, it also possesses high strength. Consequently, during the FSW of stainless steels, the tool is subjected to severely adverse conditions of heat and stress, which may cause deformation and wear of the tool. The tool must be resistant to fatigue, fracture, mechanical and chemical wear. Therefore, mechanical properties of the tool sufficient at the high temperatures are required and the tool must be chemically inert to welded materials. Thus, selection of a suitable tool material with proper design, which often has a complex geometry and is also cost-effective, is a critical issue for friction stir welding of stainless steel (Siddiquee, 2014; Bhadeshia, 2009).

Not many tool materials are suitable for stainless steel FSW due to the difficult welding conditions. Nevertheless, researchers all over the world have used several kinds of welding tools made of refractory materials or ceramic-based composites for welding stainless steel successfully.

PCBN

PCBN as FSW tool material was used for welding of various high melting temperature materials in countless applications (Sato, 2009; Chen, 200; Sato, 2005; Santos, 2016) after Collier and others stated that friction stir processing (FSP) of ferrous alloys, in particular stainless steels grades AISI 304L and AL-6XN, is possible using a tool made of PCBN. Failure modes identified in their tests were mechanical-, chemical- and diffusion wear. They also stated that PCBN machining insert wear mechanisms correlate directly with PCBN FSP tool wear mechanisms. Regarding the present work, the following statement was significantly important: machining tests of AL-6XN can be used as a screening method to determine PCBN FSP tool performance [Collier, 2003]. It is acceptable to perform model tests with potential tool materials, with materials that need to be welded, before the development of the final tool, to avoid excessive costs in tool development. Park et al. investigated the wear of the PCBN tool and its effect on the second phase formation in stainless steel friction-stir welds. The FSW was applied to five grades of stainless steels (ferritic, duplex, and austenitic). B-rich phase evolution and interstitial pickup were also investigated in their work. Additionally, besides study of tool effect on the weld quality, they suggested that tool wear during FSW can be attributed to high flow stresses in austenitic stainless steels (Park, 2009).

WC- and W-based alloys

Tungsten (W) has a high melting point and mechanical properties at elevated temperatures. WC-based hardmetals are characterized by high hardness and resistance to wear as well as acceptable strength and fracture toughness. Wear and plastic deformation of tools were observed mainly due to high temperature and stresses prevailing during welding and affecting the wear mechanism while welding stainless steel with WC-based hardmetals. Temperature and stresses vary depending on the location on the tool. The tool degradation and wear mechanism are slightly different depending the location on the tool profile (pin root, bottom face of the pin, shoulder) but main reasons for wear are diffusion, adhesion and plastic deformation. Such conclusions were drawn by Siddiquee and Pandey as they investigated the effect of FSW parameters on the behavior of the WC-Co tool employed in the welding of AISI 304 stainless steel (Siddiquee, 2014).

Tool degradation can be divided into two main categories – wear and deformation – also in the case of W-based FSW tools. Such conclusions were reached by Thompson and Babu as they investigated degradation mechanisms of FSW tools made from W-based alloys for welding high speed steels (HSS). Material processing plays a significant role in material's ability to resist tool failure (Thompson, 2010) and both materials, WC-Co and W-based alloy, strongly influence the weld structure and were hardly worn. Formation of ferrite phase with high W content and formation of a large number of coarse $M_{23}C_6$ -type carbides in the stir zone during the FSW of AISI304 stainless steel was shown (Sato, 2011). WC-based hardmetals (Muneo, 2015; Siddiquee, 2011; Ueji, 2006) and W-based alloys (Lakshminarayanan, 2010; Klingensmith, 2005; Meran, 2010) tools have also been used to weld other high melting temperature materials.

Ir-based alloy

Iridium (Ir) has a high melting point, high mechanical properties and oxidation resistance at elevated temperatures. Although Ir is a rare, costly metal and very difficult to machine, Miyazawa et al. developed an Ir-based alloy tool. They succeeded to weld over 75 m long defect-free joints of AISI 304 stainless steel without shielding gas. Wear of the Ir-based alloy tool was less than or equal to that of the PCBN tool (Miyazawa, 2012). They also developed the Ir-based alloy tool alloyed by additional elements, such as Re (Miyazawa, 2011) and Zr (Miyazawa, 2012) to improve the FSW tool. Ir was slightly oxidized at elevated temperatures and adding Re increased the high temperature strength and high temperature hardness. Although the wear was seen clearly in the probe of the Ir-Re tool, the Ir-Re-Zr tool was hardly worn and had better properties than other tested Ir-based alloys (Miyazawa, 2012).

Other tool materials

In addition to the tool materials characterized above for stainless steel FSW, some other attempts were made to develop the tools capable enough of withstanding the thermal, impact and shear forces that occur during the FSW of stainless steel. The atmospheric plasma spray (APS) and plasma transferred arc (PTA) hardfacing processes were performed to deposit refractory ceramic-based composites coatings on the Inconel 738 alloy by Lakshminarayanan et al. (Lakshminarayanan et al., 2014). They stated that the low values of bond and shear strength of the APS coatings led to the unwanted failure of the coated tool during the plunging stage of the FSW process. Nevertheless, the PTA hardfaced tool effectively withstood the temperature and high stresses produced during the motion of the FSW tool during welding of stainless steel, proving its capability to be used as a candidate FSW tool material to weld high melting temperature materials (Siddiquee, 2014).

1.3 Aim and objectives of the study

Tool degradation is a limiting factor during friction stir welding (FSW) of high melting point metals and is also important in terms of tools durability during welding of low melting point metals. Therefore, the **aim** of the study was to develop and utilize reliable, durable and cost-effective tool materials for the FSW of metals with a wide range of melting temperatures. Ceramic-metal composites, in particular TiC- and TiCN-based cermets as well as WC-based hardmetals possessing a good combination of hardness, strength, toughness and resistance to wear at ambient and elevated temperatures can be considered as significant FSW tool material candidates.

Hypothesis of the study is that ceramic-metal composites (TiC- based cermets and WC- based hardmetals), have potential to perform as reliable and cost-effective tool materials for the FSW of metals with different compositions, solid state welding temperatures and mechanical characteristics.

The objectives of the research are:

- Development and application of laboratory scale model-testing methodology for assessment of tools degradation during the working of low- and high melting point metals at the regular FSW temperatures.
- Comparative study for revealing the performance of ceramic-metal composites as potential tool materials for the FSW of metals with different welding temperatures: aluminium alloy, copper and stainless steel.

- Improving understanding of the effect of composition and characteristics of ceramic-metal composites and workpiece materials (aluminium alloy, copper and stainless steel) on the degradation rate and mechanism during model tests and welding using FSW tool prototypes.
- Tools prototypes production and FSW feasibility studies in laboratory conditions (welding of copper and stainless steel) and in industrial environment (welding of aluminium alloys).

2 Materials and experimental methods

Hardmetals (WC-based ceramic-metal composites) are extensively used in the conditions require high stiffness and wear resistance, e.g., in forming and metal cutting tools. The remarkable wear resistance of the hardmetals is because of their high hardness, wear resistance and moderate fracture toughness (Brookes, 1996). Cobalt is widely used as the binder system due to its excellent wetting performance and high mechanical properties. Hardmetals are used as a FSW tool material, especially FSW of high melting point alloys (Choi, 2009; Siddiquee, 2014) or materials with hard particulates (Liu, 2005). Cermets consist of ceramic particles bonded with a metal matrix, except for hardmetals that are WC-based (Hardmetals, Sarin, 2014). Cermets demonstrate high hardness and wear resistance at high cutting speeds in machining, as compared to WC-based hardmetals. The most common binder systems of TiC- and Ti(C,N)-based cermets are Ni alloys. Nevertheless, Fe alloys have positive aspects over Ni and Co as metallic phase, such as possibility to heat treatment, high strength and affordable cost. For that reason, study of Ni- and Co-free metal composites has been escalated during the last decades (Lapman, 1993). Generally, TiC- and Ti(C,N)-based cermets are used where moderate density, good wear resistance or high temperature oxidation resistance is necessary (Mari, 2014). For example, TiC-cermets with a iron-based binder have demonstrated their superiority over WC-based hardmetals in metalforming because of their perfect adhesive wear resistance and low fatigue sensitivity (Klaasen, 2004; Klaasen 2010).

2.1 Materials

2.1.1 Tool materials

The following factors have to be taken into account when selecting of the tool materials for FSP/FSW: good compressive yield strength at high temperatures, no reaction with welded material, resistance to wear, excellent strength and creep resistance, low cost etc. (Zhang, 2012; Meilinger, 2013; Cui, 2018; Mishra, 2014). Therefore, ceramic-metal composites can be used as FSW tool material because their excellent properties (Brookes, 1996).

In this research, TiC-based cermets were investigated due to following aspects: raw materials availability, environmental impact, healthcare related to the utilization of W and Co (Critical Raw Materials, online; REACH, online). The most common binder phase of TiC- and Ti(C,N)-based cermets are NiMo alloys (Hardmetals, Sarin, 2014). Fe-alloys, in particular TiC-FeCr and TiC-FeNi cermets were also studied as potential FSW tool materials because of their advantages over Co and Ni such as low cost, potential to heat treatment and high strength,

The chemical composition, powder particle size and supplier of initial powders for preparation of ceramic-metal composites are shown in Table 4. The starting chemical composition and carbide content in the sintered carbide composites are shown in Table 5 (Publication V).

Table 4. Characteristics of the starting powders (Publication V).

Material	Chemical composition (wt.%)	Powder particle size (μm)	Supplier
WC	W—base; C—6.13; oth. < 0.14	D50 = 0.86	Wolfram Bergbau und Hütten AG (Sankt Martin im Sulmtal, Austria)
TiC	Ti—base; C _{total} —19.12; C _{free} —0.15; oth. < 0.31	2.0–3.0	Pacific Particulate Materials Ltd. (New Westminster, Canada)
Co	Co—99.5; oth.—0.5	5.0–6.0	Pacific Particulate Materials Ltd. (New Westminster, Canada)
Fe	Fe—99.72; Si—0.01; P—0.07; Mn—0,02; oth—C	40–90	Rio Tinto (London, United Kingdom)
Ni	Ni—99.8; oth.—0.2	3.0–5.0	Pacific Particulate Materials Ltd. (New Westminster, Canada)
Mo	Mo—99.8; oth.—0.2	1.0–3.0	Pacific Particulate Materials Ltd. (New Westminster, Canada)
AISI430L	Fe—base; Fe—16.8; Mn—0.69; Si—0.64; oth < 0.05	10–45	Sandvik Osprey Ltd. (Neath, United Kingdom)

Table 5. Chemical composition of tool materials under investigation (Publication IV).

Designation	Initial composition (wt.%)		Carbide content after sintering (vol.%)
	Carbide	Binder	
85WC-Co	85WC	15Co	76.4
90WC-Co	90WC	10Co	83.7
94WC-Co	94WC	6Co	90.0
70TiC-NiMo	70TiC	20Ni; 10Mo	87.7
75TiC-NiMo	75TiC	16.7Ni; 8.3Mo	89.9
80TiC-NiMo	80TiC	13.3Ni; 6.7Mo	92.1
70TiC-FeCr	70TiC	24.9Fe; 5.1Cr	84.0
70TiC-FeNi	70TiC	25.8Fe; 4.2Ni	79.3

The carbide volume content in cermets was calculated taking into account the dissolution of Mo in TiC and the formation of secondary Cr-based carbides in TiC-NiMo and TiC-FeCr ceramic-metal composites, respectively (Publication III; Kolnes, 2018). The microstructures of the selected carbide composites are shown in Figure 3.

All the composites were produced using conventional powder metallurgy (PM) technology routes for hardmetals and cermets. Powder mixtures for starting powders were prepared using the conventional ball mill with WC-Co lining and balls for a duration of 72 h at the ball to the powder weight ratio of 10:1. Isopropyl alcohol was used as a milling liquid. WC-Co contamination from milling was approximately 5 wt.% in the case of TiC-based cermets. Tungsten carbide dissolves in titanium carbide and cobalt in metallic binder during the liquid phase sintering of cermets. Milled powders were mixed with 3 wt.% paraffin, granulated, dried and compacted into green bodies with 100 MPa

of uniaxial pressure. Pressureless liquid phase sintering (LPS) in vacuum (0.1–0.5 mbar) during 30 min was carried out to obtain specimens for the mechanical, model (cutting) tests and for production of FSW tool prototypes. The optimal sintering temperatures of 1450–1500 °C (depending on the composition) for achieving near-full density (low porosity) and maximal mechanical characteristics were used. Heating rate up to the sintering temperature was 10 °C·min⁻¹, followed by dwelling at the final temperature and cooling with furnace (Publication V).

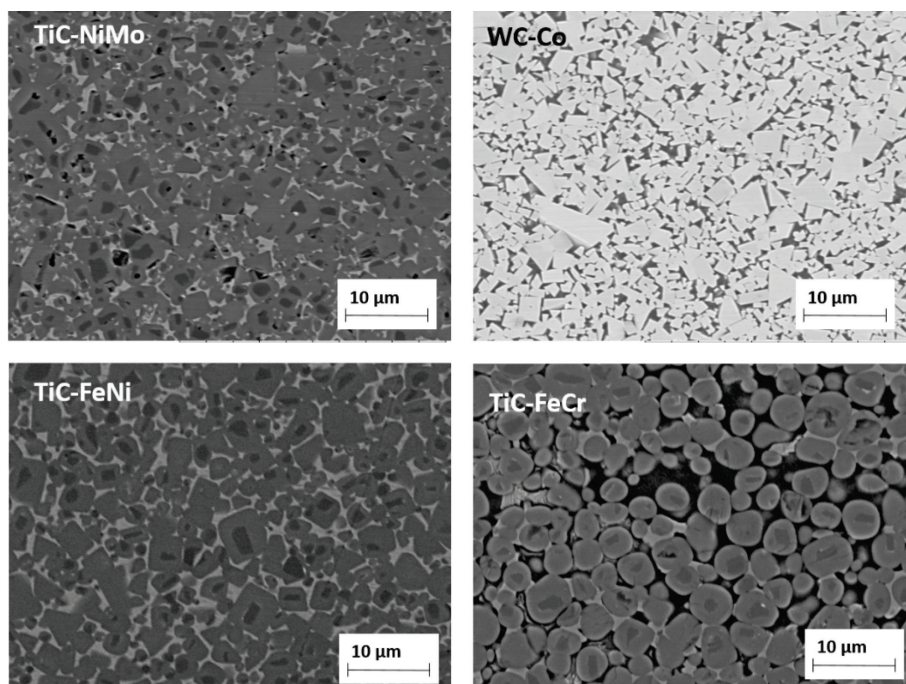


Figure 3. SEM micrographs of ceramic-metal composites 75TiC-NiMo, 85WC-Co, 70TiC-FeNi and 70TiC-FeCr (Publication V).

2.1.2 Workpiece materials

In this study, we focused on aluminium, copper and stainless steel because of their quite poor weldability as compared to the low-carbon steel liquid phase welding (Olson, 1993). The chemical composition of the workpiece materials used is shown in Table 6.

Table 6. Chemical composition of workpiece materials for the model and FSW tests (Publication V).

Workpiece Material	Chemical Composition (wt.%)					
Aluminium alloy (AW6082-T6)	96.9 Al	1.1 Si	0.5 Mn	0.8 Mg	0.7 Other	
Copper (Cu-ETP)	99.9 Cu					0.1 Other
Stainless steel (AISI 304)	70.7 Fe	1.6 Mn	18.0 Cr	8.1 Ni	0.3 Si	1.3 Other

2.2 Experimental details

2.2.1 Model wear tests

To evaluate the wear performance of different carbide composites during the FSW of aluminium alloy, copper and stainless steel, the model tests were performed on a universal lathe (see Figure 4a), using cutting tools from carbide composites with specific geometry (see Figure 4b). Tools were grounded to achieve a nose angle of 134° , side cutting edge angle of 23° and side relief angle of 8° . A set of three specimens were produced for every tested material, to assess the reliability and the reproducibility of experimental results. The investigated material bars were machined at high speed, up to 630 m/min, 470 m/min and 280 m/min to achieve the cutting zone temperature approximately similar to that of the welding temperature for aluminium alloy (400°C), copper (600°C) and stainless steel (1000°C), respectively. The feed rate and the depth of the cut were kept constant during testing at 0.39 mm/rev and 0.125 mm, respectively. Common FSW temperatures for Al-alloys ($\sim 400^\circ\text{C}$) and stainless steel ($\sim 1000^\circ\text{C}$) were achieved at described cutting speeds, while for copper temperature of 600°C , which is somewhat below regular FSW temperature ($700\text{--}750^\circ\text{C}$), was achieved as maximum (Publication V).

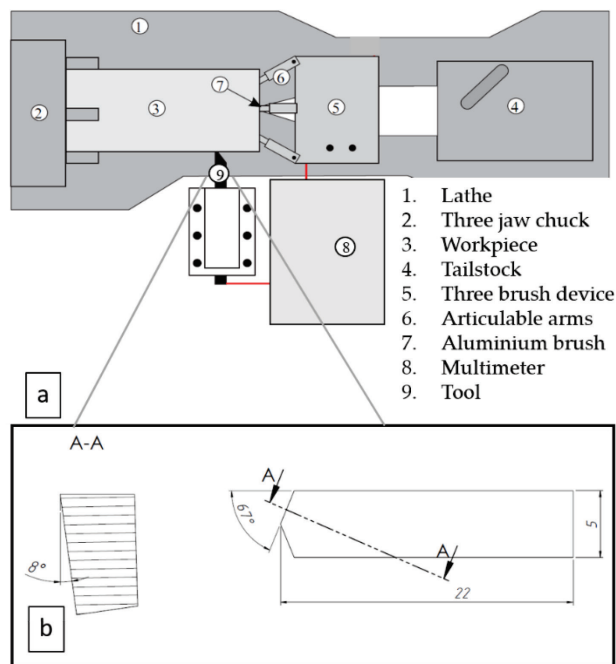


Figure 4. Schematic of the tool-workpiece thermocouple system (a) and cutting tool geometry (b) (Publications II and III).

The wear rate of the tool was determined as the shortening in the length of the cutting tool nose tip of the model test specimens. Shortening of the cutting nose tip was measured on the top surface of the tool in the case of aluminium alloy and copper as workpiece materials, using the images made from the top surface of the cutting tool by Hitachi TM 1000 Tabletop scanning electron microscope (Hitachi High-Tech, Krefeld, Germany) (see Figure 5). In the model tests with stainless steel, the height of the wear

pattern was measured on the front surface of the tool because the tool wear rate was much more intensive. These measurement results were recalculated to the shortening of the cutting nose tip on the top surface for better comparison. To measure the cutting temperature in the cutting point, a tool-workpiece thermocouple method was used for all tested materials (Publication V).

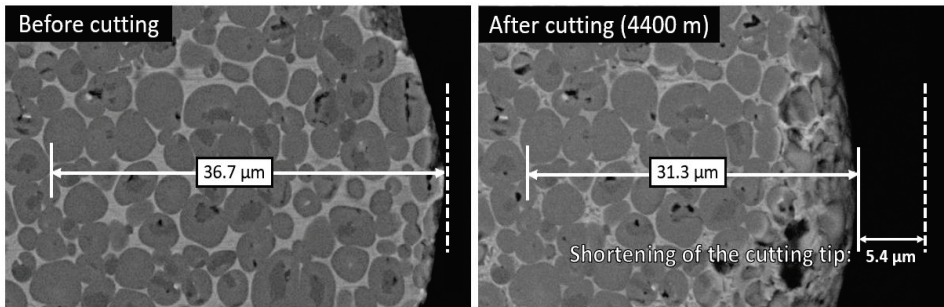


Figure 5. The measurement of the shortening of 70TiC-FeCr tool nose tip on the top surface of the cutting tool after cutting aluminium alloy (cutting distance 4400 m) (Publication V).

Working temperature measurement

Currently, the most used method to measure cutting temperature is the tool-workpiece thermocouple method, which uses Seebeck's principle. Previous studies have proved that a metal subjected to a temperature differential undergoes a non-uniform distribution of free electrons, which subjects this metal to an electromotive force differential (Recktenwald, 2010; Publication III). This method requires two different metals joined in one part. Along the paths of the thermocouple circuit, the electromotive force is given by the product of the difference between the Seebeck's coefficients of thermocouple materials and the temperature gradient between the thermocouple closed and open junctions. With the tool-workpiece thermocouple method, the amount of electromotive force is an indication of the average temperature in the tool-workpiece interface. On some occasions, the electromotive force does not correspond to the average cutting temperature of the interface, it only corresponds in the cases when the temperature is uniform, or if the thermoelectric obtained from the tool-workpiece combination varies linearly along with the cutting temperature (Publication III). The tool-workpiece thermocouple method has also recently been used for measuring the FSW process temperature (De Backer, 2013).

The scheme of the system used is presented in Figure 4a. The workpiece and the turning tool were insulated from the lathe. The cold end of the tool and the three-bush device were connected to the voltmeter to measure the electromotive force (Publication III).

To ensure reliable temperature measurements, the tool-workpiece thermocouple is required to be the only high temperature point in the system. All the other material connections have to be at the room temperature. To maintain the electrical conductivity in the tool-workpiece thermocouple circuit during turning of aluminium alloy, copper and stainless steel, a three-brush device was used. The main function of the three-brush device is to maintain the electrical continuity of the tool-workpiece thermocouple circuit with the workpiece in rotational movement. The device used is similar to that used by Santos Jr. et al. (Santos et al., 2017; Publication III).

In this work, calibrations of the tool-workpiece thermocouple were carried out with tool materials under research. Long bars of the tool materials (hardmetals, cermets) were prepared with one end joined with all workpiece materials (aluminium alloy, copper and stainless steel). The calibration thermocouples were introduced into an electrical furnace and heated up to 500 °C, 700 °C and 1100 °C in the case of aluminium alloy, copper and stainless steel, respectively. Which are similar temperatures to the FSW conditions (Threadgill, 2009; Nakata, 2005; Prasanna, 2010). Electromotive force was measured on the outside ends of the ceramic-based composite bar and the workpiece material chip, which were at the room temperature. Therefore, the electromotive force was dependent only on the temperature of the contact point between the tool and the workpiece materials. Figure 6 shows the calibration curves of the three tested thermocouple materials tested with Al alloy (Publication III).

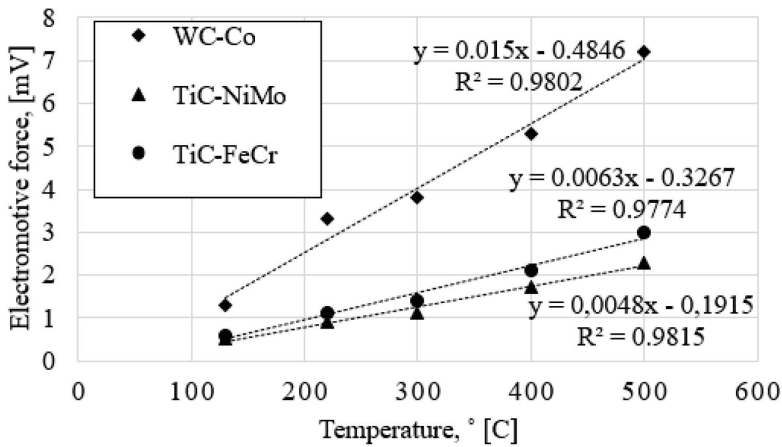


Figure 6. Relationship between the temperature and the electromotive force for three ceramic-based materials tested with aluminium alloy (Publication III).

2.2.2 Diffusion testing

In this study, reaction diffusion experiments were conducted for deeper understanding of the diffusion controlled processes that may result in harmful reactions between the tool and the workpiece materials, incurring tool degradation. The reaction diffusion of the tool material is one of the important reasons of FSW tool degradation by intergrain fracture during the working of metallic alloys, especially taking into account the acceleration of diffusion by temperature and contact stresses developed in the FSW. Fragments of the FSW tool material are deformed and detached from the FSW tool by a fracture along the embrittled grain boundaries under the shear stress developed on the surface of the tool during FSW (Tarasov, 2014). Diffusion of workpiece material elements to tool is a special concern in FSW/FSP of high-melting point metals (Publication V), in particular Cu-, Fe- and Ti-alloys. As an example, FSW tool wear by rapid-rate diffusion of elements from Ti- alloy into W-Re alloy tool causing degradation and wear by subsurface fracture has been reported (Thompson, 2011). Similar processes are significant, considering the FSW of steels and copper characterized by much higher working temperatures and contact stresses as compared to aluminium alloys (Publications IV-VI).

During the FSW of copper alloys and aluminium alloys, tribological deposits cover FSW tool (Tarasov, 2014). Such layers enable analysis of diffusion processes in the contact region of tool-workpiece. Unfortunately, the formation of such tribological layers is not evident during the model tests using stainless steel as workpiece materials. Therefore, special test samples were prepared for all tool and workpiece materials groups (Publications IV-VI).

Ceramic-metal composites with the highest binder fraction from each tested tool material group were selected (85WC-Co, 70TiC-NiMo, 70TiC-FeCr, 70TiC-FeNi) to achieve deeper diffusion of elements from the workpiece materials into the tool. The test samples for the study of diffusion-controlled processes were prepared using spark plasma co-consolidation of sintered carbide composite specimens and workpiece material or material powder with similar chemical composition to obtain a permanent bond between the tool material and the metal (Al-alloy, copper, stainless steel). Reaction diffusion tests were performed by heating the test samples up to approximately the same temperature as in the model tests, followed by 4 h dwelling at that temperature in vacuum furnace. Such heating time is relatively short in comparison with the FSW tool life during welding of aluminium alloys and copper (Publication V).

To understand the distribution of chemical elements in the microstructure in the tool-workpiece contact region, the scanning electron microscope (Zeiss EVO MA15) equipped with energy-dispersive X-ray spectroscopy system INCA (Oxford Instruments) was used.

2.2.3 FSW feasibility studies

A vertical milling machine OPTImill MT 220S (vertical spindle power, 4 kW; spindle speeds, 60-1750 rpm; table travel speed, max 800 mm/min) was used to perform the feasibility study of the FSW tool prototypes made from ceramic-metal composites. The welding trials consisted of one-sided butt welding of 4 mm sheets at ambient conditions (without gas shielding). Short welds were performed to examine tool resistance to failure during the initial plunge stage of the FSW process. Weld length depends on the workpiece material: 10 m, 10 m and 50 mm in the case of aluminium alloy, copper and stainless steel, respectively.

FSW tools used in the experiments had 3.8 mm (2.4 mm in case of stainless steel welding) long conical tapered pin with a root diameter of $\varnothing 6.4$ mm. The concave shoulder end surface was used to produce welds. Shoulder end diameter was $\varnothing 15$ mm. The rotation speed of 1235 rpm, the traverse speed of 150 mm/min and tilt angle of 2° were used and welding tool geometry in the case of aluminium alloy and copper welding, is shown in Figure 7. The rotation speed of 1750 rpm, the traverse speed of 30 mm/min and tilt angle of 2° were used in case of working of stainless steel.

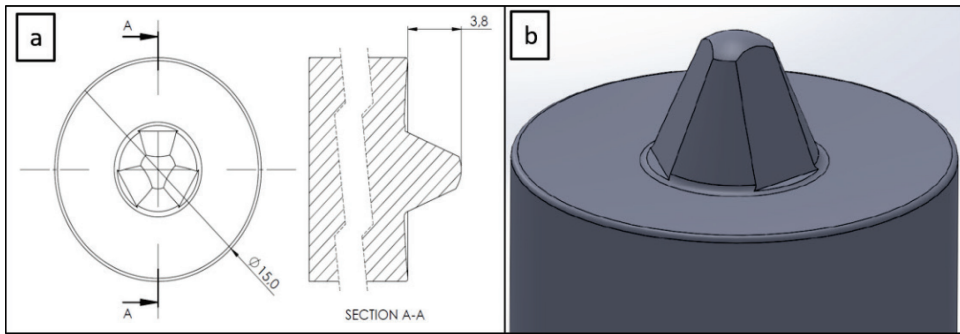


Figure 7. Drawing (a) and 3D model (b) of FSW tool used in the present research (Publication II and VI).

2.2.4 Material characterization methods

Mechanical properties

Hardness and fracture toughness K_{1c} of sintered composites were determined using ground test specimens of 5 mm × 5 mm × 17 mm. Hardness (HV30) was measured with a hardness tester Indentec 5030KV. Fracture toughness was evaluated with the indentation method (Palmqvist method) using an equation described in (Evans, 1976; Publication V).

Microscopy

The porosity of the consolidated ceramic-metallic composites was below 0.5 vol.%. The porosity was evaluated by measuring the surface area of pores on the optical image of the microstructure at the magnification of 200 times. Optical microscope Axiovert25 and software Buehler Omnimet were used (Publication V). For microstructural investigation, the scanning electron microscope (SEM) Zeiss EVO MA15 was used.

3 Performance of cermets and hardmetals as tool materials for FSW of low- and high-melting point metals

Tool materials used in the model cutting tests, diffusion tests and applied in FSW feasibility studies of aluminium alloy, copper and stainless steel are shown in Table 7 and mechanical properties and average carbide particle size of used tool materials in Table 8.

Table 7. Selection of materials for the model, diffusion and feasibility test.

Workpiece Material	Tool Materials							
	85WC -Co	90WC -Co	94WC -Co	70TiC-NiMo	75TiC-NiMo	80TiC-NiMo	70TiC-FeCr	70TiC-FeNi
Model cutting test								
Aluminium alloy (AW6082-T6)	•		•		•		•	
Stainless steel (AISI 304)	•	•	•	•	•	•	•	•
Copper (Cu-ETP)	•	•	•	•	•	•	•	•
Diffusion test								
Aluminium alloy (AW6082-T6)	•				•		•	
Stainless steel (AISI 304)	•			•			•	•
Copper (Cu-ETP)	•			•			•	
FSW feasibility test								
Aluminium alloy (AW6082-T6)	•				•			
Stainless steel (AISI 304)	•				•			
Copper (Cu-ETP)	•				•			

Table 8. Average carbide particle size and mechanical properties of tool materials under investigation (Publication V).

Designation	Hardness HV30	Fracture toughness, (MPa·m ^{1/2})	Average carbide particle size, (µm)
85WC-Co	1150 ± 20	17.8 ± 0.5	0.91
90WC-Co	1238 ± 6	16.7 ± 0.3	1.19
94WC-Co	1765 ± 25	7.2 ± 0.3	0.48
70TiC-NiMo	1340 ± 21	12.6 ± 0.3	1.21
75TiC-NiMo	1403 ± 25	11.4 ± 0.4	1.14
80TiC-NiMo	1492 ± 16	10.1 ± 0.4	1.60
70TiC-FeCr	1352 ± 6	9.1 ± 0.7	1.99
70TiC-FeNi	1379 ± 21	15.2 ± 0.5	1.60

3.1 FSW of aluminium alloy

3.1.1 Model wear tests

Chromium-molybdenum hot work tool steel X40CrMoV (AISI H13) is the most common tool material for the FSW of aluminium and aluminium alloys (see Table 2). AISI H13 is the most common choice also for FSW/FSP of copper (Rai, 2011; Arulmoni, 2015). Our study showed that WC-based hardmetal and TiC-based cermet as ceramic-metal composites outperform remarkably this air hardening tool steel in the low-temperature (70 °C) model cutting tests of aluminium alloy (Publication I and II). Both carbide composites outperform in such testing conditions markedly, also cobalt-chromium (CoCr) alloy commonly used in gas turbines and other application fields due to the wear- and corrosion resistance and incredible strength at high temperatures (Publication I). Remarkable degradation (wear) resistance of ceramic-metal composites makes them interesting as potential durable tool material in FSW.

The performance of hardmetals and cermets in the model tests at different temperatures (70 °C and 400 °C) was studied. It was shown that TiC-based cermets (TiC-NiMo, TiC-FeCr) demonstrate superiority over WC-Co hardmetal at both low (70 °C) and elevated (400 °C) working temperature (see Figure 8). The highest wear resistance at low working temperature was demonstrated by the Fe-alloy bonded composite TiC-FeCr, while at the elevated temperature by the Ni-alloy bonded cermet TiC-NiMo (Publication III). This composite demonstrated also the lowest temperature sensitivity to tool degradation (see Figure 8). Enhanced high-temperature strength of the Ni-based metallic binder of the composite as well as enhanced carbide volume fraction are the reasons behind the high wear performance of TiC-NiMo cermet (Publication III).

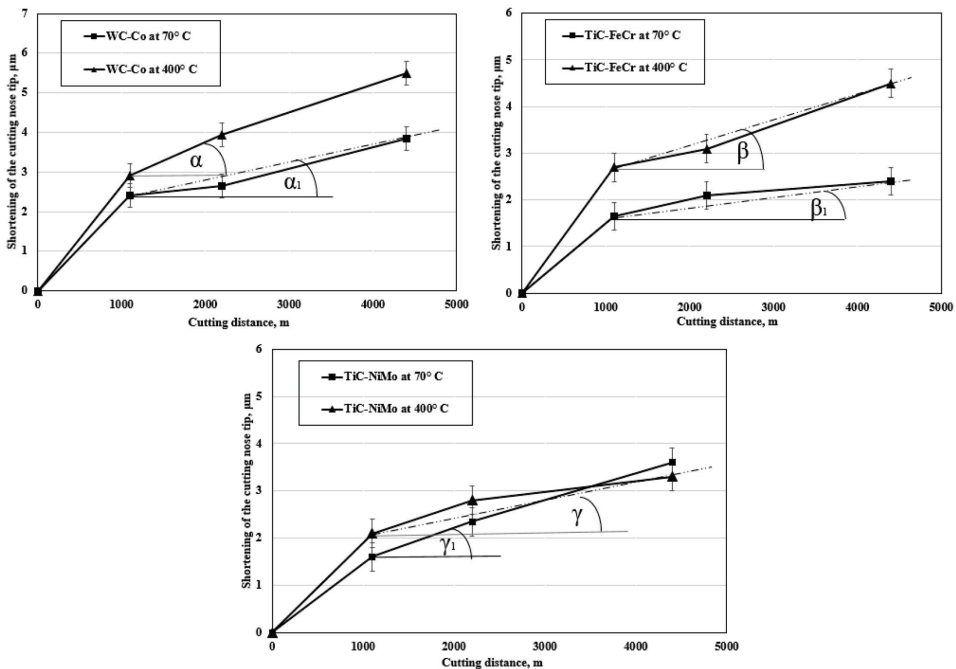


Figure 8. Wear of the carbide composites vs aluminium alloy (cutting) distance at different temperatures (adapted from Publication III).

Figure 9 demonstrates the wear rate plotted against the cutting distance of the WC-Co hardmetal and TiC-based cermets at the working temperature of 400 °C. Wear of ceramic-metal tools during the model tests with workpiece from aluminium alloy at 400 °C is very small even at considerable cutting distances up to 8800 m. WC-Co hardmetal 85WC-Co demonstrated the highest wear rate during testing. This ceramic-metal composite showed also the highest wear gain during an increase of the cutting distance. 94WC-Co hardmetal with substantially higher carbide fraction and hardness (and the lowest fracture toughness) suffered structural failure after comparatively short cutting distances. All TiC-based cermets showed an advantage over the hardmetal. However, cermet with the NiMo binder is at advantage over the composites with Fe-alloy binders (FeCr and FeNi), independent of the working distance (Publication V).

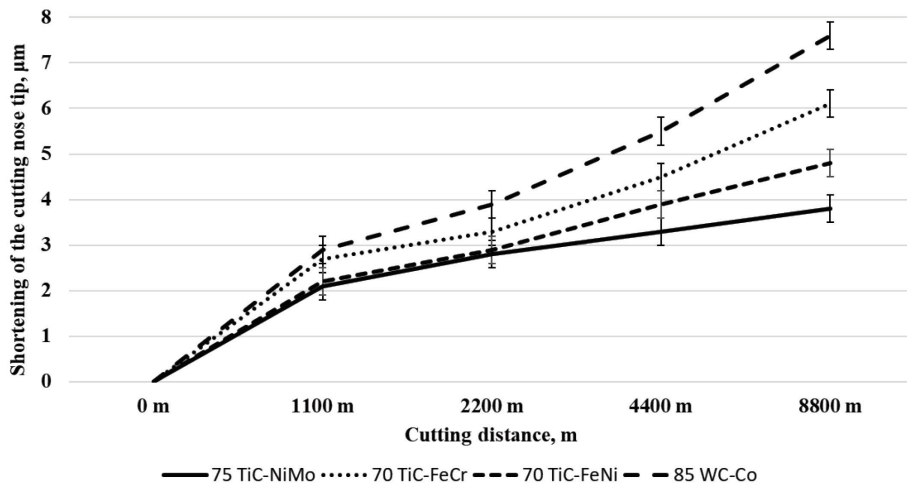


Figure 9. Wear of ceramic-metal composites vs. cutting distance in the case of aluminium alloy at 400 °C (Publication V).

During the working (cutting) of plastic metals with the fractional content of hard second phases, tools fail most commonly by mechanisms based on adhesion and diffusion. Adhesion as the key wear mechanism is the reason why TiC-based cermets, in particular TiC-NiMo composites, demonstrate superiority over the WC-Co hardmetal during the working of aluminium alloy. Adhesion as the wear mechanism is confirmed by strongly adherent workpiece metal deposits (layers) on the rake face of ceramic-metal and also FSW tools (see Figure 14 b). Other researchers addressing the wear mechanism of tools during the FSW of Al- (Tarasov, 2014), Ti- alloys (Nabhani, 2001) and Cu alloys (Sahlot, 2017; Sahlot, 2019) have made similar observations. Also, Al diffusion has been shown to be a degradation factor in the tools used for the FSW of aluminium (Tarasov, 2014; Publications III and V).

SEM studies (Figure 10) demonstrate failure (material removal) of the cutting tool tip after wear tests of carbide composites. The structure of a worn cutting nose tip is distinctive, proving that failure starts preferably in the binder continuing by extraction of carbides. This wear mechanism in the model testing conditions used is similar to that in previous studies of the adhesive wear of cermets and hardmetals (Klaasen, 2010; Publication III).

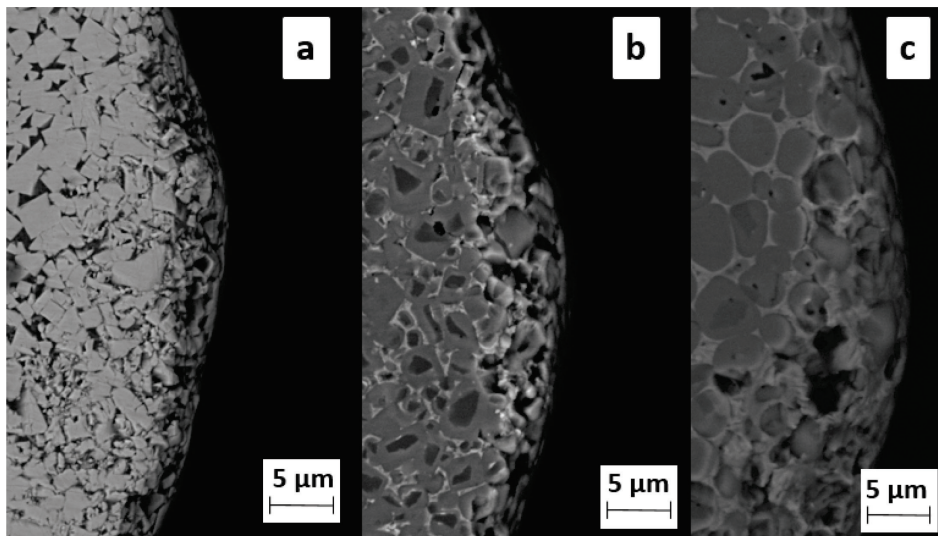


Figure 10. The worn out cutting nose tip (cutting distance 4400m) of carbide composites WC-Co (a), TiC-NiMo (b) and TiC-FeCr (c) (Publication III).

3.1.2 Diffusion tests

In addition to adhesion, also diffusion has been shown to be a degradation factor in the tools used for the FSW of aluminium and aluminium alloys (Tarasov, 2014). These diffusion controlled degradation processes are possible due to the combination of both local high mechanical and thermal loading effects on the tool. These processes may lead to the formation of brittle intermetallic compounds in the heat-affected zone of metallic binders of ceramic-metal composite tools. The embrittlement created at the grain boundaries of the tool material may increase the likelihood of degradation under severe stresses that the tool surfaces are exposed to (Publication V).

At the working temperature of 400 °C, the ceramic-metal tools are covered by the workpiece metal, Al alloy. Figure 11 shows the results of EDS line scans in tool-workpiece contact zones after 4 h heat treatment at 400 °C. The diffusion of Al into the cobalt binder is slightly higher than its diffusion into the iron-chromium and nickel-molybdenum binder (see Figure 11 a, b, c) (Hirano, 1962; Alamadadi, 2017). At the same time, titanium diffusion but not that of tungsten into aluminium was observed (Publication III).

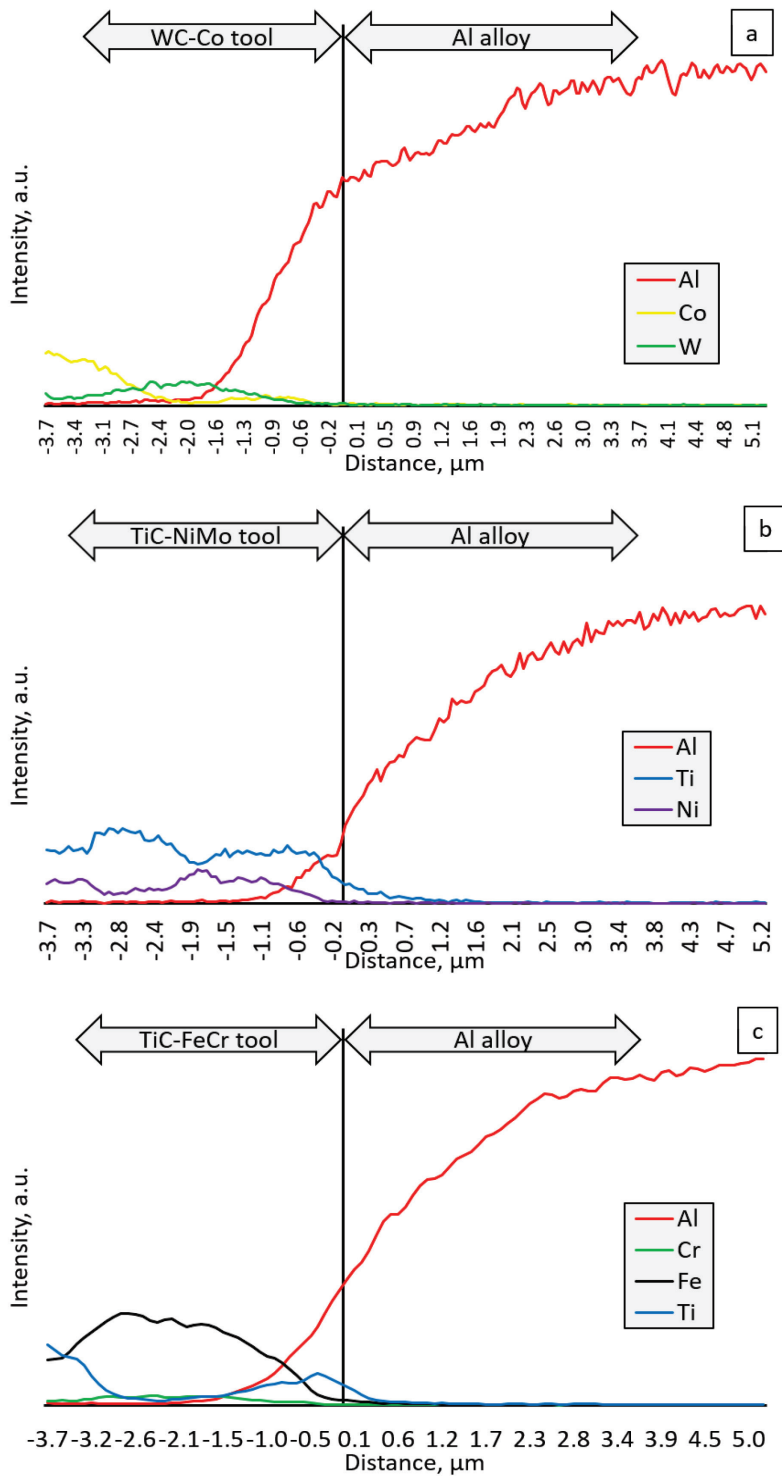


Figure 11. EDS line scan of the WC-Co, TiC-NiMo and TiC-FeCr tools-workpiece (aluminium alloy) contact zones after diffusion heat treatment for 4 h at 400 °C (Publication III).

Figure 12 demonstrates the EDS mapping of Co-, Ni- and Fe-based binders in contact with Al-based workpiece material after heat treatment of 4 h at 400 °C. In the study, the test samples were prepared using spark plasma co-consolidation of sintered carbide composite specimens and aluminium alloy powder with similar chemical composition as that of the workpiece used in the model tests. Diffusion of aluminium into ceramic-metal composites metallic phase is quite marginal as compared to the diffusion of copper and stainless steel components at 600 °C and 1000 °C, respectively (see Figure 18 and Figure 23). However, the highest wear gain during an increase of the cutting distance of the WC-Co hardmetal can be explained by the higher diffusion depth to Co binder, resulting in the formation of hard and brittle intermetallic phases in the contact region of the tool-workpiece, whereas their fraction increases with an increase in the content of aluminium (Publication V).

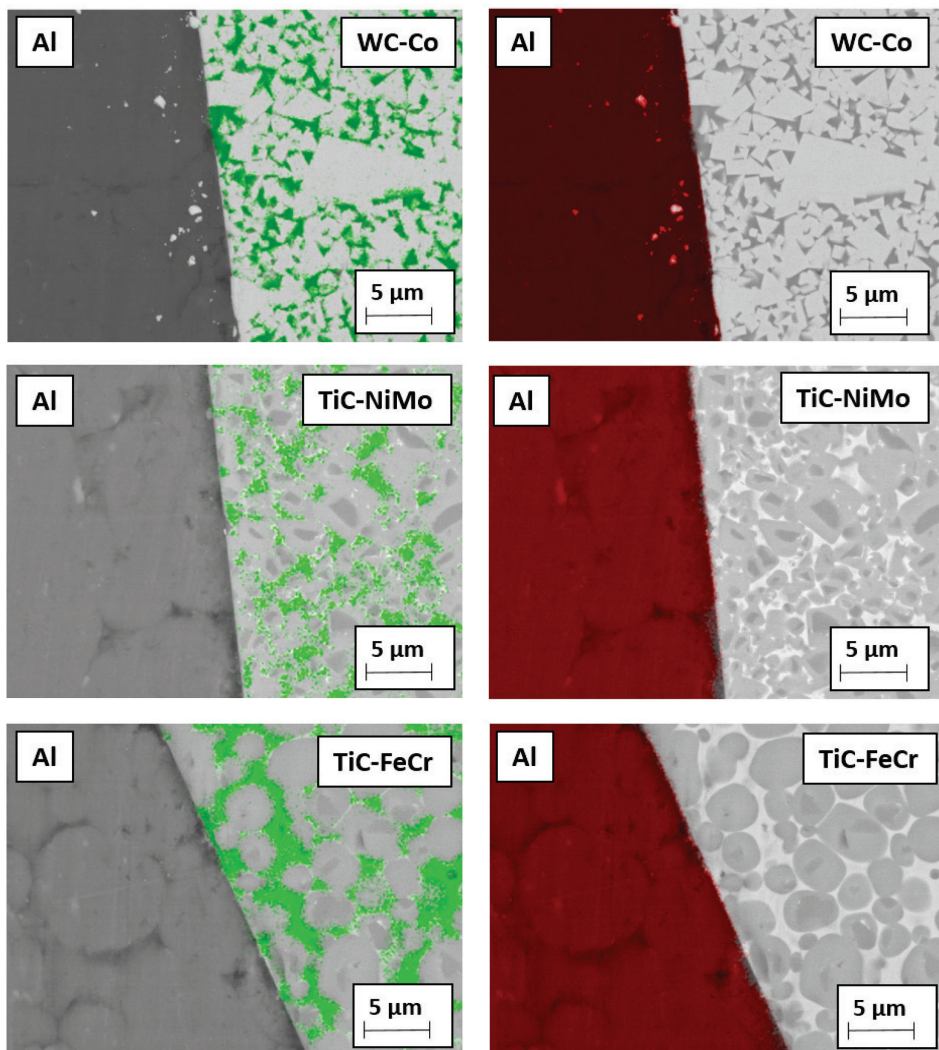


Figure 12. EDS mapping of permanent bond between tool materials and aluminium alloy heating in vacuum during 4 h at 400 °C: green—metallic binder (Co, Ni, Fe), red—aluminium (Publication V).

3.1.3 Friction stir welding trials

FSW trials in laboratory conditions were performed using a vertical milling machine. 4 mm thick sheets from aluminium alloy were one-side butt welded at ambient conditions using a FSW tool with geometry presented in Figure 7. The welding distance was 10 m. The macroscopically defect-free welds were produced (see Figure 13 a) using both WC-Co hardmetal and TiC-NiMo cermet. Figure 13 b demonstrates the cross section of the weld and Figure 14 demonstrates the FSW tool (75TiC-NiMo) before welding (as sintered) (a) and after welding of 10 m (b).

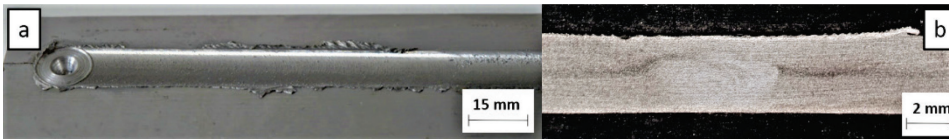


Figure 13. Image of the visually macroscopic defect-free weld of aluminium alloy (a) and cross section of the same weld (b). Image of the FSW tool (75TiC-NiMo) before (a) and after welding of aluminium alloy (b).

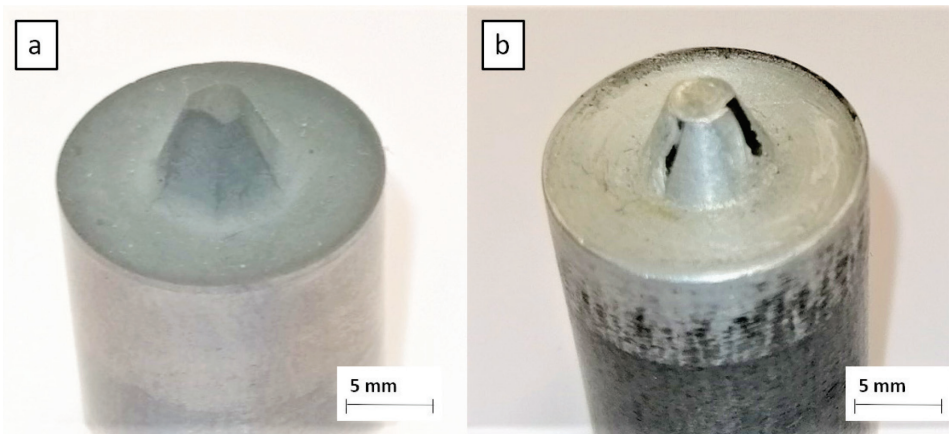


Figure 14. Image of the FSW tool (75TiC-NiMo) before (a) and after welding of aluminium alloy (b).

3.1.4 Summary

Research results of the performance of ceramic-metal composites (WC-based hardmetals and TiC-based cermets) as potential tool materials for the FSW of aluminium alloy can be summarized as follows:

- TiC-based cermets with Ni- and Fe-alloy binders demonstrate superiority over WC-Co hardmetals both at low ($\sim 70^\circ\text{C}$) and FSW temperature ($\sim 400^\circ\text{C}$) in the model tests with Al alloy. The highest wear performance at the high working temperature was demonstrated by TiC-NiMo cermets.
- The lowest temperature sensitivity of wear resistance was demonstrated by Ni-alloy bonded cermets TiC-NiMo.
- Adhesion as one of the wear mechanisms is confirmed by strongly adherent workpiece metal (Al alloy) deposits (layers) on the rake face of ceramic-metal cutting as well as FSW tools.
- The high diffusion depth and intensity of Al into the WC-Co hardmetals as compared to that of TiC-based cermets (in particular TiC-NiMo cermets) is

probably behind the decreased wear performance of hardmetals as compared to cermets in the model tests at the weld temperature (~400 °C).

- FSW feasibility studies showed that it is possible to produce macroscopically defect free welds using FSW tools from WC-based hardmetals and TiC-based cermets.

3.2 FSW of copper

3.2.1 Model wear tests

The wear performance plotted against the cutting distance of WC- TiC- based ceramic-metal composites of different composition, and fraction of carbides is shown in Figure 15. The testing results for the most wear resistant grades of WC-Co hardmetals and TiC-NiMo cermets (Publication V) are presented. Table 9 presents the wear rates of all tool materials (shortening of the cutting tool nose tip) at the maximal cutting distance of 920 m.

Table 9. Tool material wear rate in the model (cutting) tests of copper at the maximal cutting distance of 920 m (Publication V).

Wear rate (shortening of the cutting tool nose tip), μm							
85WC-Co	90WC-Co	94WC-Co	70TiC-NiMo	75TiC-NiMo	80TiC-NiMo	70TiC-FeCr	70TiC-FeNi
28	26	23	37	38	31	27	36

Increase in the carbide (WC or TiC) fraction improves the wear performance of both WC-Co hardmetals and TiC-NiMo cermets (see Table 9). As different from the model tests with workpieces from aluminium alloy and stainless steel, WC-Co hardmetals with 90–94 wt.% WC demonstrated the best performance. It should be pointed out that 70TiC-FeCr cermet also showed high wear resistance. Regardless of substantial performance of TiC-NiMo cermets in the model tests with Al alloy (Figure 10) and stainless steel (Figure 21), NiMo-alloy bonded cermets compare unfavourably with WC-Co hardmetals when the counterpart is copper. These results demonstrate different wear mechanisms during testing (cutting) of workpieces from different metals at substantially different temperatures and contact stresses (Publication V).

While tool wear during the FSW of aluminium and aluminium alloys, steels and titanium and its alloys has attracted interest of several researchers, only a few studies have focused on copper alloys (Nakata, 2005; Sahlot, 2017; Sahlot, 2019). Investigation of the wear mechanism for the H13 steel tool during the FSW of Cu-Cr-Zr alloy showed severe wear due to high stresses at elevated temperatures (Shalot, 2017). The sticking of Cu alloy over the steel tool surface occurred due to diffusion bonding between copper and steel. Adhesion as one of the wear mechanisms was also confirmed by copper metal deposits at the FSW ceramic-metal tool surfaces (see Figure 20) as well as during the model cutting tests. It is the result of high stresses acting on the tool at high temperatures (Publications V and VI).

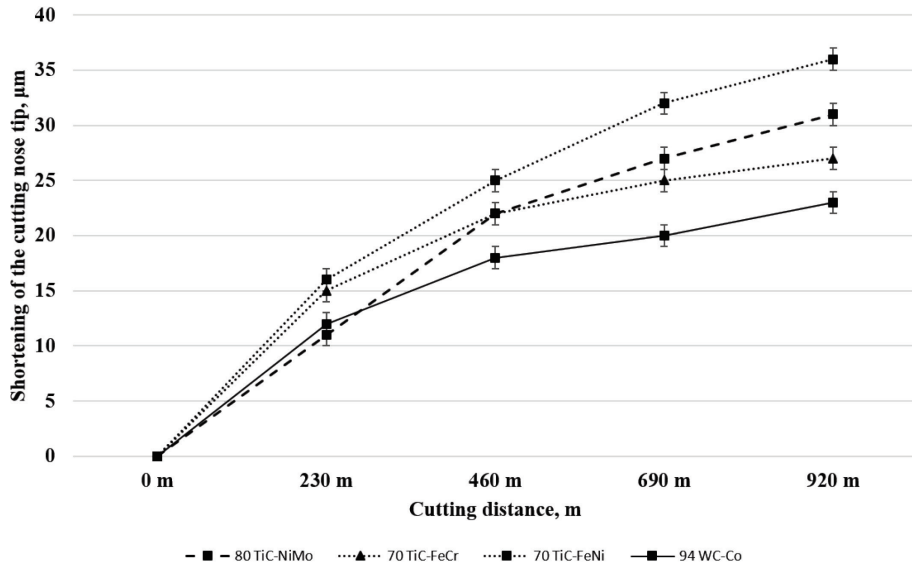


Figure 15. Wear of ceramic-metal composites vs cutting distance in the case of copper at 600 °C (Publication V).

3.2.2 Diffusion tests

In addition to adhesion, diffusion is one of the aspect for tool wear. The studies showed that diffusion of Cu from the workpiece and Fe from the tool takes place across the interface. Diffused Cu and Fe form a solid solution layer over the tool surface without any intermetallic formation as per the Fe-Cu phase diagram. High stresses on the tool surface at elevated temperature results in dislodging of this layer on the FSW tool surface (Sahlot, 2017). Currently, no studies addressing the wear mechanism of cermets or hardmetals during the FSW of copper or copper alloys are available.

At FSW temperatures, the ceramic-metal tools are covered by the workpiece metal, copper, similar to that during the working of the Al alloy. It enables analysis of the diffusion processes in the tool-workpiece contact zone. Figure 16 a and b demonstrates FSW tool-workpiece interface images with EDS line scans after welding of copper.

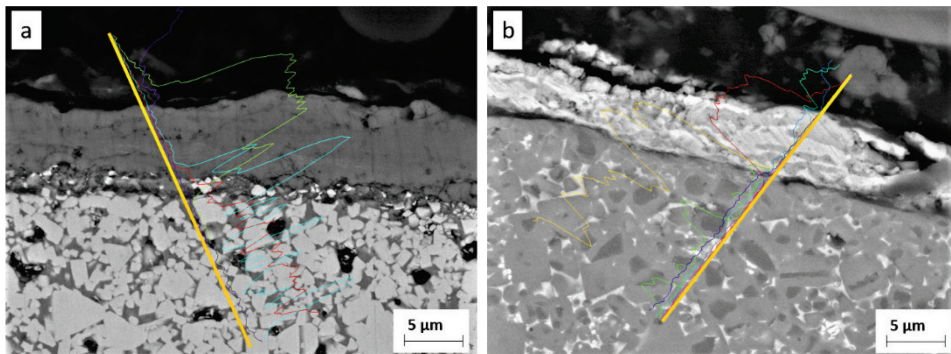


Figure 16. Tool-workpiece images with EDS line scans after 10 m welding of copper: a) WC-Co tool, b) TiC-NiMo tool (adapted from Publication VI).

Figure 17 shows results the EDS line scans of ceramic-metal tools and Cu workpiece interfaces after friction stir welding (~10 m weld) during about 1 h (Figure 17 a and c) and also after diffusion tests during 4 h at 600 °C (Figure 17 b and d). The figure demonstrates a relatively higher diffusion depth of Cu in the TiC-NiMo cermet as compared to diffusion in WC-Co both during FSW trials (Figure 17 a and c) and during prolonged heat treatment at 600 °C (Figure 17 b and d). Apparently, almost no diffusion of the components of ceramic-metal tools, in particular Co and Ni to workpiece, during the FSW process can be observed (Figure 17 a and c). A continuous movement (slip) and replacement of Cu layer on the tool surface during welding unlike during prolonged diffusion model tests (Figure 17 b and d) are behind such a result. Loss of nickel due to diffusion to workpiece exceeds that of cobalt.

The results are in agreement with phase diagrams Co-Cu and Ni-Cu. Enhanced diffusion rate of Cu to Ni-based metallic binder of the cermet resulting in higher fraction of Cu in the surface regions of the tool (see Figure 17 c) is probably the reason behind the enhanced wear rate of TiC-NiMo tools as compared to that of WC-Co in the model tests (see Figure 15).

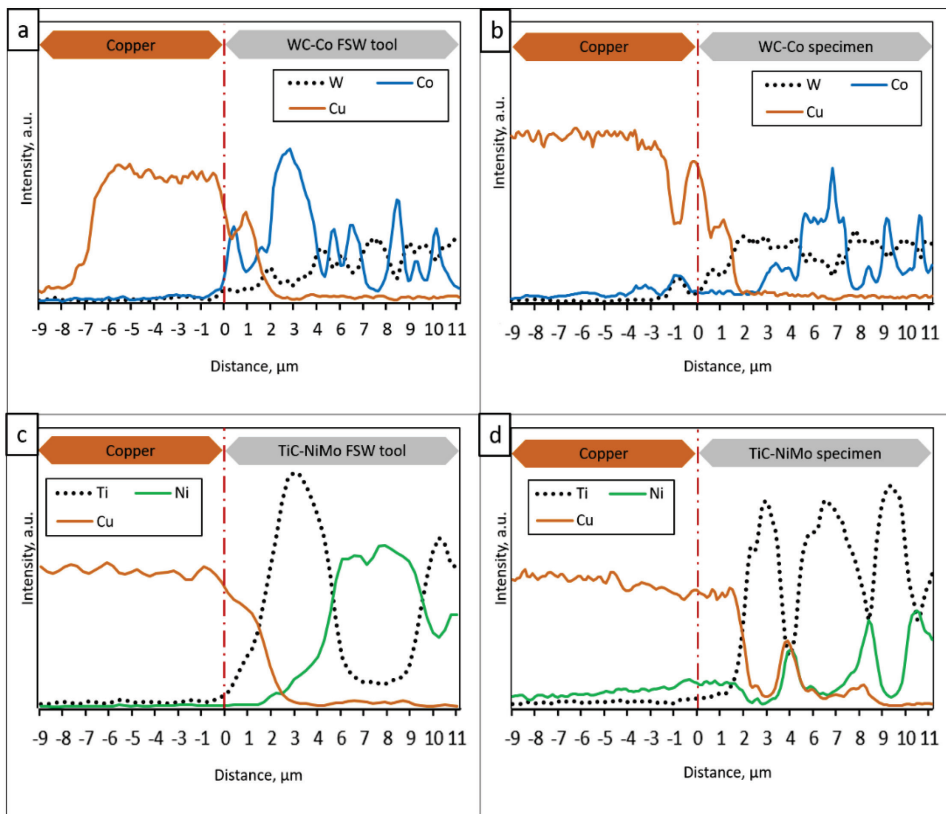


Figure 17. EDS line scans of WC-Co (a) and TiC-NiMo (c) FSW tools surface in the welding test after 10 m welds (1 h), and WC-Co (b) and TiC-NiMo (d) diffusion model test specimens in contact with copper after heat treatment for 4 h at 600 °C (adapted from Publication VI).

Figure 18 demonstrates the EDS mapping of the ceramic-metal composites with Co-, Ni- and Fe-based binders in contact with copper after model diffusion tests (heat treatment) at 600 °C. The EDS mapping confirms the results of EDS-line scan studies (Figure 17). Figure 18 demonstrates a relatively higher diffusion depth of copper in the Ni alloy of the TiC-NiMo cermet as compared to copper diffusion in WC-Co and TiC-FeCr composites. It is in agreement with the correspondent phase diagrams Co-Cu, Fe-Cu and Ni-Cu, demonstrating high mutual solubility of Cu and Ni and very low in Fe-Cu and Co-Cu systems even at the temperature 600 °C. Intensive diffusion of copper into the TiC-NiMo binder phase (Cu diffuses faster in Ni than Ni in Cu) results in increased fraction of copper in the surface regions of a cermet tool and decrease of hardness. It may cause enhanced wear rate of TiC-NiMo cermet and also TiC-FeNi cermet as compared to WC-Co hardmetals and TiC-FeCr cermets (Publication V).

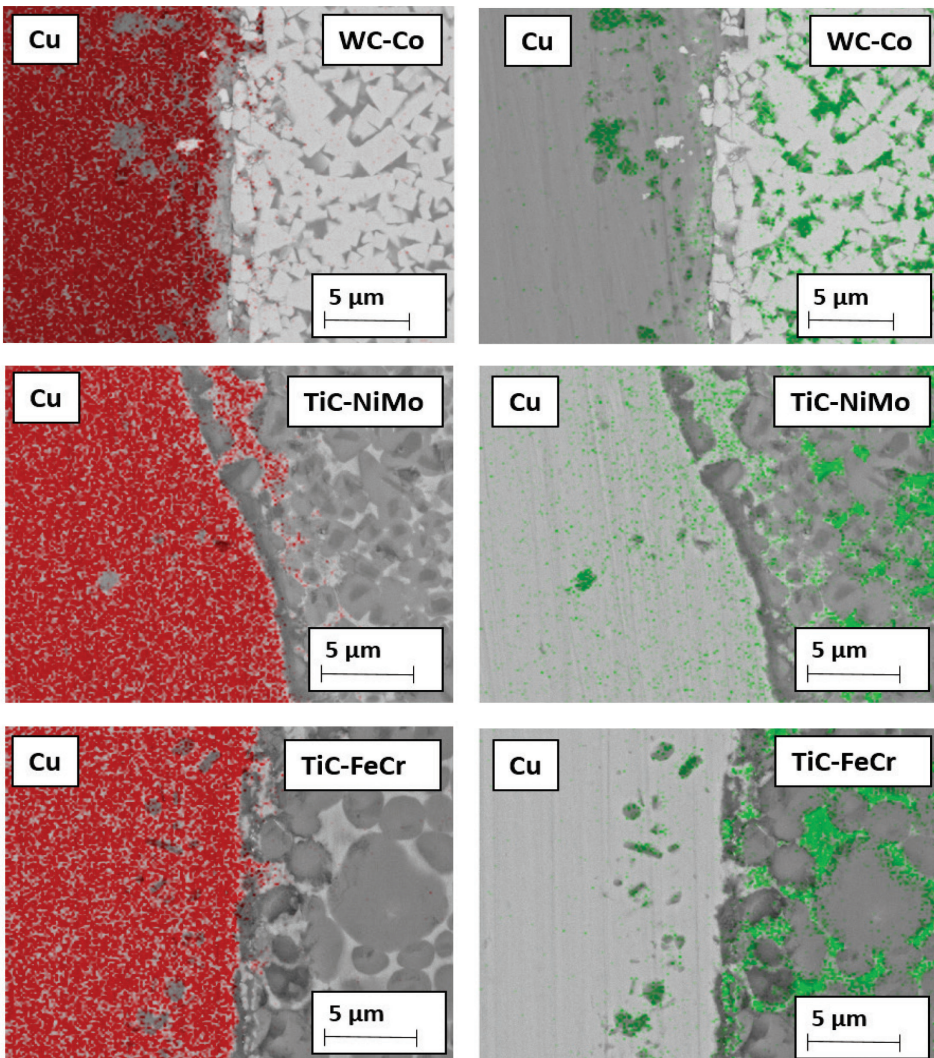


Figure 18. EDS mapping of permanent bond between copper tool and materials after heat treatment in vacuum during 4 h at 600 °C: red—copper, green—metallic binder (Co, Fe, Ni) (Publication V).

3.2.3 Friction stir welding trials

Figure 19 shows the image of macroscopically defect-free weld of copper (Figure 19a) and the cross section of the same weld (Figure 19b). Figure 20 demonstrates the FSW tool before welding (as sintered) (a) and after welding of 10 m (b). From the point of view of the geometry of the FSW tool, special attention should be paid to the fact that cut-outs on the sides of the tool pin are most likely not necessary, as they were not filled with copper (see Figure 20).

Savolainen (Savolainen, 2004) has shown that FSW tools from TiC-NiMo and TiC-NiW cermets (50 wt.% TiC) show low mechanical properties and, as a result, low reliability during welding of Cu and Cu-alloys. Our research demonstrated feasibility of employing WC-Co hardmetals and TiC-NiMo cermets as tool materials for the FSW of copper and copper alloys. Tools from these ceramic-metal composites (with a similar geometry as the Savolainen tools) did not fail during multiple plunges as well as traverse welding distances. Macroscopic wear was not observed after traverse distance of 10 m (Publication VI).

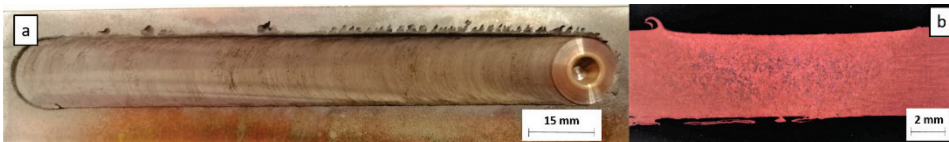


Figure 19. Image of the visually macroscopic defect-free weld of copper (a) and cross section of the same weld (b) (adapted from Publication VI).

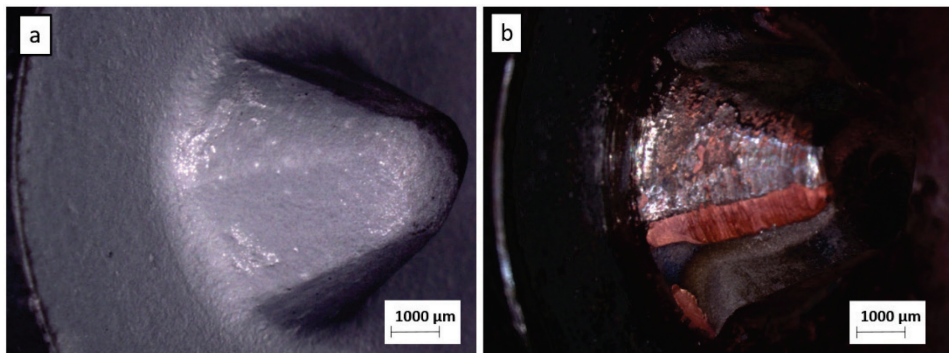


Figure 20. Image of the FSW tool (75TiC-NiMo) before (a) and after welding of copper (b) (adapted from Publication VI).

3.2.4 Summary

Research results of the performance of WC-based hardmetals and TiC-based cermets as potential tool materials for the FSW of copper can be summarized as follows:

- WC-Co hardmetals (90...94 wt.% WC) outperform most of TiC-based cermet grades in the model tests (working temperature of 600 °C) with copper. Hardmetals show better wear performance as compared to cermets, in particular TiC-NiMo cermets, even if they compare unfavourably with hardness.
- Adhesion as one of the wear mechanisms is confirmed by adherent workpiece metal (copper) deposits on the rake face of ceramic-metal cutting tools as well as FSW tools.

- Diffusion is one of the factors of ceramic-metal tools degradation in the working of comparatively high-melting point copper. The high diffusion rate of Cu to TiC-NiMo cermets, resulting in enhanced fraction of copper in the surface regions of tools, is probably the reason behind decreased wear performance of TiC-NiMo cermets as compared to WC-Co hardmetals during the model tests at the weld temperature (600 °C).
- FSW feasibility studies demonstrated that it is possible to produce macroscopically defect-free welds using FSW tools from the WC-Co hardmetals and TiC-based cermets.

3.3 FSW of stainless steel

3.3.1 Model wear tests

Figure 21 demonstrates wear (shortening of the cutting tool nose tip) plotted against the cutting distance of ceramic-based composites of different composition and carbide fraction. For clarity, Figure 21 shows testing results only for the most wear resistant grades of WC-Co hardmetals and TiC-NiMo cermets (Publication V). Table 10 presents the wear rate of all carbide composites at the maximal cutting distance of 150 m.

Table 10. Wear rate of tool materials in the model (cutting) tests of stainless steel at the maximal cutting distance of 150 m (Publication V).

Wear rate (shortening of the cutting tool nose tip), μm							
85WC-Co	90WC-Co	94WC-Co	70TiC-NiMo	75TiC-NiMo	80TiC-NiMo	70TiC-FeCr	70TiC-FeNi
258	174	147	108	42	50	298	191

Unlike the result in model test with aluminium alloy (at 400 °C) or copper workpiece (at 600 °C), the wear of cermet and hardmetal tools was pronounced during cutting of stainless steel (at 1000 °C) even at comparatively short cutting distances (see Figure 21). Increase in the volume fraction of the carbide phase and hardness in the composites enhances the wear performance of WC-Co hardmetals and TiC-NiMo cermets. Regardless of high chromium content, ensuring enhanced resistance to oxidation, FeCr alloy bonded cermet showed the highest wear rate as well as wear gain during the increase of the cutting distance (see Figure 21 and Table 10). An alternative Fe-alloy bonded 70TiC-FeNi cermet exhibited better wear performance at the level of WC-Co hardmetals. TiC-NiMo cermets with 75–80 wt.% TiC demonstrated superior wear performance in such conditions. Results prove different wear mechanisms during the working of aluminium alloy or copper workpiece and stainless steel at substantially different working temperatures (Publications IV and V).

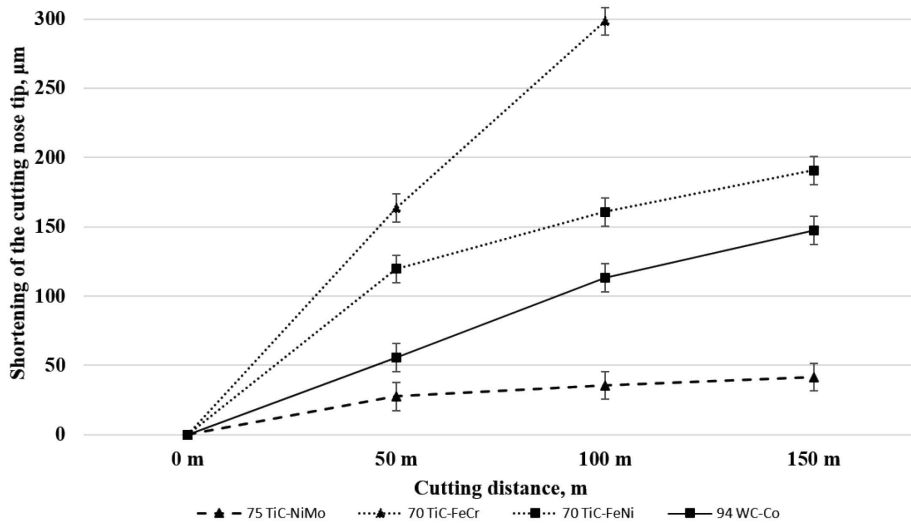


Figure 21. Wear of selected tested ceramic-metal composites vs. cutting distance in the case of stainless steel at 1000 °C (Publication V).

Ni-based alloys can withstand severe operating conditions involving high temperature and corrosion environments. Such alloys with excellent elevated temperature properties, in particular NiMo alloys, are used at the highest homologous temperatures as compared to any common metallic alloy systems (ASM Handbook, 1993; Brooks, 1984). The Ni-based binders in cermetts can decidedly handle the heat generated during FSW as well as during the model cutting process better than cobalt in the WC-Co hardmetals and the Fe-based alloy in the TiC-FeNi and TiC-FeCr cermetts (Publication V).

Experimental investigation of WC-based tool materials wear during the FSW of stainless steel has shown that the wear at a pin root and at the bottom face of the pin is attributed mainly to diffusion, adhesion and attrition mechanisms (Siddiquee, 2014). Hot adhesion is one of the wear mechanisms behind the result that TiC-NiMo cermetts demonstrate superiority over abrasive wear resistant WC-Co hardmetals during the working of stainless steel (Publication V).

3.3.2 Diffusion tests

During cutting of stainless steel, tool materials are exposed to high temperatures affecting remarkably the mechanism of wear. The presence of Fe and Cr in stainless steel strongly influences the dissolution of carbide particles present in the WC-Co hardmetal as well as in TiC-based cermet tool materials. Dissolution of WC leads to the formation of carbon deficient forms of tungsten carbide W_2C , Co_xW_yC compounds (eta phase) and $M_{23}C_6$ phases (Lou, 2003). During processing at high temperatures, the Fe present in the steel also diffuses into the FSW tool and forms a solid solution with cobalt (Siddiquee, 2014). The carbon liberated during the dissolution of WC dissolves in the Co-Fe solid solution and its solubility increases as the amount of Fe in the solid solution increases. Brittle metallic carbide compounds are easily removed by mechanical action, giving rise to craters on the surface of the tool (Siddiquee, 2014). These diffusion-controlled processes—formation of carbon deficient forms of tungsten carbide and metallic

carbides in Co binder—remain relevant wear processes during FSW and during cutting in the model wear tests with the WC-Co tool (Publication V).

Figure 22 demonstrates the EDS line scan of the WC-Co hardmetal and TiC-based cermet in contact with stainless steel after diffusion model tests (heat treatment) 4 h at 1000 °C. Figure 22 demonstrates intensive two-way diffusion of chemical elements of stainless steel (Fe, Cr, Ni) and TiC-based cermets and WC-Co hardmetal. As a result of diffusion, Fe and Cr from stainless steel were revealed in the surface layers of WC-Co hardmetal and TiC-NiMo cermet.

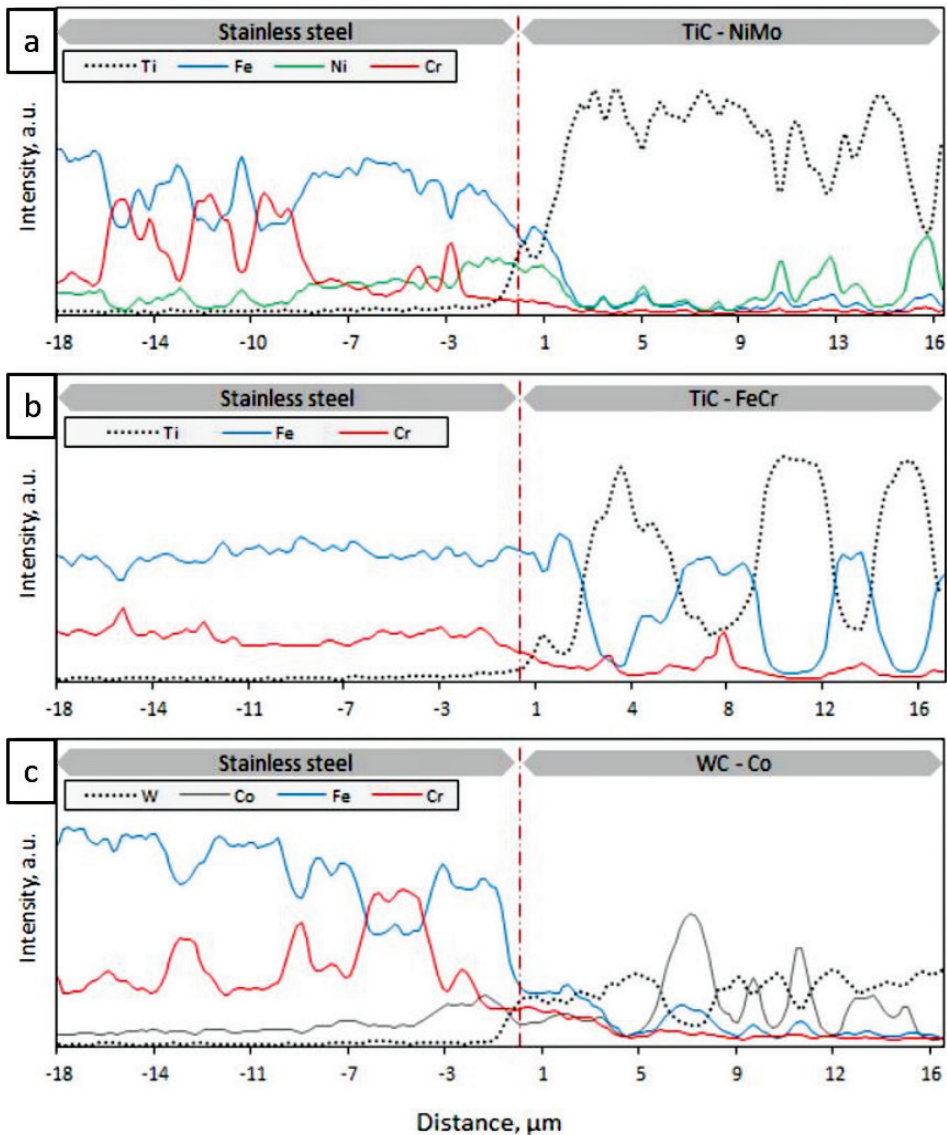


Figure 22. EDS line scans of TiC-NiMo (a), TiC-FeCr (b) and WC-Co (c) diffusion model test specimens in permanent bond with stainless steel after heating for 4 h at 1000 °C.

Figure 23 shows the results of EDS mapping of the ceramic-metal composites with Co-, Ni- and Fe-binders in contact with stainless steel after diffusion tests at 1000 °C. The figure shows the formation of brittle carbon deficient tungsten carbide (eta phase) interaction layer at the interface between the hardmetal and steel. High stresses acting on the tool at high temperature during the cutting process may lead to dislodging of this layer on the tool surface. This diffusion-controlled mechanism is probably the reason behind the decreased wear performance of the WC-Co hardmetal as compared to the wear of TiC-NiMo cermets (Publication V).

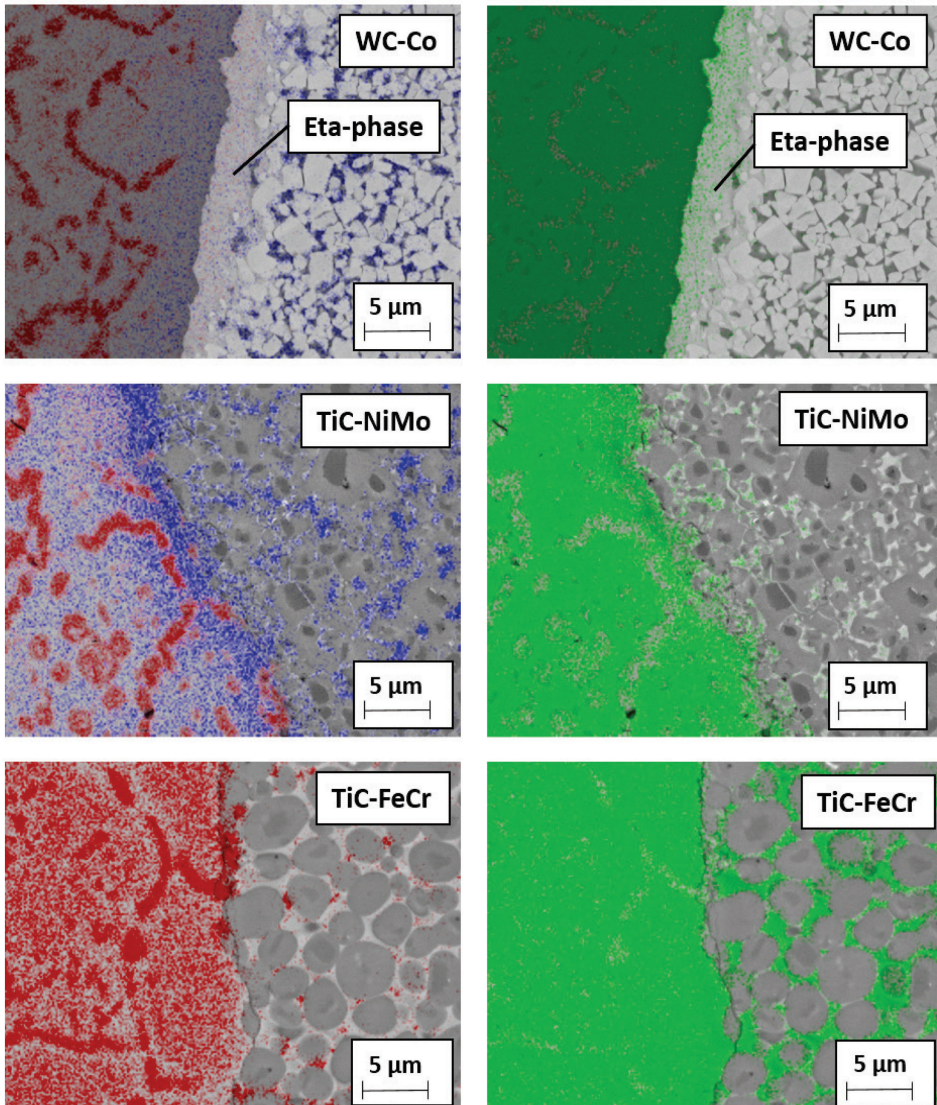


Figure 23. EDS mapping of permanent bond between stainless steel and tool materials after heat treatment in vacuum during 4 h at 1000 °C: red—chromium, green—iron, blue—metallic binder (Co, Ni) (Publication V).

As different from tungsten carbide (WC), titanium carbide (TiC_x) exists as a homogeneous phase over a relatively wide range of carbon content. Dissolution of TiC leads to the formation of substoichiometric carbide particles, not special carbon deficient forms of carbide. As a result, no clear interaction layer at the interface cermet-steel was observed (see Figure 23), i.e., high-temperature diffusion-controlled wear mechanism of TiC-based cermets is different. At high temperatures of the model tests, the iron present in the stainless steel diffuses into the TiC-NiMo cermet tool, forming a solid solution with Ni (see Figure 23). The carbon liberated during the dissolution of TiC dissolves in the Ni-based binder, favouring formation of additional metallic carbides. Also, diffusion of carbon to low-carbon austenitic stainless steel takes place during the reaction diffusion tests, favouring formation of the network of chromium carbides in steel (see Figure 23). During the working of stainless steel, this process is similar both to the WC- and TiC- based ceramic-metal composites (Publication V).

TiC-FeCr cermet demonstrated the highest wear rate (the lowest wear performance) during the model testing. This composite showed also the highest wear gain rate during the increase of the cutting distance (see Figure 21). Diffusion-controlled processes play probably a secondary role in such a rapid degradation process of a cermet tool. The wear performance decrease may be explained by strong chromium steel-to-chromium steel adhesion and tool surface attrition in the contact region of a tool-workpiece (Publication V).

3.3.3 Friction stir welding trials

FSW trials in laboratory conditions were performed using a vertical milling machine. 4 mm thick sheets with partial penetration depth (2.5 mm) from austenitic stainless steel were one-side butt welded at ambient conditions using a FSW tool. The macroscopically defect-free welds were produced (see Figure 24 a) using TiC-NiMo cermet (75TiC-NiMo) as tool material. Figure 25 shows the tool before (a) and after (b) welding of the workpiece. AS different from aluminium alloy and copper as workpiece materials, intensive wear of the FSW tool was observed after travel distance of 50 mm (see Figure 25 b).

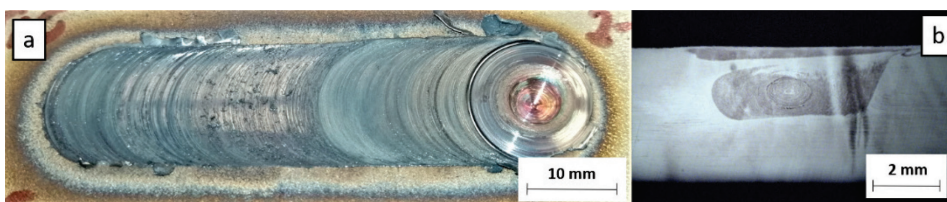


Figure 24. Image of the visually macroscopic defect-free weld of stainless steel (a) and cross section of the same weld (b).

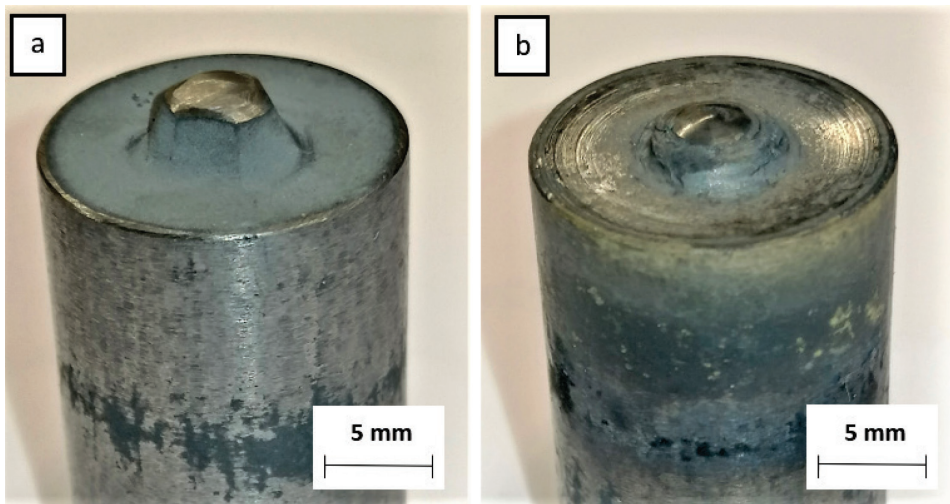


Figure 25. Image of the FSW tool (75TiC-NiMo) before (a) and after (b) welding of austenitic stainless steel.

3.3.4 Summary

Research outcomes of the performance of ceramic-metal composites (TiC-based cermets and WC-based hardmetals) as potential tool materials for the FSW of austenitic chrome-nickel stainless steel can be summarized as follows:

- TiC-NiMo cermets (75...80 wt.% TiC) demonstrate the highest performance in the model tests (working temperature of 1000 °C) using workpiece material from austenitic stainless steel. A great elevated temperature performance of Ni-alloys bonded cermets, which can handle the heat generated during FSW and the model wear tests better than Co in WC-Co hardmetals and Fe in Fe-based alloys in the TiC-FeNi and TiC-FeCr cermets, is the reason behind the high wear resistance of TiC-NiMo cermets.
- TiC-FeCr cermet demonstrating high wear performance during the model wear tests with low melting point metal (aluminium alloy) showed the highest wear rate as well as wear gain during the increase of the working distance as compared to other ceramic-metal composites. Such a behaviour can be explained by strong chromium steel-to-chromium steel adhesion and tool surface attrition in the contact surfaces of the tool-workpiece.
- The high-temperature diffusion is an important factor in addition to hot adhesion of ceramic-metal tools degradation in the working of high melting point stainless steel. The diffusion-controlled processes resulting in formation of brittle carbon deficient forms of tungsten carbide (etc phase) interaction layers at the interface between tool and steel workpiece are probably to a great extent the reason behind the decreased degradation performance of WC-Co hardmetals as compared to TiC-NiMo cermets.
- FSW feasibility studies demonstrated that it is possible to produce short welds using FSW tools from ceramic metal composite intensive wear of the tool was observed.

4 Conclusions

The main goal of the research was to reveal the performance of ceramic-metal composites (hardmetals, cermets) as potential tool materials for friction stir welding (FSW) of workpiece metals with substantially different welding temperatures – aluminium alloy, copper and stainless steel. The effect of composition and characteristics of ceramic-metal composites and workpiece materials on the degradation rate and mechanism of tools during the model wear tests and feasibility FSW tests was also under investigation. The following conclusions can be drawn:

1. The laboratory scale model testing methodology for assessment of cutting tools degradation (wear) during the working of low- and high-melting point metals at different temperatures, in particular regular FSW temperatures, was developed and applied.
2. The comparative study of the performance of ceramic-metal composites as potential tool materials for FSW of metals with different melting and working temperatures has shown that:
 - TiC-based cermets with Ni- and Fe-alloy binder systems demonstrate the highest resistance to degradation in the model tests (working temperature of 400 °C) with the workpiece from aluminium alloy. The highest wear performance and the lowest temperature sensitivity to tool degradation was demonstrated by Ni-alloy bonded cermets TiC-NiMo.
 - WC-Co hardmetals (90...94 wt.% WC) outperform most of TiC-based cermets in the model tests (working temperature of 600 °C) with copper. Hardmetals showed better wear performance as compared to cermets (TiC-NiMo cermets) even if they compare unfavourably with the volume fraction of carbides and hardness.
 - TiC-NiMo cermets (75...80 wt.% TiC) demonstrate the highest performance in the model tests (working temperature of 1000 °C), using a workpiece material from austenitic stainless steel. An outstanding elevated temperature performance of Ni-alloys bonded cermets is the reason behind the high resistance to the tool degradation of TiC-NiMo cermets.
3. The study of the effect of composition and characteristics of ceramic-metal composites and workpiece materials (aluminium alloy, copper, stainless steel) on the degradation rate and the mechanism during the model and feasibility FSW tests has shown that:
 - Irrespective of workpiece metal, the most common wear mechanisms of tools from ceramic-metal composites in the model wear tests and during FSW are adhesion and diffusion.
 - In addition to adhesion, the high diffusion depth and intensity of Al into the WC-Co hardmetal as compared to that of TiC-based Ni- or Fe-alloy bonded cermets is probably the reason behind the decreased degradation performance WC-based, Co bonded hardmetal (at the weld temperature of 400 °C).
 - In addition to adhesion, the high diffusion rate and depth of Cu to TiC-NiMo cermets (Ni-based binder), resulting in an enhanced fraction of Cu in the surface regions of tools, is probably the reason behind the

decreased wear performance of TiC-NiMo cermets as compared to WC-Co hardmetals during the model wear tests (at the weld temperature of 600 °C).

- The high-temperature diffusion is an important factor (in addition to hot adhesion) of ceramic-metal tools degradation in the working of high melting point stainless steel (at the weld temperature of 1000 °C). The diffusion-controlled process, resulting in the formation of brittle carbon deficient forms of tungsten carbide (etc. phase) interaction layers between the tool and the stainless steel workpiece, is probably to a great extent the reason behind the decreased wear performance of WC-Co hardmetals as compared to TiC-NiMo cermets.
4. Prototypes of FSW tools from the ceramic-metal composites were prepared. The FSW feasibility studies demonstrated the possibility to produce macroscopically defect-free welds from copper, stainless steel and aluminium alloy workpieces.

References

- Adesina, A.Y.A.; Al-Badour, F.A.; Gasem, Z.M. Wear resistance performance of AlCrN and TiAlN coated H13 tools during friction stir welding of A2124/SiC composite. *Journal of Manufacturing Processes*, 2018, 33, 11-125.
- Adesina, A.Y.; Gasem, Z.M.; Al-Badour, F.A. Characterization and evaluation of AlCrN coated FSW tool: A preliminary study. *Journal of Manufacturing Processes*. 2017, 25, 432-442.
- Alimadadi, H.; Kjartansdottir, C.; Burrows, A.; Kasama, T.; Møller, P. Nickel-aluminum diffusion: A study of evolution of microstructure and phase, *Materials Characterization*, 2017, 130, 105-112.
- Arulmoni, V.J.; Ranganath, M.S.; Mishra, R.S. Friction stir processed copper: A review. *Int. Res. J. Sustain. Sci. Eng.* 2015, 3, 1-11.
- Bhadeshia, H.K.D.H.; DebRoy, T. Critical assessment: friction stir welding of steels, *Science and Technology of Welding and Joining*. 2009, 14/3, 193- 196. I
- Bist, A.; Saini, J.S.; Sharma, B.A review of tool wear prediction during friction stir welding of aluminium matrix composite. *Trans. Nonferrous Met. Soc. China*, 2016, 26, 2003-2018.
- Boopathi, S.; Kumaresan, A.; Manohar, N.; Moorthi, K.R. Review on Effect of Process Parameters - Friction Stir Welding Process. *IRJET*. 2017, 4/7, 272-278.
- Bozkurt, Y.; Boumerzoug, Z. Tool material effect on the friction stir butt welding of AA2124-T4 Alloy Matrix MMC. *J. Mater. Res. Technol.* 2018, 7(1). 29-38.
- Brookes, K.J. *World Directory and Handbook of Hardmetals and Hard Materials; Metal Powder Industry: London, UK*, 1996.
- Brooks, C.R.; Spruiell, J.E.; Stansbury, E.E. Physical metallurgy of nickel-molybdenum alloys. *Int. Met. Rev.* 1984, 29, 210-248.
- Cam, G.; Ipekoglu, G.; Küçükörneroglu, T.; Aktarer, S.M. Applicability of friction stir welding steels, *Journal of Achievements in Materials and Manufacturing Engineering*, 2017, 80/2, 65-85.
- Chen Y.C.; Fujii, H.; Tsumura, T.; Kitagawa, Y.; Nakata, K.; Ikeuchi, K.; Matsubayashi, K.; Michishita, Y.; Fujiya, Y.; Katoh, J. Friction stir processing of 316 stainless steel plate, *Science and Technology of Welding and Joining* 2009, 14/3, 197-201.
- Choi, D.H.; Lee, C.W.; Ahn, B.W.; Choi, J.H.; Yeon, Y.M.; Song, K.; Park, H.S.; Kin, Y.J.; Yoo, C.D.; Jung, S.B. Frictional wear evaluation of WC-Co alloy tool in friction stir spot welding of low carbon steel plates. *Int. J. Refract. Met. Hard.* 2009, 27, 931-936.
- Collier, M.; Steel, R.; Nelson, T.; Sorensen, C.; Parker, S. Grade development of polycrystalline cubic boron nitride for friction stir processing of ferrous alloys, *Materials Science Forum*, 2003, 426-432, 3011-3016.
- Cui, L; Zhang, C.; Liu, Y.C.; Liu, X.G.; Wang, D.P.; Li, H.L.J. Recent progress in friction stir welding tools used for steels, *J. Iron Steel Res. Int.* 2018, 25, 477-486.
- Critical Raw Materials. Available online: https://europa.eu/growth/sectors/raw-materials/specific-interest/critical_et (29.03.2020).
- Darvazi, A.R.; Irnmanesh, M. Thermal modeling of friction stir welding of stainless steel 304L, *Int. J. Adv. Manuf. Technol.* 2014, 75, 1299-1307.
- De Backer, J., Bolmsjö, G., Thermoelectric method for temperature measurement in friction stir welding, *Science and Technology of Welding and Joining*, 2013, 18:7, 558-565.

- Elangovan, K; Balasubramanian, V.; Valliappan, M. Influences of tool pin profil and axial force on the formation of friction stir processing zone in AA6061 aluminium alloy. *Int. J. Adv. Manuf. Technol.* 2008, 38, 285-295.
- Emamian, S.; Awang, M.; Yusof, F.; Hussain, P.; Mehrpouya, M.; Kakooei, S.; Moayedfar, M.; Zafar, A. A review of friction stir welding pin profile. 2nd International Conference on Mechanical, Manufacturing and Process Plant Engineering, 2017, 1-16.
- Evans, A.G.; Charles, E.A. Fracture toughness determinations by indentation. *J. Am. Ceram. Soc.* 1976, 59, 371-372.
- Fernandez, G.J.; Murr, L.E. Characterization of tool wear and weld optimization in the friction-stir welding of cast aluminum 359+20% SiC metal-matrix composite. *Materials Characterization.* 2004, 52, 65-75.
- Fujii, H. Friction stir welding of steels, *Welding International.* 2011, 25/4, 260-273.
- Fuller, C.B., Friction stir tooling: Tool materials and designs, *Friction stir welding and processing*, ASM International, 2007, 7-35.
- Hardmetals. *Comprehensive Hard Materials*, 1st Ed.; Sarin, V.K.; Elsevier: Amsterdam, The Netherlands, 2014.
- Hirano, K.L., Agarwala, R. P., Cohen, M. Diffusion of iron, nickel and cobalt in aluminium, *Acta Metallurgica*, 1962, 10, 857-863.
- Hwang, Y.M.; Fan, P. L.; Lin, C. H. Experimental study on friction stir welding of copper metals. *J. Mater. Process. Technol.* 2010, 210, 1667-1672.
- Jannet, S.; Mathewa, P.K.; Raja, R. Comparative investigation of friction stir welding and fusion welding of 6061-T6 – 5083-O aluminum alloy based on mechanical properties and microstructure. *J. Achiev. Mater. Manuf. Eng.* 2013, 61/2, 181-186.
- Jeganathan Arulmoni, V.; Ranganath, M.S.; Mishra, R.S. Friction stir processed copper: A review. *Int. Res. J. Sustain. Sci. Eng.* 2015, 3, 1–11.
- Johnson, R.; Threadgill, P.L. Friction stir welding of magnesium alloys, *Essential readings in magnesium technology.* 2003, 487-492.
- Kah, R.; Tajan, R.; Matrikainen, J.; Suoranta, R. Investigation of weld defects in friction-stir welding and fusion welding of aluminium alloys. *Int. J. Mech. Mater. Eng.* 2015, 10, 26.
- Kaur, M.; Singh, T.; Singh, K. Comparison between Friction stir welding & Fusion welding of Aluminium Alloys based on mechanical properties & microstructure: A Review. *Special Issue in IJRAET*, 2016, 4/2, 1-4.
- Khodaverdizadeh, H.; Heidarzadeh, A.; Saeid, T. Effect of tool pin profile on microstructure and mechanical properties of friction stir welded pure copper joints. *Materials & Design*, 2013, 45, 265-270.
- Klaasen, H.; Kübarsepp, J.; Roosaar, T.; Viljus, M.; Traksmaa, R. Adhesive wear performance of hardmetals and cermets. *Wear* 2010, 268, 1122-1128.
- Klaasen, H.; Kübarsepp, J. Wear of advanced cemented carbides for metalforming tool materials. *Wear*, 2004, 256, 846-853.
- Klingensmith, S.; DuPont, J.N.; Marder, A.R.; Microstructural characaterization of a double-sided friction stir weld on a superaustenitic stainless steel, *Welding Journal*, 2005, may, 77-85.
- Kolnes, M.; Mere, A.; Kübarsepp, J.; Viljus, M.; Maaten, M.; Tarraste, M. Microstructure evolution of TiC cermets with ferritic AISI 430L steel binder. *Powder Metall.* 2018, 61, 197-209.

- Kumar, A.; Gautam, S.S.; Kumar, A. Heat input & joint efficiency of three welding processes TIG, MIG and FSW using AA6061. *Int. J. Mech. Eng. & Rob. Res.* 2014, 1, 89-94.
- Lakshminarayanan, A.K.; Balasubramanian, V.; An assessment of microstructure, hardness, tensile and impact strength of friction stir welded ferritic stainless steel joints, *Materials and Design*, 2010, 31, 4592-4600.
- Lampman, S.; Zore, T.B. Properties and selection: Nonferrous alloys and special purpose materials. In *ASM Handbook*, 3rd ed.; ASM International: Cleveland, OH, USA, 1993; Volume 2, pp. 428-445.
- Li, H.B.; Jiang, Z.H.; Weng, H.; Zhang, S.C.; Li, L.; Han, P.D.; Misra, R.D.K.; Li, J.Z. Microstructure, Mechanical and corrosion properties of friction stir welded high nitrogen nickel-free austenitic stainless steel, *Materials and Design*. 2015, 84, 291-299.
- Liu, F.C.; Hovanski, Y.; Miles, M.P.; Sorensen, C.D.; Nelson, T.W. A review of friction stir welding steels: tool, material flow, microstructure, and properties, *Journal of Materials Science & Technology*, 2018, 34, 39-57.
- Liu, H.J.; Feng, J.C.; Fujii, H.; Nogi, K. Wear characteristics of a WC-Co tool in friction stir welding of AC4AC30 vol%SiCp composite. *International Journal of Machine Tools & Manufacture*. 2005, 45, 1635-1639.
- Liu, H.J.; Feng, J.C.; Fujii, H.; Nogi, K. Wear characteristics of a WC-Co tool in friction stir welding of AC4A + 30 vol% SiCp composite. *Int. J. Mach. Tool Manu.* 2005, 45, 1635-1639.
- Lohwasser, D.; Chen, Z. Friction stir welding: From basics to applications. Woodhead Publishing Limited and CRC Press LLC, Padstow, Cornwall, UK, 2010.
- Lou, D.; Hellman, J.; Luhulima, D.; Liimatainen, J.; Lindroos, V.K. Interactions between tungsten carbide (WC) particulates and metal matrix in WC-reinforced composites. *Mater. Sci. Eng. A*. 2003, 340, 155-162.
- Mall, P.P.; Panchal, J. Friction Stir Welding Process & Parameters: A Review, *Int. j. adv. res. technol.* 2017, 06/06, 15-18.
- Mari, D. Mechanical Behavior of Hardmetals at High Temperature, in: Sarin, V.K.; Mari, D.; Llanes, L. (Eds.), *Comprehensive Hard Materials*, Elsevier Ltd., Oxford, 2014.
- Meilinger, A.; Török, I. The importance of friction stir welding tool. *Production processes and Systems*, 2013, 6/1, 25-34.
- Meran, C.; Canyurt, O.E. Friction Stir Welding of austenitic stainless steels, *Journal of Achievements in Materials and Manufacturing Engineering*, 2010, 43, 432-439.
- Mishra, R.; De, P.S.; Kumar, N. Friction Stir Welding and Processing; Springer International Publishing: Berlin/Heidelberg, Germany, 2014.
- Miličić, M.; Gladović, P.; Bojanić, R.; Savković, T.; Stojić, N. Friction stir welding (FSW) process of copper alloys. *Metalurgija*, 2016, 55/1, 107-110.
- Miyazawa, T.; Iwamoto, T.; Maruko, T.; Fujii, H. Development of Ir based tool for friction stir welding of high temperature materials, *Science and Technology of Welding & Joining*, 2011, 16/2, 188-192.
- Miyazawa, T.; Iwamoto, Y.; Maruko, T.; Fujii, H. Development of high strength Ir based alloy tool for friction stir welding, *Science and Technology of Welding and Joining*, 2012, 17/3, 213-218.
- Miyazawa, T.; Iwamoto, Y.; Maruko, T.; Fujii, H. Friction stir welding stainless of 304 steel using Ir based alloy tool, *Science and Technology of Welding and Joining*, 2012, 17/3, 207-212.

- Muneo, M.; Yasushi, K.; Rinsei, I. Applicability of friction stir welding (FSW) to steels and properties of the welds, JFE Technical Report, 2015, 20, 133-140.
- Murr, L. E.; Liu, G.; McClure, C. A TEM study of precipitation and related microstructures in friction-stir-welded 6061 aluminium, Journal of Material Science, 1998, 33, 1243-1251.
- Nabhani, F. Wear mechanisms of ultra-hard cutting tools materials. J. Mater. Process. Technol. 2001, 115, 402-412.
- Nakata, K. Friction stir welding of copper and copper alloys. Weld. Int. 2005, 19:12, 929-933.
- Olson, D.L.; Siewert, T.A.; Liu, S.; Edwards, G.R. Welding, brazing and soldering. In ASM Handbook; ASM International: Cleveland, OH, USA, 1993; Volume 6.
- Padro, R.A.; Murr, L.E.; Shindo, D.J.; Soto, K.F. Tool wear in the friction stir welding of aluminium alloy 6061+20% Al₂O₃: a preliminary study. Scripta Materialia, 2001, 45, 75-80.
- Park, H.S.; Lee, B.W.; Murakami, T.; Nakata, K.; Ushio, M.; Friction stir welding of oxygen free copper and 60%Cu-40%Zn copper alloy. Materials Science Forum, 2008, 580-582, 447-450.
- Park, S.H.C.; Sato, Y.S.; Kokawa, H.; Okamoto, K.; Hirano, S.; Inagaki, M.; Boride formation induced pcBN tool wear in friction-stir-welded stainless steel, Metallurgical and Materials Transactions, 2009, 40A, 625-635.
- Park, S.H.; Sato, Y.S.; Kokawa, H.; Okamoto, K.; Hirano, S.; Inagaki, M. Microstructural characterization of stir zone containing residual ferrite in friction stir welded 304 austenitic stainless steel, Science and Technology of Welding and Joining. 2005, 10/5, 550-556.
- Prado, R.A.; Murr, L.E.; Soto, K.F.; McClure J.C. Self-optimization in tool wear for friction-stir welding of Al 6061+20% Al₂O₃ MMC. Materials Science and Engineering. 2003, A349, 156-165.
- Prasanna, P.; Rao, B.S.; Rao, G.K.M. Finite element modeling for maximum temperature in friction stir welding and its validation. Int. J. Adv. Manuf. Technol. 2010, 51, 925-933.
- Properties and selection: Nonferrous alloys and special purpose materials. In ASM Handbook, 3rd ed.; ASM International: Cleveland, OH, USA, 1993; Volume 2, pp. 428-445.
- Rai, R.; De, A.; Bhadeshia, H.K.D.H.; DebRoy, T. Review: Friction stir welding tools. Sci. Technol. Weld. Join. 2011, 16, 325-342.
- REACH (Registration, Evaluation, Authorization and Restriction of Chemical Substances). Available online: http://ec.europa.eu/environment/chemicals/reach/reach_intro.htm (29.03.2020).
- Recktenwald, G. Conversion of thermocouple voltage to temperature, Apostila, Portland 2010.
- Reynolds, A.P.; Tang, W.; Posada, M.; Deloach, J. Friction stir welding of DH36 steel, Science and Technology of Welding and Joining. 2003, 8/6, 455-460.
- Sahlot, P.; Jha, K.; Dey, G.K.; Arora, A. Quantitative wear analysis of H13 steel tool during friction stir welding of Cu-0.8%Cr-0.1%Zr alloy. Wear, 2017, 378-379, 82-89.
- Sahlot, P.; Mishra, R.S.; Arora, A. Wear mechanism for H13 steel tool during friction stir welding of CuCrZr alloy. Int. J. Min. Met. Mater. 2019, 59-64.

- Santos, M.C., Jr.; Araujo Filho, J.S.; Barrozo, M.A.S.; Jackson, M.J.; Macchado, A.R. Development and application of temperature measurement device using the tool-workpiece thermocouple method in turning at high cutting speeds. *Int. J. Adv. Manuf. Tech.* 2017, 89, 2287-2298.
- Santos, T.F.A.; Lopez, E.A.T.; da Fonseca, E.B.; Ramirez, A.J. Friction stir welding of duplex and superduplex stainless steels and some aspects of microstructural characterization and mechanical performance, *Materials Research* 2016, 19/1, 117-131.
- Sato, Y.S.; Muraguchi, M.; Kokawa, H. Tool Wear and Reactions in 304 Stainless Steel during Friction Stir Welding, *Materials Science Forum*, 2011, 675-677, 731-734.
- Sato, Y.S.; Nelson, T.W.; Sterling, C.J.; Steel, R.J.; Pettersson, C.O. Microstructure and mechanical properties of friction stir welded SAF 2507 super duplex stainless steel, *Materials Science and Engineering* 2005, A397, 376-384.
- Sato, Y.S.; Harayama, N.; Kokawa, H.; Inoue, H.; Tadokoro, Y.; Tsuge, S. Evaluation of microstructure and properties in friction stir welded superaustenitic stainless steel, *Science and Technology of Welding and Joining* 2009, 14/3, 202-209.
- Savolainen, K.; Mononen, J.; Saukkonen, T.; Hänninen, H.; Koivula, J. Friction stir weldability of copper alloys. 5th International Friction Stir Welding Conference, September 14-16 (2004), Metz, France.
- Schneider, J. A. Temperature distribution and resulting metal flow, *Friction stir welding and processing*, ASM International, 2007, 37-49.
- Shen, J.J.; Liu, H.J.; Cui, F. Effect of welding speed on microstructure and mechanical properties of friction stir welded copper. *Materials & Design*, 2010, 31, 3937-3942.
- Siddiquee, A.N.; Pandey, S.; Khan, N.Z. Friction stir welding of austenitic stainless steel: a study on microstructure and effect of parameters on tensile strength, *Materials Today: Proceedings*, 2015, 2, 1388-1397.
- Siddiquee, A.N.; Sunil Pandey, S. Experimental investigation on deformation and wear of WC tool during friction stir welding (FSW) of stainless steel, *Int. J. Adv. Manuf. Technol.* 2014, 73, 479-486.
- Sun, Y.F.; Fujii, H. Investigation of the welding parameter dependent microstructure and mechanical properties of friction stir welded pure copper. *Mater. Sci. Eng. A*, 2010, 527, 6879-6886.
- Strand, S. Joining plastics-can friction stir welding compete. In *Proceedings of the Electrical Insulation Conference and Electrical Manufacturing and Coil Winding Technology Conference*, Indianapolis, IN, USA, 25-25 September 2003; pp. 321-326.
- Tang, W.; Guo, X.; McClure, J. C.; Murr, L. E. Heat Input and Temperature Distribution in Friction Stir Welding, *Journal of Materials Processing and Manufacturing Science*, 1998, 7, 163-172.
- Tarasov, S. Yu.; Rubtsov, V.E.; Kolubaev, E.A. A proposed diffusion-controlled wear mechanism of alloy steel friction stir welding (FSW) tools used on an aluminium alloy, *Wear* 2014, 318, 130-134.
- Tarasov, S. Yu.; Rubtsov, V. E.; Kolubaev, E.A. The effect of friction stir welding tool wear on the weld quality of aluminium alloy AMg5M, *AIP Conf. Proc.* 2014, 1623, 635-638.
- Thomas, W.M.; Nicholas, E.D.; Needham, J.C.; Murch, M.G.; Temple-Smith, P.; Dawes, C.J.G.B. Patent 9,125,978.8, Friction welding, 06.12.1991.

- Thompson, B.; Babu, S.S.; Lolla, T. Application of diffusion models to predict FSW tool wear. In Proceedings of the Twenty-first International Offshore and Polar Engineering Conference, Maui, HI, USA, 19–24 June 2011; pp. 520-526.
- Thompson, B.; Babu, S.S. Tool Degradation Characterization in the Friction Stir Welding of Hard Metals, *Welding journal*, 2010, 89, 256-261.
- Threadgill, P.L.; Leonard, A.J.; Shercliff, H.R.; Withers, P.J. Friction stir welding of aluminium alloys. *Int. Mater. Rev.* 2009, 54, 49-93.
- Uejii, R.; Fujii, H.; Cui, L.; Nishioka, A.; Kunshige, K.; Nogi, K. Friction stir welding of ultrafine grained plain low-carbon steel formed by martensite process, *Materials Science and Engineering*, 2006, A 423, 324-330.
- Welding Handbook. Vol. 5 Materials and Applications. (9th edition) Miami, American Welding Society, 2015, 255-226.
- Wieckowski, W.; Wiczorek, P.; Lacki, J. Investigation of anti-wear coatings in terms of their applicability to tools in the FSW process. Proceedings of XIX International Scientific Conference, 2019, 135, 177-182.
- Zhang, Y.N.; Cao, X.; Larose, S.; Wanjara, P. Review of tools for friction stir welding and processing, *Canadian Metallurgical Quarterly*. 2012, 51, 250-260.
- Yi, D.; Onuma, T.; Mironov, S.; Sato, Y.S. Evaluation of heat input during friction stir welding of aluminium alloys. *Science and Technology of Welding and Joining*, 2016, 22/1, 41-46.

Acknowledgements

First, I would like to thank my supervisor prof. Jakob Kübarsepp, co-supervisor prof. Fjodor Sergejev for providing excellent working conditions and continuous support throughout my studies.

I would like to thank co-authors of the papers related to the thesis and colleagues in the Department of Mechanical and Industrial Engineering for their support, especially Märt Kolnes, Marek Tarraste for numerous scientific discussions. Also, I would like to thank Mart Viljus and Rainer Traksmäa for materials characterization.

Finally, my sincere thanks are due to my family for support and encouragement.

The study was supported by the following projects:

- IUT 19-29 – Multi-scale structured ceramic-based composites for extreme applications (Estonian Research Council, 2014-2019)
- PRG665 – Composites “ceramics-Fe alloy” for a wide range of application conditions (Estonian Research Council, 2020)

This work has been partially supported by ASTRA “TUT Institutional Development Programme for 2016-2022” Graduate School of Functional Materials and Technologies (2014-2020.4.01.16-0032).

Abstract

Performance of ceramic-metal composites as tool materials for friction stir welding

Arc welding and oxyfuel gas welding were among the first industrial joining processes developed late in the 19th century. Resistance welding followed soon after. Demand for reliable and inexpensive joining methods for metal alloys used widely in industrial scale impelled advancement of welding technology during 20th century.

A comparatively new solid state welding process – friction stir welding (FSW) – was invented less than 30 years ago (in 1991) at the Welding Institute of the United Kingdom, initially applied to aluminium alloys. Today it is possible to weld a wide range of metals including titanium alloys, stainless steel, copper alloys etc.

FSW as the solid-state welding technique uses a special non-consumable rotating tool to join materials without melting them. Due to solid-state nature, FSW leads to several advantages over fusion welding processes, such as ability to join materials that are difficult to fusion weld (in particular, alloys of Al, Mg, Cu and stainless steel), low distortion and shrinkage, excellent mechanical properties of welds etc. In addition, FSW is a green joining technology due to energy efficiency and low environmental impact.

The welding tool geometry and its material are critical for the successful use of the process. The tool material to be used depends on the workpiece material and the desired tool life. Literature overview shows that studies on the FSW tool materials development, selection and wear mechanism are scarce. According to the author's knowledge, no comparative studies have been conducted for revealing the performance and degradation mechanisms of ceramic-metal composites as potential tool materials for the FSW of different metals. Therefore, the **motivation** of the present study was to develop, select and apply reliable, durable and cost-effective tool materials for the FSW of metals with a wide range of melting temperatures. Ceramic-metal composites, in particular WC-based hardmetals and TiC-based cermets possessing a good combination of hardness, wear resistance, strength and toughness at ambient and elevated temperatures, can be considered as significant FSW tool material candidates. Following the necessity to develop advanced tool materials for the FSW of metals that are difficult to fusion weld, the author of the thesis posed the following **hypothesis**: *Ceramic-metal composites, in particular WC-based hardmetals and TiC-based cermets, have potential to perform as reliable and cost-effective tool materials for the FSW of metals with different composition, solid-state welding temperature, structure and mechanical characteristics.*

The **objectives** of the present research were: (1) development and application of the model testing methodology for assessment of tools degradation (wear) during the working of low- and high-melting point metals at the regular FSW temperatures; (2) a comparative study of ceramic-metal composites as potential tool materials for the FSW of metals with substantially different welding temperatures; (3) improving understanding of the effect of composition and characteristics of tool and workpiece materials on the degradation rate and mechanism during the model wear tests and FSW feasibility studies; (4) production of tool prototypes for conducting FSW feasibility studies.

The test specimens and FSW tool prototypes from the TiC-based cermets bonded with Ni- and Fe alloys and WC-based WC-Co hardmetals were produced using the conventional powder metallurgy approach: mechanical milling of initial carbide and metal powders, uniaxial pressing and liquid-phase vacuum sintering. Aluminium alloy,

copper and austenitic stainless steel were used as workpiece materials both during the model (cutting) tests and FSW feasibility studies. The reaction-diffusion of the tool and workpiece material elements is one of the important reasons of FSW tool degradation. Special diffusion test samples were prepared for selected tool and workpiece material groups to study the diffusion-controlled processes in the tool-workpiece contact zone. Distribution of chemical elements in the tool-workpiece contact regions was performed using X-ray spectroscopy (EDS). A vertical milling machine was used to perform the feasibility study of ceramic-metal tools behavior during the FSW of workpiece materials under investigation.

The main **outcomes** of the present research were as follows.

1. The model testing methodology for assessment of tools degradations during working at regular FSW temperatures was developed and applied.
2. A comparative study for revealing the performance of ceramic-metal composites for the FSW of metals with different melting and working temperatures was performed. It was shown that: (1) TiC-based cermets have the highest performance during the working of aluminium alloy. (2) WC-Co hardmetals outperform TiC-based cermets during the working of workpiece from copper. (3) TiC-NiMo cermets demonstrate the highest performance in the model tests using counterpart from austenitic stainless steel.
3. Study of the effect of composition and characteristics of ceramic-metal composites and workpiece materials on the tool degradation mechanism has shown that irrespective of workpiece metal, the most common degradation (wear) mechanisms in the model wear tests and during FSW feasibility studies are adhesion and diffusion.
4. Prototypes of FSW tools from the ceramic-metal composites were prepared and FSW feasibility studies in laboratory and industrial environments were performed. The possibility to produce macroscopically defect-free welds from aluminium alloy, copper and stainless steel was proved.

Lühikokkuvõte

Keraamilis-metalsed komposiidid otshõõrdkeevituse tööriistamaterjalidena

Esimesed 19. sajandi lõpus tööstuslikeks rakendusteks väljatöötatud metallide liitmisprotsessid olid elektrikaarkeevitus ja gaaskeevitus. Jätkuv vajadus laia tööstusliku rakendatavusega, usaldusväärsete ja hinnalt mõistlike liitmistehnoloogiate järele tõukas tagant arendusi keevitustehnoloogiate valdkonnas läbi kogu 20. sajandi.

Tööstusliku rakenduse aspektist suhteliselt uus tardfaaskeevitusprotsess – otshõõrdkeevitus – leiutati vähem kui 30 aastat tagasi (1991) Ühendkuningriigi Keevitusinstituudis (Welding Institute of the United Kingdom). Uudset keevitustehnoloogiat rakendati esmaselt alumiiniumisulamitest toorikute liitmiseks. Tänapäeval on tõestatud võimalikkust kasutada seda liitmetehnoloogiat paljud metallide sh. titaanisulamite, roostevaba terase, vasesulamite jne. keevitamiseks.

Otshõõrdkeevitus kui tardfaaskeevituse puhul kasutatakse spetsiaalset pöörlevat ja korduskasutatavat (sulamatut) tööriista materjalide liitmiseks hõõrdumisel eralduva soojuse toimet neid sulatamata. Tänu tardfaaskeevitusprotsesside tehnilistele iseärasustele on otshõõrdkeevitusel sulafaaskeevitusega võrreldes rida eeliseid: võimalus keevitada sulakeevitusmeetodiga raskelt liidetavaid metalle (sh. Al-, Mg-, Cu-sulamid, roostevaba teras), väike keevitusdeformatsioonide oht, keevisõmbluse suurepärase kvaliteet (struktuur, mehaanilised omadused) jne. Otshõõrdkeevitus on “roheline” liitmetehnoloogia tänu energiatõhususele ja väikesele keskkonnamõjule.

Tööriista geomeetria ja materjal on otshõõrdkeevitusprotsessi kriitilisteks aspektideks. Tööriistamaterjalide valik sõltub töödeldavast/keevitatavast materjalist ning soovitatavast tööriista püsivusajast. Kirjanduse ülevaade võimaldab järeldada, et uuringuid, mis käsitlevad tööriistamaterjalide arendust, valikut ja kulumist on piiratud. Käesoleva töö autori seisukohast puuduvad uuringud, millistes käsitletakse keraamilis-metalsed komposiidide kui potentsiaalsete tööriistamaterjalide püsivust ja kulumismehhanismi erinevate metallide otshõõrdkeevitamisel. Selletõttu käesoleva uurimistöo peamiseks **motivatsiooniks** oli vajadus arendada, valida ja rakendada usaldusväärseid, suure püsivusega ja majanduslikult tasuvaid tööriistamaterjale sulamistemperatuuri laia vahemikuga metallide otshõõrdkeevituseks. Keraamilis-metalsed komposiidid, sh. WC-baasil kõvasulamid ja TiC-baasil kermised, milliseid iseloomustab hea kõvaduse, kulumiskindluse, tugevuse ja sitkuse kombinatsioon normaal- ja kõrgendatud temperatuuridel, omavad head potentsiaali tööriistamaterjalidena otshõõrdkeevitamisel. Tulenevalt vajadusest arendada kaasaegseid tööriistamaterjale sulakeevitusega raskelt (probleemselt) keevitatavate metallide otshõõrdkeevitamiseks käesoleva doktoritöö autori **hüpotees** on: *“Keraamilis-metalsedel komposiididel – WC-baasil kõvasulamid ja TiC-baasil kermised – on potentsiaal olla usaldusväärseteks ja majanduslikult tasuvateks tööriistamaterjalideks erineva koostise, tardfaaskeevituse temperatuuri, struktuuri ja mehaaniliste omadustega metallide otshõõrdkeevituseks.”*

Käesoleva uurimistöo **eesmärgid** olid: (1) mudelkatsete metoodika arendamine võimaldamaks hinnata tööriistade kulumist madala ja kõrge sulamistemperatuuriga metallide töötlemisel tavapärasel otshõõrdkeevitamise temperatuuridel; (2) keraamilis-metalsed komposiidide kui potentsiaalsete otshõõrdkeevituse tööriistamaterjalide toimivuse (kulumise) uurimine erineva keevitustemperatuuriga metallide (Al-sulam, vask ja roostevaba teras) töötlemisel mudelkatsetmetoodikat rakendades; (3) arusaama parandamine seosest keraamilis-metalsed komposiidide (kõvasulamid, kermised) ning

töödeldavate materjalide (Al-sulam, vask, roostevaba teras) koostise ja omaduste ning tööriista kulumise (purunemise) intensiivsuse ja mehhanismi vahel mudelkatsetes ja tööriista prototüüpidega otshõõrdkeevitamisel; (4) tööriista prototüüpide valmistamine otshõõrdkeevitamiseks ning nendega teostatavusekatsete läbiviimine laboratoorsetes (vask ja roostevaba teras) ja tööstuslikes (Al-sulam) tingimustes.

Proovikehad (mudelkatseteks, mehaaniliste omaduste määramiseks) ja tööriista prototüübid otshõõrdkeevituseks TiC-baasil (Ni- ja Fe-sulamist metallsideainega) kermistest ja WC-Co kõvasulamitest valmistati pulbermetallurgilist tehnoloogiat kasutades: lähtepulbrite (karbiidid, metallid) mehaaniline jahvatus, pulbritest proovikehade ja tooteprototüüpide pressimine ning vedelfaaspaagutus vaakumis. Alumiiniumi sulamit, tehniliselt puhast vaske ja austeniitset roostevaba terast kasutati töödeldava materjalina nii mudelkatsetes kui ka otshõõrdkeevitamisel. Tööriista ja töödeldava materjali elementide vastastikune difusioon on üks oluline otshõõrdkeevituse tööriistade kulumise põhjuseid. Difusiooniprotsesside uurimiseks kontaktpindadel tööriist-toorik otshõõrdkeevituse temperatuuridel valmistati valikuliselt spetsiaalsed proovikehad. Keemiliste elementide ümberjaotust kontaktsoonis tööriist-toorik uuriti kasutades röntgenspektroskoopiat (EDS). Otshõõrdkeevituse teostatvusuuringutes keraamilis-metalletest tööriistamaterjalidest tööriistaprototüüpe kasutades kasutati vertikaalfreespinkki.

Uurimustöö peamised **tulemused** on alljärgnevad:

1. Arendati ja rakendati mudelkatsete meetodikat hindamaks tööriistade kulumist erineva otshõõrdkeevituse temperatuuriga metallide töötlemisel.
2. Viidi läbi erineva koostise ja struktuuriga keraamilis-metalletest komposiididest tööriistade püsivuse (kulumise) uuringud erineva sulamis- ja töötlustemperatuuriga metallide töötlemisel. Uurimustöö võimaldab teha alljärgnevad järeldused: (1) TiC-baasil kermised demonstreerivad parimat kulumiskindlust Al-sulami töötlemisel; (2) WC-baasil kõvasulamid näitasid oma eelseid TiC-baasil kermiste ees vase töötlemisel; (3) TiC-NiMo kermiste kulumiskindlus ületas teiste tööriistamaterjalide oma mudelkatsetes roostevaba terasega.
3. Uuringud seostest keraamilis-metalletest komposiidide (kõvasulamid, kermised) ning töödeldavate materjalide (Al-sulam, vask, roostevaba teras) koostise ja omaduste ning tööriistade kulumise (purunemise) intensiivsuse ja mehhanismi vahel näitasid, et töödeldava materjali koostisest sõltumatult on peamisteks kulumise mehhanismideks nii mudelkatsetes kui otshõõrdkeevitusel adhesioon ja difusioon.
4. Valmistati keraamilis-metalletest komposiididest tööriistaprototüüpe ja viidi läbi esialgsed otshõõrdkeevituse teostatavusuuringud. Uuringud demonstreerisid makroskoopiliselt defektivabade keevisõmbluste valmistamise võimalust Al-sulami, vase ja roostevaba terase otshõõrdkeevitamisel.

Appendix

Publication I

Kolnes, M., Kübarsepp, J., Sergejev, F., Kolnes, M. Comparative study of adhesive wear for CoCr, TiC-NiMo, WC-Co as potential FSW tool materials. In: R. Bendikienė, K. Juzėnas (Ed.). *Materials Engineering 2017 (224–228)*.10.10.2017 Trans Tech Publications Ltd. (Solid State Phenomena; 267), 2017.

Comparative Study of Adhesive Wear for CoCr, TiC-NiMo, WC-Co as Potential FSW Tool Materials

Mart Kolnes^a, Jakob Kübarsepp^b, Fjodor Sergejev^c and Märt Kolnes^{d*}

Department of Mechanical and Industrial Engineering, Tallinn University of Technology,
Ehitajate tee 5, 19086 Tallinn, Estonia

^amart.kolnes@ttu.ee, ^bjakob.kubarsepp@ttu.ee, ^cfjodor.sergejev@ttu.ee, ^dmart.kolnes1@ttu.ee

Keywords: friction stir welding; cermet; hardmetal; adhesive wear.

Abstract. Friction stir welding (FSW) is a novel promising joining process. In FSW, most common tool failure occurs because of transformation of geometry caused by wear. We qualify it as adhesive wear. Lathe testing of adhesion wear was conducted to compare wear resistance of the following materials: Co-25wt%Cr, TiC-25wt.%Ni/Mo and WC-15wt%Co. According to their characteristics, materials are prospective alternative tool materials for conventional frictional stir welding used in FSW of aluminium alloys. Adhesive wear tests were performed by turning aluminium alloy AW6082-T6 at low speed; travel length, turning speed and feed rate were selected to simulate FSW conditions. The adhesive wear was determined as the change of the geometry of the cutting edges of the tool measured using SEM images. In terms of adhesive wear resistance, WC-Co hardmetal is the most promising tool material. Two main stages of wear were distinguished: first, the appearance of intensive adhesion wear, followed by steady state wear. Adhesive wear is complemented by surface fatigue wear.

Introduction

Friction stir welding is a solid-state joining process that uses a non-consumable tool to join samples without melting the materials. For aluminium alloys, the temperature range of FSW is between 425 and 500 °C [1]. Heat is generated by friction between the rotating tool and the workpiece material [2]. Tool steels are the most widely used tool material for aluminium alloys. For FSW of high strength materials, the welding tools are usually made of hard metals and carbide based composites, such as WC-Co hardmetals, TiC based cermets and cubic boron nitrides. To ensure high quality of the weld, the FSW tool may not change its geometry considerably during the whole welding process. The failure of the welding tool is caused mainly by adhesive and abrasive wear [3].

Klaasen et al. have investigated adhesive wear of cemented carbides and cermets using a special lathe cutting method by turning mild steel at low speed [4]. Cemented carbides are composite materials known for their excellent wear resistance coupled with a good combination of mechanical characteristics [5]. Tungsten carbide based hardmetals are most widely used in wear conditions, e.g. metal cutting or forming tools [6]. Titanium carbide based cermets are also commonly used in high temperature applications [7].

Cobalt-chromium alloys can be generally described as alloys characterized by high strength and heat-resistance. They are non-magnetic, and have favourable resistance to wear, corrosion, tarnish. In addition, these alloys are easily 3-D printable. Heat treatment of CoCr increases the hardness of the alloys remarkably [8].

This paper is focused on the assessment of the wear behaviour of some materials promising for FSW of aluminium alloys using the method of lathe turning testing. Wear performance is related to the mechanical properties and microstructure of materials.

Experimental Details

For adhesive wear testing, the following materials were used: ceramic-metal composites WC-Co, TiC-NiMo and alloy CoCr. Chemical compositions of the materials are presented in Table 1 and microstructures carbide composites are shown in Fig. 1.

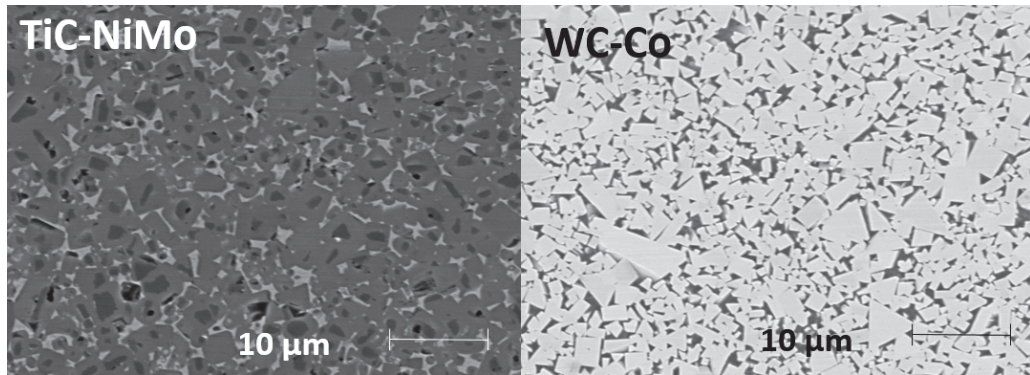


Fig. 1. SEM micrographs of the carbide composites studied

Material selection was performed as follows. As the first approximation, we chose the hardmetal WC- 6wt% Co because of its high hardness and good wear resistance. During the lathe test the cleavage fractures occurred due to fragility of that material. The test pieces were shattered during the lathe turning test. A new material WC- 15wt.% Co with higher Co content, lower hardness but higher fracture toughness was selected. Secondly, TiC-NiMo(NiMo = 2:1) with approximately the same carbide content (vol.%) as WC-15wt.%Co was chosen, considering that most of the Mo dissolves in TiC during sintering. We chose the TiC-25wt.%Ni/Mo cermet as an alternative carbide composite. The CoCr alloy material of composition Co-25wt.% Cr was chosen because it is used in industry.

Hardmetals and cermets were produced using the conventional powder metallurgical method. Composites were ball milled and vacuum sintered. CoCr samples were metal printed using a selective laser sintering technology followed by heat treatment in vacuum at temperature of 850 °C during 10 min, followed by natural cooling in furnace.

Table 1. Composition of the investigated FSW tool materials

Designation	Carbide content [vol.%]	Carbide content	Ni	Mo	Co	Cr	W
WC-Co	76.4	85	–	–	15	–	–
TiC-NiMo	89.9	75	16.7	8.3	–	–	–
CoCr	–	–	–	3.5	62	25	9.5

Adhesive wear tests were performed using a special cutting method [4], by turning aluminium AW6082-T6 at low speed. Nose angle, side cutting-edge angle and side relief angle of the turning tool were 46°, 67° and 8°, respectively. The chemical composition and mechanical properties of the AW6082-T6 alloy are shown in Table 2.

Table 2. Mechanical properties and chemical composition of counterpart (AW6082-T6 alloy)

Mechanical Properties									
Tensile strength [MPa]		Yield strength (0.2% offset) [MPa]			Elongation [%]		Hardness [HB]		
391		365			11.5		116		
Chemical composition [%]									
Al	Si	Fe	Cu	Mn	Mg	Cr	Zn	Ti	Other
96.94	1.1	0.27	0.04	0.5	0.8	0.1	0.05	0.05	0.15

Lathe wear test conditions and specimen geometry are shown in Fig. 2. Three specimens were prepared from each material. The side cutting edge angle is the same as the end cutting edge angle, at 23 degrees; the side relief angle is the same as the end relief angle, at 8 degrees. The cutting speed used in the experiments was 16 – 19 m/s. The total cutting distance on each specimen was 4400 m (4 h cutting time). The feed rate at 0.39 mm/rev and the depth of cut at 0.25 mm were constant.

The adhesion wear rate was determined as the shortening in the length of the cutting nose tip of the specimen. Changes in the geometry of the specimens were measured using the images of Hitachi TM 1000 Tabletop scanning electron microscope. Measurements were performed at certain distances (1100, 2200 and 4400 meters) and before each measurement the specimen was cauterized using the sodium hydroxide solution (NaOH 20 wt.%). Cutting distances were chosen depending on the number of passes.

Indentation fracture toughness and hardness were determined using the ground and polished specimens of 5 x 5 x 17 mm. Hardness measurements (Vickers hardness) were carried out in accordance with the standard EN-ISO-6507 using an Indentec 5030 hardness tester. The fracture toughness (K_{IC} , $\text{MPa}\cdot\text{m}^{1/2}$) was determined using the method of fracture by Vickers indentation with the most commonly used empirical equations for fragile materials proposed by Evans [9].

Results and Discussions

Klaasen et al. have investigated adhesive wear of cemented carbides and cermets using a special lathe cutting method by turning mild steel at low speed [4]. These carbide composites demonstrated acceptable adhesive wear resistance and therefore were selected as promising tool materials for FSW.

Table 3. Mechanical properties and shortening of the cutting nose tip of the specimen at different cutting distances

Designation	Hardness [HV30]	Fracture toughness [$\text{MPa}\cdot\text{m}^{1/2}$]	Shortening of the cutting nose tip of the specimen [μm]		
			1100 [m]	2200 [m]	4400 [m]
WC-Co	1183 ± 22	17.76 ± 0.4	1.1 ± 0.6	3.2 ± 2.1	5.5 ± 0.8
TiC-NiMo	1378 ± 25	5.35 ± 0.5	11.4 ± 2.6	16.4 ± 1.0	18.7 ± 2.4
CoCr	582 ± 7	-	238.3 ± 35.0	247.0 ± 29.8	254.0 ± 26.2

Table 3 demonstrates the mechanical properties of the tool materials and shortening of the length of the cutting nose tip at different cutting distances. The hardness of CoCr alloy was 2.3 times lower than TiC-NiMo and 2 times lower than WC-Co. Fracture toughness of CoCr samples is not available, because indentation marks have no cracks in the corners due to high plasticity of the alloy. The wear rate of specimens from the CoCr alloy was more than ten times higher than TiC-NiMo and more than forty times higher than WC-Co in equivalent cutting distance (see Fig. 3, right). Carbide composites showed significantly higher wear resistance than those of the CoCr alloy. One WC-Co hardmetal tool shortening in different cutting distances is shown in Fig. 3 (left). After 1100 m all tested materials reached the steady state wear conditions.

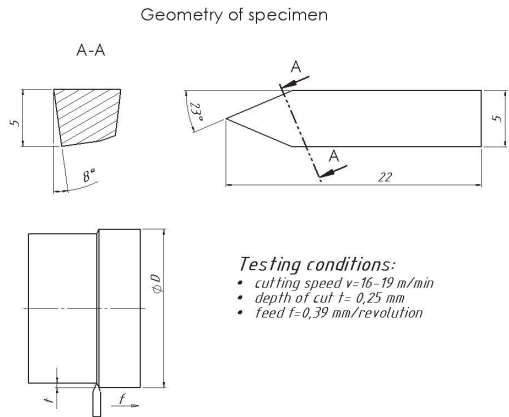


Fig. 2. The adhesive wear testing conditions and geometry of specimen

Material wear resistance is commonly evaluated by hardness. Our study also shows the importance of fracture toughness and sensitivity to fatigue. As WC-Co demonstrates excellent hardness and the wear rates of this carbide composite are markedly lower than those of TiC-NiMo cermet.

According to Wang, in the case of WC-Co hardmetals, the ductile binder phase in the worn areas of the specimens is substantially decreased during machining of commercially pure aluminium with a WC-Co tool [10]. This indicates that the Co binder phase on the specimen surface wears down during turning (see Fig. 4, left). The decrease of the binder phase simplifies the removal of the carbide grains. Similar wear schemes have been observed at static and cyclic loading of cemented carbides and cermets [11].

Wear of CoCr was analysed only for comparison; therefore, wear mechanism of this material was not studied.

The Fig. 4 (left) shows that in the WC-Co cemented carbide, the WC grains are not simply removed from the surface, but are crushed to smaller pieces, and then removed. Cracks are visible in the larger grains near the tip. The ability of WC grains to absorb fracture energy is related to their higher plasticity compared to TiC grains [12].

Similar mechanism is characteristic of the TiC-NiMo cermets wear during turning against aluminium alloy, as many small dimples can be seen on the surface of the worn-out cutting nose (see Fig. 4, right).

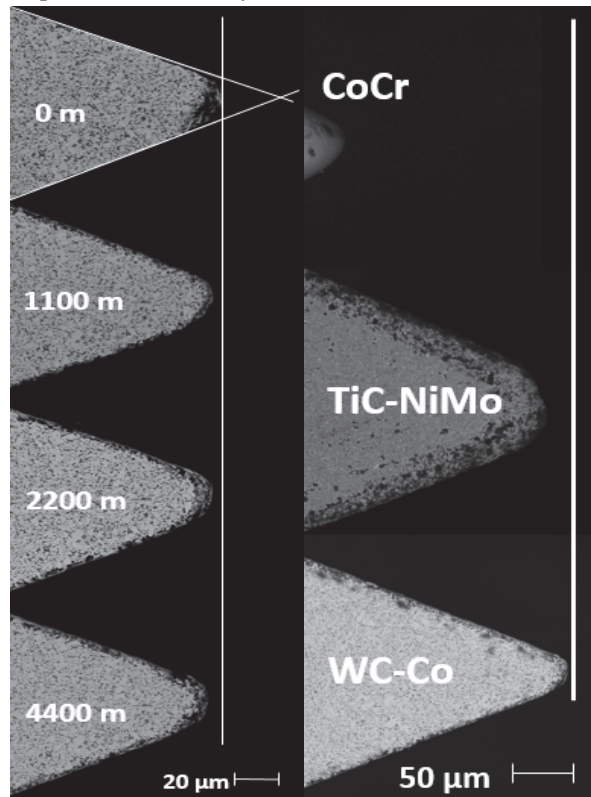


Fig. 3. Wear of WC-Co specimen in different cutting distances (left) and shortening of the length of the cutting nose tip of different materials at 4400 m

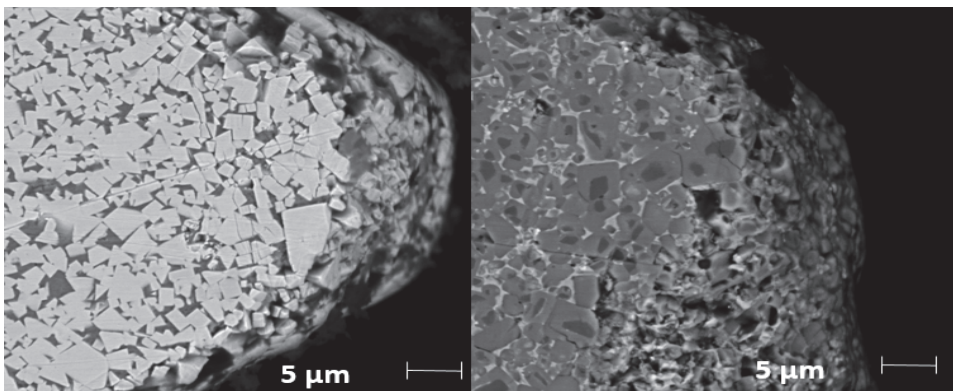


Fig. 4. The worn-out cutting nose tips of WC-Co (left) and TiC-NiMo (right)

Higher resistance to embrittlement during cyclic loading of TiC-based cermets [12] leads to lower fatigue sensitivity of these composites [11, 13]. The same conclusion can be drawn in the

present research – the TiC-based cermet tool is subjected to a lower increase of wear than that with WC based cemented carbide. In steady state wear conditions – the lowest increase in wear during the increase of the cutting distance was demonstrated by the CoCr alloy.

Summary

The following conclusions can be derived from the results of the adhesive wear lathe tests of tools made from carbide composites and the CoCr alloy:

- WC-Co hardmetal compares favourably with TiC-NiMo cermet in adhesive wear conditions. Both carbide composites (hardmetal and cermet) outperform the CoCr alloy in the testing conditions used in the present research.
- SEM study of worn tools made from hardmetal and cermet shows that binder extraction due to adhesion followed by pull-out of carbide particles and their fragments takes place.
- When increasing the cutting distance during adhesive wear testing, TiC-NiMo cermets demonstrate markedly lower increase in wear than WC- Co hardmetal. It can be explained by of lower fatigue sensitivity of TiC-based carbide composites.

Acknowledgment

This work was supported by institutional research funding IUT 19-29 of the Estonian Ministry of Education and Research.

References

- [1] P.L. Threadgill, A.J. Leonard, H.R. Shercliff, P.J. Withers, Friction stir welding of aluminium alloys, *International Materials Reviews*. 54 (2009) 49-93.
- [2] R.S. Mishra, Z.Y. Mab, Friction stir welding and processing, *Materials Science and Engineering*. 50 (2005) 1-78.
- [3] Y.N. Zhang, X. Cao, S. Larose, P. Wanjara, Review of tools for friction stir welding and processing, *Canadian Metallurgical Quarterly*. 51 (2012) 250-260.
- [4] H. Klaasen, J. Kūbarsepp, T. Roosaar, M. Viljus, R. Traksmāa, Adhesive wear performance of hardmetals and cermets, *Wear*. 263 (2010) 1122-1128.
- [5] I. Hussainova, J. Kūbarsepp, J. Pirso, Mechanical properties and features of cermets, *Wear*. 250 (2001) 818-825.
- [6] K.J. Brookes, *World Dictionary and Handbook of Hardmetals and Hard Materials*. London, 1996.
- [7] D. Mari, Mechanical Behavior of Hardmetals at High Temperature, in: V. K. Sarin, D. Mari, L. Llanes (Eds.), *Comprehensive Hard Materials*, Elsevier Ltd., Oxford, 2014.
- [8] Y.S. Al Jabbari, Physico-mechanical properties and prostodontic applications of Co-Cr dental alloys: a review of the literature, *The Journal of Advanced Prosthodontics*. 6 (2014) 138-145.
- [9] A.G. Evans, E.A. Charles, Fracture toughness determinations by indentation, *J. Am. Ceram. Soc.* 59 (1976) 371-372.
- [10] X. Wang, P.Y. Kwon, WC/Co tool wear in dry turning of commercially pure aluminium, *Journal of Manufacturing Science and Engineering*. 136 (2014) 1-7.
- [11] J. Kūbarsepp, H. Klaasen, F. Sergejev, Performance of cemented carbides in cyclic loading wear conditions, *Materials Science Forum*. 534-536 (2007) 1221-1224.
- [12] H. Klaasen, J. Kūbarsepp, A. Tšinjan, F. Sergejev, Performance of carbide composites in cyclic loading wear conditions, *Wear*. 271 (2011) 837-841.
- [13] F. Sergejev, I. Preis, I. Hussainova, J. Kūbarsepp, Fatigue mechanics of TiC-based cemented carbides, *J. Eng. Trib.* 222 (2008) 201-209.

Publication II

Kolnes, M., Kübarsepp, J., Sergejev, F., Kolnes, M. Adhesive wear of WC- and TiC-based friction stir welding tool materials for aluminium alloy welding. *Euro PM2018 proceedings*, 2018, 1-8.

Manuscript refereed by Chairman Name (Company, Country)

Adhesive Wear of WC- and TiC–based friction stir welding tool materials for aluminium alloy welding

Mart Kolnes (Department of Mechanical and Industrial Engineering, Tallinn University of Technology, Ehitajate tee 5, 19086 Tallinn, Estonia) mart.kolnes@ttu.ee; Jakob Kübarsepp (Department of Mechanical and Industrial Engineering, Tallinn University of Technology, Ehitajate tee 5, 19086 Tallinn, Estonia) jakob.kubarsepp@ttu.ee; Fjodor Sergejev (Department of Mechanical and Industrial Engineering, Tallinn University of Technology, Ehitajate tee 5, 19086 Tallinn, Estonia) fjodor.sergejev@ttu.ee; Märt Kolnes (Department of Mechanical and Industrial Engineering, Tallinn University of Technology, Ehitajate tee 5, 19086 Tallinn, Estonia) mart.kolnes1@ttu.ee

Abstract

Focus is on the adhesive wear performance of WC-based cemented carbides and TiC-based cermets bonded with Ni and Fe alloys. Adhesive wear tests were performed by turning aluminium alloy AW6082-T6 at low speed on the lathe. The AISI H13 tool steel, a well-known friction stir welding (FSW) tool material was used as reference material. The short-duration FSW tests were conducted to prove the comparison of mechanical stability of the tool during the initial phase of welding (plunge phase). The tools were prepared using the powder metallurgy technology for ceramic-based composites and selective laser sintering (SLS) for the AISI H13 tool steel. Microscopic investigations showed that the tool surfaces were partly covered with tribological mechanically mixed layer of aluminium alloy. The adhesive wear resistance of WC–Co cemented carbides and TiC-FeCr cermets was found superior over other tested materials.

Introduction

Friction stir welding (FSW) is a relatively new welding technique, which uses a specially designed tool to join materials without melting them; the process temperature does not exceed 0.7 of the melting temperature of aluminium [1]. Sufficient heat is produced by friction between the tool and the workpiece (base metal). Welded material is mixed by the rotation of the FSW tool of special geometry. No filler material is required, as the weld is formed from the base metal. FSW is a joining process successfully used in shipbuilding, aerospace and automotive industries, especially in applications where high strength and excellent quality welds are needed.

Although FSW was initially invented to join aluminium alloys, today a wide variety of materials can be welded by this welding process [2, 3]. Most widely used FSW tool material for aluminium welding is chromium–molybdenum hot worked air hardening tool steel AISI H13 (X40CrMoV5-1) [4] and high-speed steels. However, there is lack of information about using other tool materials for FSW of aluminium alloys.

Studies of the wear mechanisms of tool materials in FSW are scarce; but abrasion, adhesion and diffusion are the wear mechanisms expected [4, 5]. Prevailing wear mechanism depends both on the material to be welded and the tool material. A rationale behind the tool wear in the FSW of aluminium alloys could be strong adhesion of aluminium alloy to a tool and the following reaction diffusion of the tool material into aluminium due to high temperatures developed during welding [5]. Therefore, the higher the resistance to adhesion, the lower should the wear of the tool be. In this context, ceramic-based composites, such as cemented carbides and cermets, could be promising FSW tool materials.

Ceramic-based materials that are commonly used as tools offer superior wear resistance and reasonable strength and fracture toughness. Sufficient strength and toughness is of crucial importance in addition to wear as FSW tools are subjected to severe stresses during initial plunge into joinable workpieces. FSW tools, especially those made of brittle materials, are more likely to fail in the initial plunge stage than later in the welding process [6]. Cemented WC–Co carbides have been used as tool materials for FSW, but the brittle nature of ceramic-based composites may result in fracture during the tool plunging phase [6]. As a result, short-duration welds are usually performed to examine durability of the tool during an initial plunge.

The objective of this work is to investigate the wear at prevalent adhesion and the reliability of tool materials promising for friction stir welding of aluminium alloys – ceramic-based composites. The focus was on WC-Co hardmetal and TiC- based cermets with different composition (Ni- and Fe-based) and structure of the binder. Ni and Co are known as metals of high supply risk and also for their toxicity. Therefore, cermets with iron- based binders were included in the research programme. Abundant availability and non-toxicity of iron and most iron alloys makes it an excellent replacement

as a binder metal in ceramic-based composites. The most widely used tool steel AISI H13 utilized for the FSW of aluminium and aluminium alloys was used as reference material.

Experimental Details

Previous research has shown that TiC-Ni/Mo cermets compare unfavourably with WC-Co hardmetal (at comparable carbide volumetric content) regarding to adhesive wear resistance [7]. Therefore, alternative TiC-based cermets with iron alloy (FeNi and FeCr) binders were selected.

The heat resistant tool steel AISI H13 (X40CrMoV) alloy was used as reference material because it is the most widely used FSW tool material in industry. Composition of ceramic-based composites (cemented carbide and cermets) and tool steel AISI H13 is presented in Table 1 and mechanical properties in Table 2.

Table 1. Composition of the FSW tool materials

Designation	Carbide content	Carbide content	C	Fe	Ni	Mo	Co	Cr	V	Mn	Si
	[vol.%]	[wt.%]									
WC-Co	76.4	85	-	-	-	-	15	-	-	-	-
TiC-NiMo	89.9	75	-	-	16.7	8.3	-	-	-	-	-
TiC-FeNi	79.0	70	-	25.8	4.2	-	-	-	-	-	-
TiC-FeCr	79.0	70	-	24.9	-	-	-	5.1	-	-	-
H13 (X40CrMoV)	-	-	0.4	90.6	-	1.4	7	5.15	1.03	0.38	0.97

Adhesive wear testing and friction stir welding tools from ceramic-metal composites were produced using a conventional powder metallurgical press and the sintering method.

Table 2. Mechanical properties of the materials

	WC-Co	TiC-NiMo	TiC-FeNi	TiC-FeCr	X40CrMoV
Hardness [HV30]	1100 ± 20	1378 ± 25	1323 ± 21	1225 ± 6	562 ± 8
Fracture toughness [MPa·m ^{1/2}]	17.8 ± 0.5	11.35 ± 0.4	18.0 ± 0.5	10.2 ± 0.7	-

The difficulty in machining of complex features such as flutes and flats on the tool profile can be overcome using 3D printing. Therefore, reference material samples were metal printed using the laser sintering technology. The most significant benefit of the selected laser sintering technology over conventional manufacturing methods is the outstanding flexibility in the component design. To ensure parts with low porosity and high quality, optimal parameters of selective laser melting were used [8].

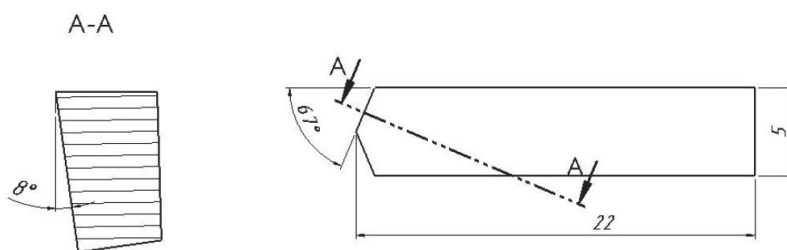


Fig. 1. Geometry of the specimen

The special lathe cutting method was used to perform wear tests with domination of adhesion - aluminium alloy AW6082-T6 was turned using tools from the investigated materials at low speed, simulating the FSW process conditions. Wear testing conditions and geometry of the specimen geometry (see Fig. 1) were the same as in previous research [7]. The chemical composition and mechanical properties of the AW6082-T6 alloy are shown in Table 3.

Three cutting tools were prepared from each material. The cutting speed used in the wear experiments was 16 – 19 m/s. Cutting speed was not constant, because the diameter of the blank was reduced by turning. The total cutting distance for each specimen was 4400 m. The feed rate at 0.39 mm/rev and the depth of the cut at 0.125 mm were constant.

Table 3. Mechanical properties and chemical composition of counterpart for adhesive wear testing (AW6082-T6 alloy)

Chemical composition [%]									
Al	Si	Fe	Cu	Mn	Mg	Cr	Zn	Ti	Other
96.94	1.1	0.27	0.04	0.5	0.8	0.1	0.05	0.05	0.15
Mechanical Properties									
Tensile strength [MPa]		Yield strength (0.2% offset) [MPa]		Elongation [%]		Hardness [HB]			
391		365		11.5		116			

The adhesion wear rate was determined as the shortening in the length of the cutting nose tip of the specimen. Changes in the geometry of the specimens were measured using the images made of the face or top surface of the cutting tool by Hitachi TM 1000 Tabletop scanning electron microscope. Measurements were performed at certain distances (1100, 2200 and 4400 meters) and before each measurement, the specimen was cauterized (to make nose tip measurements) using the sodium hydroxide solution (NaOH 20 wt.%).

A vertical milling machine was used to perform the feasibility study of the FSW tools. Short (250 mm) welds were performed to examine tool resistance to failure during the initial plunge stage of the FSW process. FSW tools used in the experiments had 3.8 mm long conical tapered pin with a root diameter of $\varnothing 6.4$ mm. The concave shoulder end surface with double spiral features was used to produce welds. Shoulder end diameter was $\varnothing 12$ mm. Welding specimen geometry is shown in Fig. 2.

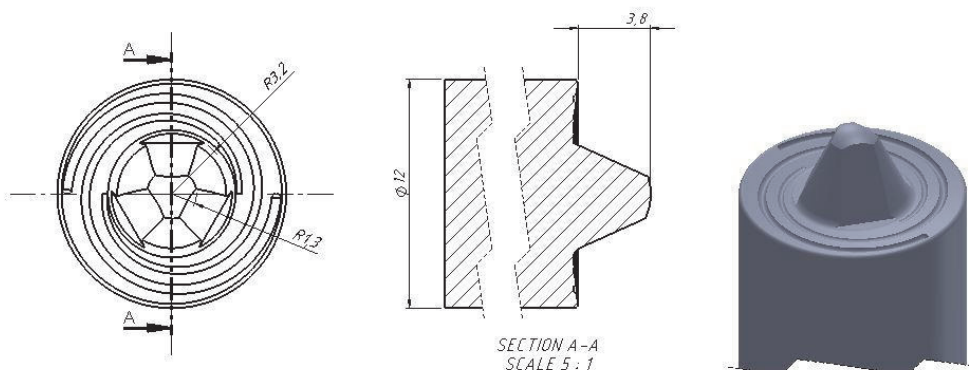


Fig. 2. Top view of the FSW tool shoulder and tip (left), diameter of the shoulder and length of the tip (center) and isometric view of tool (right)

The hardness and indentation fracture toughness were determined using the ground and polished specimens of $5 \times 5 \times 17$ mm. Hardness measurements (Vickers hardness) were carried out in accordance with the standard EN-ISO-6507 using an Indentec 5030 hardness tester. The fracture toughness (K_{IC} , $\text{MPa}\cdot\text{m}^{1/2}$) was determined as indentation fracture toughness. The fracture toughness was calculated by the most commonly used empirical equation for fragile materials proposed by Evans [9].

Results and Discussions

Carbide composites showed significantly higher adhesive wear resistance than the reference material H13. The wear rate of tool steel (H13) was more than five to ten times higher than that of hardmetal and cermets (see Table 4).

Table 4. Cutting nose tip shortening for tested materials at the final cutting distance of 4400 m

	WC-Co	TiC-NiMo	TiC-FeNi	TiC-FeCr	40CrMoV
Shortening of the cutting nose tip [μm]	3.9	7.9	5.3	2.4	39.4

Fig. 3 demonstrates the adhesive wear performance of the cemented carbide and TiC-based cermets plotted against cutting distance. The results refer to marked dependence of the wear performance of a ceramic-metal composite on their composition. In particular, the wear performance depends to a considerable extent on the composition and properties of the binder. At similar carbide volume fraction, WC-based cemented carbide and TiC-FeCr cermet demonstrate an obvious superiority over cermets bonded with NiMo and FeNi alloys.

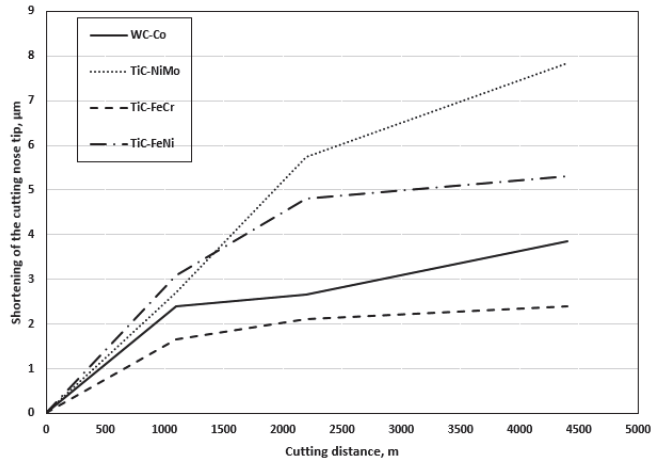


Fig. 3. Adhesive wear (shortening of the length of the cutting tool nose tip) of carbide composites vs cutting distance

Surprisingly, the results of the present research are quite similar to those obtained by Klaasen et al. where the adhesive wear test was performed by the cutting method but instead of aluminium, mild steel was used as counterpart material. Fig. 4 demonstrates the results of adhesive wear performance of different carbide composites plotted against the carbide volumetric fraction [7].

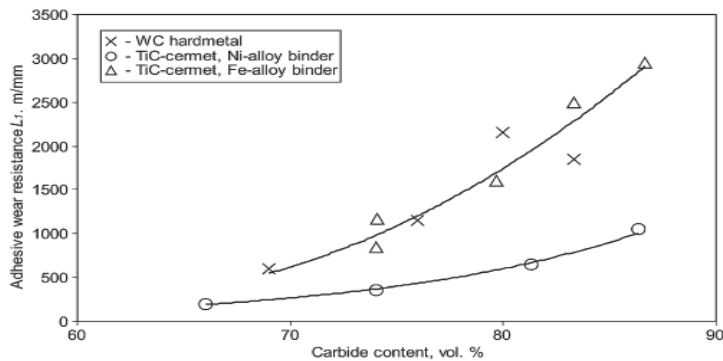


Fig. 4. Adhesive wear resistance vs. hardness of carbide composites [7]

In this investigation, TiC-based cermets with an iron alloy binder also exhibited a remarkable advantage over cermets with a NiMo binder (at an equal carbide volumetric fraction) and WC-based cemented carbides at an equal carbide volume fraction were at slight advantage over TiC-FeNi cermets.

Material removal during adhesive wear has a selective nature. As a precondition to binder selective removal, at first extrusion of the binder, its adhesive interaction has to occur [7]. Extrusion due to compressive stresses is followed by extraction and the microcutting process by abrasive particles in the surface layers of aluminium. After removal of the binder, carbides can be easily withdrawn from the surface (see Fig. 5).

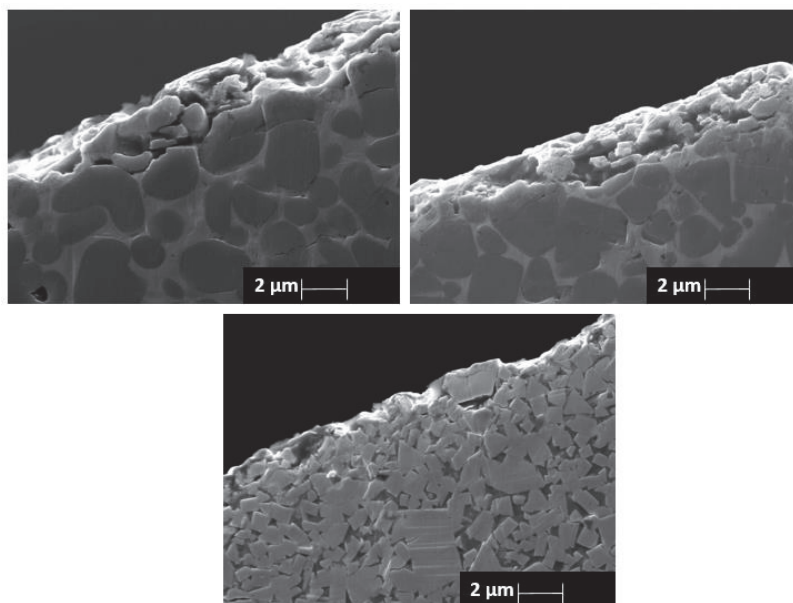


Fig. 5. Wear nature of TiC-FeCr (upper left), TiC-FeNi (upper right) and WC-Co (bottom) specimens cutting

The higher adhesive wear resistance of the WC-Co cemented carbide is the result of its higher rigidity (modulus of elasticity) – higher resistance to the elastic strains. Titanium carbide based cermets compare unfavourably with tungsten carbide based composites in terms of modulus of elasticity. The high adhesive wear resistance of TiC-FeCr cermet exceeding that of WC-Co cemented carbide (at similar volumetric fraction of binder and hardness) may be attributed to the structural peculiarity of the high-chromium cermet – secondary carbides $(Cr, Fe)_7C_3$ in the binder [10]. These carbides form hard bridges between titanium carbide particles (compare Fig. 6 left and right), increasing stiffness of the carbide skeleton and reducing metallic binder extrusion, followed by extraction and microcutting. Cermets with Ni alloy binder compare unfavourably with iron alloys (FeNi, FeCr) bonded cermets presumably due to the higher proof stress and strength of the steel binder at testing temperatures.

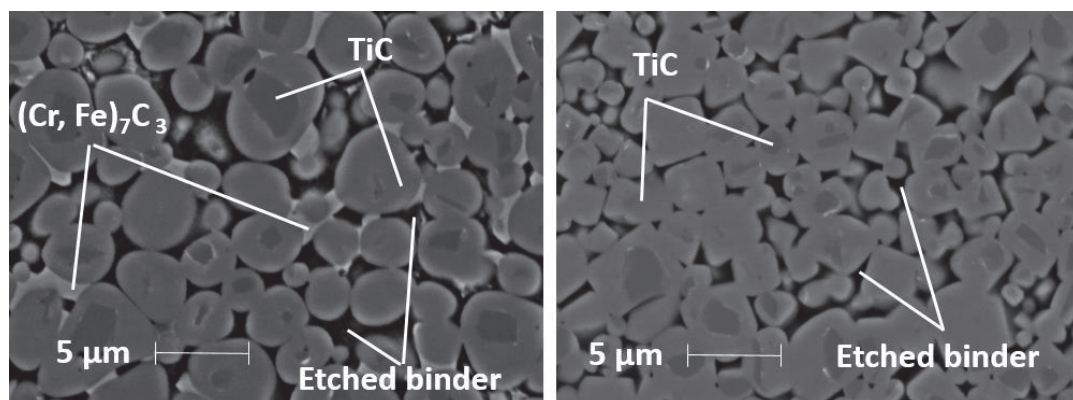


Fig. 6. SEM micrograph of the TiC-FeCr (left) and TiC-FeNi (right) after etching 90 seconds in nitric acid 5% solution

Conclusions

The wear performance at prevailing adhesion of WC-based cemented carbide and TiC-based cermets bonded with nickel and iron alloys was investigated. The following conclusions were drawn:

- Carbide composites (cemented carbide and cermets) outperform remarkably the tool steel commonly used as tool material in the FSW of aluminium alloys in wear conditions where adhesion prevails.
- At equal carbide volume fraction, WC-Co cemented carbide is at advantage over TiC-based cermets (except TiC-FeCr). Higher stiffness (modulus of elasticity) is the reason behind higher performance of the tungsten carbide-based composite.
- Adhesive wear performance of TiC-based composites with iron alloy binder is at advantage over TiC cermets with Ni alloy binder. Presumably, the reason is the higher proof stress and strength of steel binder.
- The high wear resistance of TiC-FeCr cermet exceeding that of WC-Co cemented carbide may be attributed to the structural peculiarity of high-chromium cermet – marked fraction of secondary carbides $(Cr, Fe)_7C_3$ in the binder, increasing the stiffness of carbide skeleton and decreasing the metallic binder extrusion, followed by extraction and microcutting.

Acknowledgment

This work was supported by institutional research funding IUT 19-29 of the Estonian Ministry of Education and Research. The tool preparation is supported by Smart Industry Centre (SmartIC) project, project number 2014-2020.4.01.16-0183.

References

- [1] P.L. Threadgill, A.J. Leonard, H.R. Shercliff, P.J. Withers, Friction stir welding of aluminium alloys, *International Materials Reviews*. 54 (2009) 49-93.
- [2] W.M. Thomas, P.L. Threadgill, E.D. Nicholas, Feasibility of friction stir welding steel, *Science and Technology of Welding and Joining*. 4 (1999) 365-372.
- [3] R. Johnson, P.L. Threadgill, Friction stir welding of magnesium alloys, *Essential readings in magnesium technology*. (2003) 487-492.
- [4] R. Raj, A. De, H. K. D. H. Bhadeshia, T. DebRoy, Review: friction stir welding tools, *Science and Technology of Welding and Joining*. 16 (2011) 325-342.
- [5] S. Yu. Tarasov, V. E. Rubtsov, E. A. Kolubaev, A proposed diffusion-controlled wear mechanism of alloy steel friction stir welding (FSW) tools used on an aluminium alloy, *Wear*, 318 (2014) 130-134.
- [6] Y.N. Zhang, X. Cao, S. Larose, P. Wanjara, Review of tools for friction stir welding and processing, *Canadian Metallurgical Quarterly*. 51 (2012) 250-260.
- [7] H. Klaasen, J. Kubarsepp, T. Roosaar, M. Viljus, R. Traksmaa, Adhesive wear performance of hardmetals and cermets, *Wear*. 263 (2010) 1122-1128.
- [8] P. Laakso, T. Riipinen, A. Laukkanen, T. Andersson, A. Jokinen, A. Revuelta, K. Ruusuvoori, Optimization and Simulation of SLM Process for High Density H13 Tool Steel Parts, *Physics Procedia*. 83 (2016) 26-35.
- [9] A.G. Evans, E.A. Charles, Fracture toughness determinations by indentation, *J. Am. Ceram. Soc.* 59 (1976) 371-372.
- [10] Märt Kolnes, A. Mere, J. Kübarsepp, M. Viljus, B. Maaten, M. Tarraste, Microstructure evolution of TiC cermets with ferritic AISI 430L steel Binder, *Powder Metallurgy*. (2018)

Publication III

Kolnes, M., Kübarsepp, J., Sergejev, F., Kolnes, M. Wear of potential tool materials for aluminium alloys friction stir welding at weld temperatures. Proceedings of the Estonian Academy of Sciences, 2019, 68 (2), 198-206.



Wear of potential tool materials for aluminium alloys friction stir welding at weld temperatures

Mart Kolnes*, Jakob Kübarsepp, Fjodor Sergejev, and Märt Kolnes

Department of Mechanical and Industrial Engineering, Tallinn University of Technology, Ehitajate tee 5, 19086 Tallinn, Estonia

Received 31 January 2019, accepted 20 March 2019, available online

© 2019 Authors. This is an Open Access article distributed under the terms and conditions of the Creative Commons Attribution-NonCommercial 4.0 International License (<http://creativecommons.org/licenses/by-nc/4.0/>).

Abstract. Friction stir welding is a solid-state joining process that uses a non-consumable tool to join materials by mixing them mechanically in the weld area instead of melting them. The high-quality friction stir welding (FSW) process temperatures are in the range of 400–500 °C. Adhesive wear is suggested to be the main wear mechanism for the FSW tool. Adhesive wear testing should be performed at the weld temperature or close to the welding process temperatures for better simulation of real-life FSW tool wearing conditions. Adhesive wear tests of three FSW tool materials, WC–Co and TiC based with NiMo and FeCr binders at temperatures of 70 °C (low) and 400 °C (high) were performed by turning aluminium alloy AW6082-T6. The higher temperature in the cutting zone was achieved by increasing the cutting speed. To measure the temperature at the interface of the cutting tool and the workpiece, a novel method based on the thermoelectric effect was used. The wear was determined as the change of the geometry of the cutting edges of the tool. Microscopic investigations were performed by using scanning electron microscopy. The distribution of chemical elements and the chemical composition of the tool cutting edge were analysed by energy dispersive X-ray spectroscopy. The TiC-based cermets (TiC–NiMo and TiC–FeCr) demonstrated superiority over WC–Co cemented carbide at both low (70 °C) and high (400 °C) temperatures. The highest wear performance at the low temperature was shown by the Fe-alloy bonded composite TiC–FeCr while at the high temperature the Ni-alloy bonded cermet TiC–NiMo had the highest wear performance.

Key words: friction stir welding, cermet, cemented carbide, adhesive wear, weld temperature.

1. INTRODUCTION

Friction stir welding (FSW) is a thermomechanical deformation joining process that uses a specially designed tool to join materials without melting them [1,2]. The FSW tool serves three primary functions: heating of the workpiece, movement and mixing of the material to produce the joint, and containment of the hot metal beneath the tool shoulder. Heating is produced within the workpiece both by friction between the rotating tool pin and the shoulder and by severe plastic deformation

of the workpiece [3]. Localized heating softens the material around the pin. As a result of the tool rotational action and the influence on the workpiece, if performed properly, a qualitative solid-state joint is produced. It is essential to ensure that the tool will not lose special features, such as the geometry of the pin, and/or texture features of the shoulder part of the tool and dimensional stability by the wear at weld temperature.

Excessive tool wear changes the tool shape (normally by removing tool features), thus changing the weld quality and increasing the probability of defects. In friction stirring, tool wear can occur due to adhesive, abrasive, or chemical wear (addressed subsequently as reactivity)

* Corresponding author, mart.kolnes@taltech.ee

mechanisms. The exact wear mechanism depends on the interaction between the workpiece and the tool material and the selected tool parameters [4].

The cemented carbides and cermets selected for our study as prospective FSW tool materials have relatively high abrasive wear resistance as compared to common tool materials [5,6]. For this reason, we concentrated on the adhesive wear of these materials. Previous adhesive wear studies at room temperature have shown that TiC-based cermets are of great potential in FSW applications [7]. For better simulation of real-life welding conditions, the adhesive wear was studied at temperatures close to the weld temperatures.

It is well known that temperature may influence the wear mechanism [8]. Generally, this is attributed to the decreased yield strength and increased ductility at elevated temperatures. Gåård et al. investigated the effect of frictional heating on the adhesive wear mechanism [9]. They claimed that adhesive wear is influenced by temperature, as increased temperature leads to shorter sliding distances until the onset of severe wear, distinguished as an increase of the coefficient of friction. They found that the transition to severe adhesive wear occurs at similar sliding distances for similar temperatures, although the normal loads and velocities are different. They assumed that the very high sensitivity of adhesive wear to temperature already at lower temperatures is unlikely to depend on the change in mechanical properties. Tang et al. found that the highest temperature in the welding seam is approximately 0.8 of the melting temperature of the welded material [10].

The FSW tool is commonly coated by a layer of weldable material, in particular an aluminium alloy. The problem here is that the generation of the tribological layer on the tool surface creates conditions for the diffusion of elements into the tool metal. A rationale behind the tool wear in the FSW of aluminium alloys could be strong adhesion of the aluminium alloy to a tool and the following diffusion of the tool material into aluminium due to high temperatures developed during welding [11]. The reaction-diffusion of iron into aluminium is a well-known phenomenon that has been observed in many cases [12]. Hirano et al. investigated the diffusion of iron, nickel, and cobalt in aluminium at a temperature range over 360 to 630 °C and measured

the temperature dependences of diffusivities of these materials in aluminium [13].

Currently, the most often used method to measure cutting temperature is the tool–workpiece thermocouple method, which uses Seebeck’s principle. Previous studies have proved that a metal subjected to a temperature differential undergoes a non-uniform distribution of free electrons, which subjects this metal to an electromotive force differential [14]. This method requires two different metals joined in one part. Along the paths of the thermocouple circuit, the electromotive force is given by the product of the difference between the Seebeck’s coefficients of thermocouple materials and the temperature gradient between the closed and open junctions of the thermocouple. With the tool–workpiece thermocouple method, the amount of electromotive force is an indication of the average temperature in the tool–workpiece interface. On certain occasions, the electromotive force does not correspond to the average cutting temperature of the interface; it only corresponds in the cases when the temperature is uniform, or if the thermoelectric obtained from the tool–workpiece combination varies linearly along with the cutting temperature. The tool–workpiece thermocouple method was recently used also for measuring the FSW process temperature [15].

This work focuses on the performance of carbide composites in wear conditions with the prevalence of adhesion at a low and near weld temperature during the FSW of an aluminium alloy.

2. EXPERIMENTAL DETAILS

Wear tests at different temperatures were performed on a universal lathe. The aluminium alloy AW6082-T6 (1.1% Si, 0.5% Mn, 0.8% Mg, rest Al) round bar of 200 mm diameter was machined at high speeds, up to 630 m/min. Three different cutting tool materials were used. The composition of carbide-based composites and their mechanical properties are presented in Table 1.

The carbide volume content was calculated taking into account the dissolution of Mo in TiC and the formation of secondary Cr-based carbides in cermets TiC–NiMo and TiC–FeCr, respectively. Microstructures of carbide composites are shown in Fig. 1. The TiC–FeCr

Table 1. Composition and mechanical properties of carbide composites

Designation	Initial composition, wt%		Carbide content, vol%	Hardness HV30	Fracture toughness, MPa·m ^{1/2}
	Carbide	Binder			
WC–Co	85 WC	Co(W) 15	76.4	1100 ± 20	17.8 ± 0.5
TiC–NiMo	75 TiC	Ni 16.7, Mo 8.3	89.9	1378 ± 25	11.4 ± 0.4
TiC–FeCr	70 TiC	Fe 25.8, Cr 5.1	84.0	1225 ± 6	10.2 ± 0.7

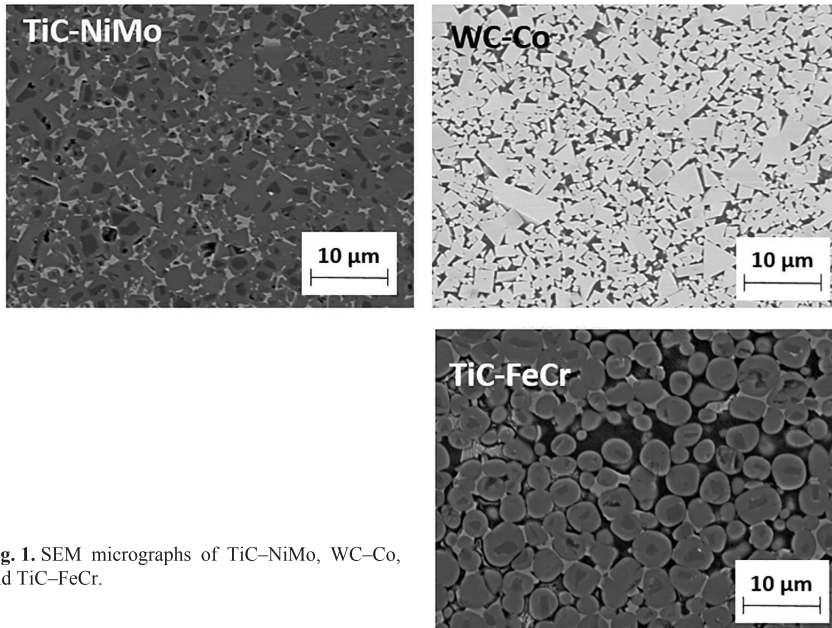


Fig. 1. SEM micrographs of TiC–NiMo, WC–Co, and TiC–FeCr.

cermet was etched in nitric acid 5% solution for 90 s to determine its carbide volume content, for which image analysis software OmniMet was used.

To measure the cutting temperature in the cutting point, a tool–workpiece thermocouple system was used

[16]. The scheme of this system is presented in Fig. 2. The workpiece and the turning tool were insulated from the lathe. The cold end of the tool and the three-bush device were connected to the voltmeter to measure the electromotive force.

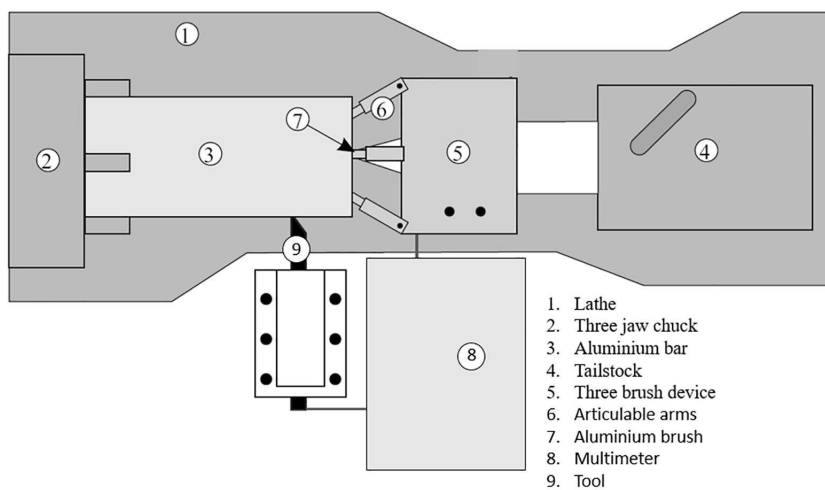


Fig. 2. Schematic of the tool–workpiece thermocouple system (top view) [16].

To ensure reliable temperature measurements, the tool–workpiece thermocouple must be the only high-temperature point in the system. All the other material connections have to be at room temperature. To maintain the electrical conductivity in the tool–workpiece thermocouple circuit during the turning of the aluminium alloy, a three-brush device was used. The main function of the three-brush device is to maintain the electrical continuity of the tool–workpiece thermocouple circuit with the workpiece in rotational movement. The device used is similar to that of Santos et al. [16].

In this work, calibrations of the tool–workpiece thermocouple were carried out with tool materials under research. Long bars of the tool materials were prepared with one end joined with an aluminium chip. The calibration thermocouples were introduced into an electrical furnace and heated up to 500 °C. The electromotive force was measured on the outside ends of the ceramic-based composite bar and the aluminium chip, which were at room temperature. Therefore, the electromotive force was dependent only on the temperature of the contact point between the composite and the aluminium chip. Figure 3 shows the calibration curves of the two tested thermocouple materials.

The electromotive force was 6.1 mV, 2.4 mV, and 1.9 mV for WC–Co, TiC–FeCr, and TiC–NiMo, respectively, at 440 °C, which is close to the maximum FSW temperature of aluminium alloy AW6082-T6. Three measurements were performed for each specimen, and the results of the temperature measured by the three-brush device are average values.

To investigate the dependence of cutting temperature on the cutting speed in the case of the cemented carbide, WC–Co tool turning tests were performed at cutting speeds up to 630 m/min. Raising the cutting speed over 500 m/min did not increase the temperature significantly (Fig. 4). The reason is that for our lathe test setup, the temperature of the cutting tool in contact stabilizes at around 410 °C. Although the approximate

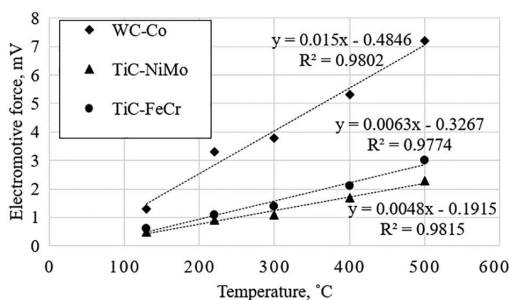


Fig. 3. Relationship between the temperature and the electromotive force for ceramic-based materials tested.

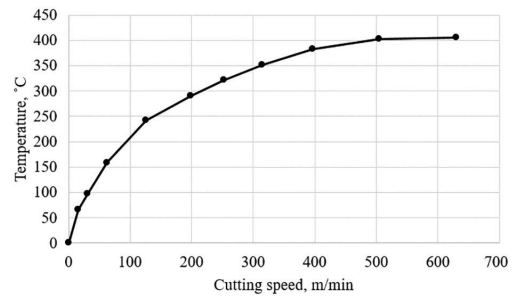


Fig. 4. Cutting speed vs cutting point temperature in the case of the WC–Co tool.

welding temperature of the aluminium alloy AW6082-T6 is about 440 °C, it was not reached during the turning tests. Therefore, 500 m/min was selected as the cutting speed for adhesive wear tests in the case of WC–Co cemented carbide. The same cutting speed to achieve the cutting temperature of approximately 400 °C was also used for the tools made from cermets. The cutting speed of 17 m/min was used in tests at low-temperature (approximately 70 °C) wear conditions.

The cemented carbide and cermets tools were ground in order to achieve a nose angle of 134°, side cutting-edge angle of 23°, and side relief angle of 8°. The total cutting distance for each specimen was 4400 m. The feed rate and the depth of cut were kept constant during testing at 0.39 mm/rev and 0.125 mm, respectively. Changes in the geometry of the specimens were measured using the images made from the top surface of the cutting tool by Hitachi TM 1000 Tabletop scanning electron microscope. The adhesion wear rate was determined as the shortening (in µm) in the length of the cutting nose tip of the specimen. Measurements were performed at certain distances (1100, 2200, and 4400 m) and before each measurement, the specimen was cauterized (to make nose tip measurements) using a sodium hydroxide solution (NaOH 20 wt%). In order to understand the distribution of chemical elements in the microstructure in the tool–workpiece contact region, the energy-dispersive X-ray spectroscopy (EDS) system INCA was used.

3. RESULTS AND DISCUSSION

Previous research [17–19] has shown that at similar volume fraction of carbides TiC-based cermets independent of their binder composition and structure are at a disadvantage compared to WC-based cemented carbides in abrasive erosion and also in abrasive wear conditions. The performance of carbide composites in

abrasion conditions is controlled primarily by the stiffness of the composite, i.e. its resistance to elastic (evaluated by the modulus of elasticity) and plastic (evaluated by proof stress) strains, and depends chiefly on the properties of the carbide phase (WC vs TiC) [17,18]. At the same time, the adhesive wear performance of cermets may be comparable to that of WC-based composites, as it is controlled primarily by composite resistance to plastic strain featured by the proof stress that depends on properties of both the metallic and the ceramic phase [17,19].

In the present research TiC-based composites (cermets) demonstrated superiority over WC-based cemented carbides at both low (70 °C) and elevated (400 °C) temperatures (see Table 2 and Fig. 5). The high

wear performance of TiC-based cermets indicates that the prevailing mechanism in the wear testing conditions used in the present research was adhesion. At the low temperature, the highest wear performance was demonstrated by the TiC–FeCr cermet while at the high temperature the TiC–NiMo cermet outperformed both WC–Co and TiC–FeCr composites (Fig. 5, Table 2).

The wear performance of cermet, bonded with the Ni alloy (TiC–NiMo) as distinct from WC–Co and TiC–FeCr composites appeared to be similar at low (70 °C) and elevated (400 °C) temperatures. In other words, the wear temperature sensitivity of the Ni-alloy bonded cermet was markedly lower compared to the other carbide composites investigated.

Figure 5 demonstrates wear performance plotted against the cutting distance at two different temperatures of the WC–Co cemented carbide and TiC–FeCr and TiC–NiMo cermets. Increase in the temperature resulted in a marked growth of wear, i.e. shortening of the cutting nose tip (except the TiC–NiMo cermet). At the same time different composites demonstrated no marked differences in the wear gain rate during the increase of the cutting distance: the wear rate increase angles (α , β , and γ) were almost similar at different temperatures (see Fig. 5).

Table 2. Cutting tool nose tip shortening for tested materials at the final cutting distance of 4400 m

Material	Shortening of the cutting nose tip, μm	
	at 70 °C	at 400 °C
WC–Co	3.9	5.5
TiC–NiMo	3.6	3.3
TiC–FeCr	2.4	4.5

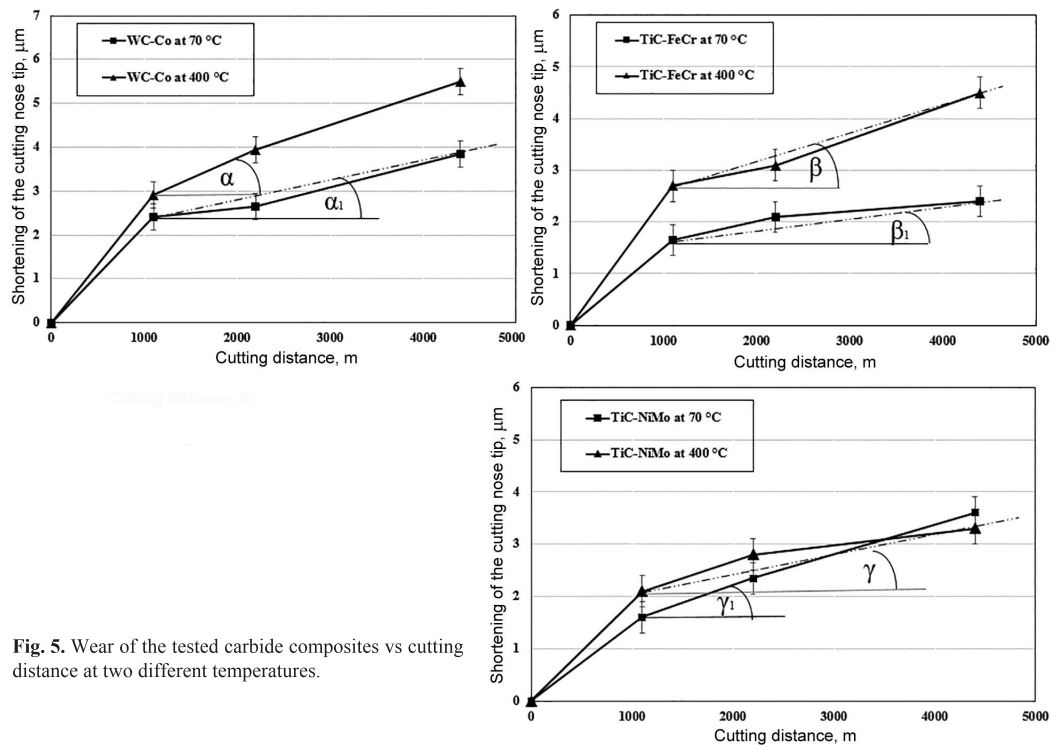


Fig. 5. Wear of the tested carbide composites vs cutting distance at two different temperatures.

The SEM studies (Fig. 6) demonstrated failure (material removal) of the cutting tool tip after the wear tests of carbide composites. Micrographs confirm our previous research results of adhesive wear performance of cemented carbides and cermets [19]. The structure of the worn cutting nose tip is distinctive, proving that adhesive failure starts preferably in the binder continuing by the extraction of carbides.

Figure 7a shows the EDS line scan of the WC–Co tool covered during the turning test by the aluminium alloy after 4-h heat treatment at 400 °C. Figure 7b presents the SEM image of the measured area. The EDS scan revealed a slight diffusion of aluminium (diffusion depth approximately 2 µm) into the cemented carbide binder phase.

Figures 8a and 9a show the EDS line scan of the TiC–FeCr and TiC–NiMo tools, respectively, covered

during the turning test by the aluminium alloy after 4-h heat treatment at 400 °C. Figures 8b and 9b present SEM images of the measured area. The EDS scan revealed a mild diffusion of aluminium (diffusion depth approximately 1 µm) into the iron- or nickel-based binder phase of the TiC-based cermets.

The diffusion of aluminium into the cobalt binder was slightly higher than its diffusion into the iron–chromium or nickel–molybdenum binder (cf. Fig. 7 and Figs 8, 9). There was no significant aluminium diffusion into the carbide phase and metallic binder diffusion into aluminium in the case of all three tested composites. At the same time, a marked diffusion of titanium but not of tungsten into aluminium was observed (cf. Fig. 7 and Figs 8, 9).

The surface failure (removal of material) during adhesive wear starts mostly in the binder by a combined

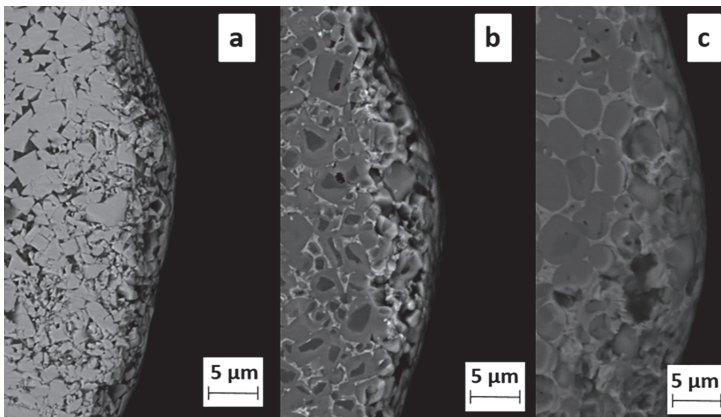


Fig. 6. Worn-out cutting nose tip (cutting distance 4400 m) of carbide composites WC–Co (a) and TiC–NiMo (b) and TiC–FeCr (c) cermets.

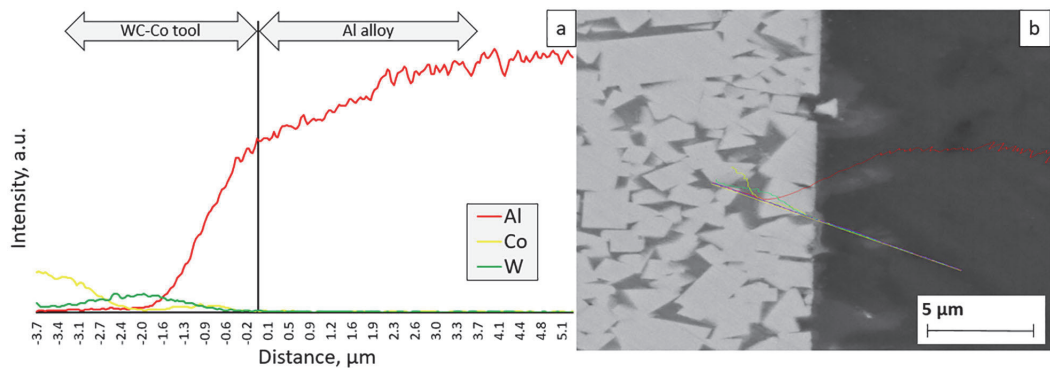


Fig. 7. EDS line scan (a) and the cross-section view of the WC–Co tool with a tribological layer (b).

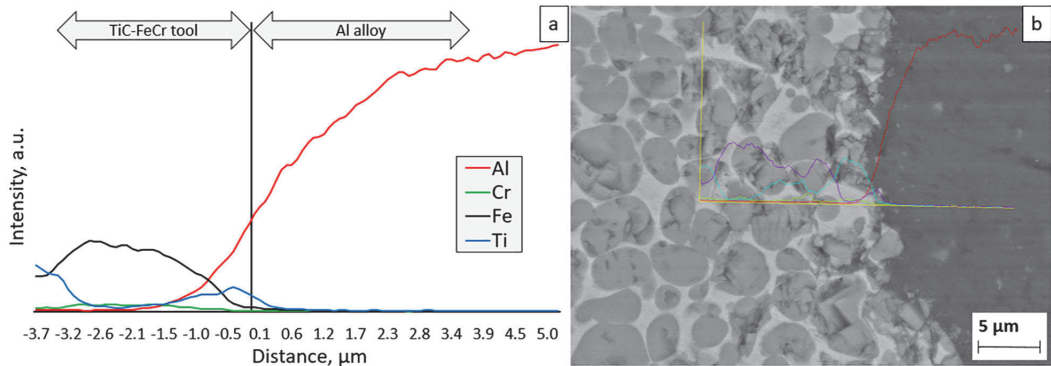


Fig. 8. EDS line scan (a) and the cross-section view of the TiC–FeCr tool with a tribological layer (b).

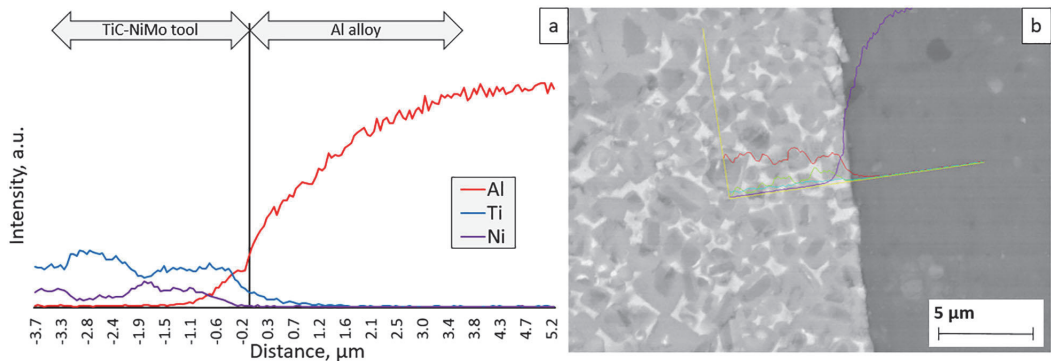


Fig. 9. EDS line scan (a) and the cross-section view of the TiC–NiMo tool with a tribological layer (b).

extrusion–extraction–microcutting process preceded by the local plastic strain that takes place prevalently in the binder of the composite. The performance of the composite in the wear conditions with predominance of adhesion depends on the carbide fraction and properties of the metallic binder. Both the increase of the volume fraction of the carbide phase in the composite and the strength of the metallic phase lead to an improvement of the adhesive wear performance of ceramic-based composites regardless of the ceramic phase composition [19]. Research of the microstructure evolution process has demonstrated that during the liquid-phase sintering of high-chromium TiC–FeCr cermets, the formation of the M_7C_3 (where $M = Cr$ and Fe) carbide takes place in the binder region of composites [20]. As a result, the fraction of the metallic binder (Fe-based solid solution) decreases while the fraction of the carbide phase increases. An enhanced volume fraction of the carbide phase

(TiC + M_7C_3 -type carbides) and a high strength of the FeCr alloy binder are predominantly behind the higher wear performance of TiC–FeCr cermets compared with WC–Co cemented carbides both at low and high temperatures (at an approximately equal TiC and WC fractions in carbide composites). The best high-temperature (400 °C) wear performance of the TiC–NiMo cermet can be attributed to the highest carbide volume fraction after sintering (*see* Table 1) and the high strength of the Ni-based binder at elevated temperatures.

In parallel to adhesive wear, diffusion-controlled wear takes place during FSW at high temperatures [11]. It is known that the cobalt inter-diffusion coefficient in aluminium exceeds markedly that of iron and nickel [13]. It is another aspect why ceramic-based composites with Fe- and Ni-based binders should demonstrate better wear performance at high temperatures in contact with Al than composites bonded with cobalt.

4. CONCLUSIONS

The performance of carbide composites bonded with Co, Ni, and Fe alloys, in particular of cermets (TiC–NiMo and TiC–FeCr) and WC–Co cemented carbide, in wear conditions with prevailing adhesion was investigated at different temperatures (including the weld temperature during the FSW of aluminium alloys). The following conclusions were drawn:

- TiC-based cermets (TiC–NiMo, TiC–FeCr) demonstrated superiority over WC–Co cemented carbide at both low (70 °C) and elevated (400 °C) temperatures.
- The highest wear performance at the low temperature (70 °C) was demonstrated by the Fe-alloy bonded composite TiC–FeCr, while at the high temperature (400 °C) the Ni-alloy bonded cermet TiC–NiMo showed the highest performance.
- The lowest temperature sensitivity of wear resistance was demonstrated by the Ni-alloy bonded cermet TiC–NiMo.
- Enhanced high-temperature strength of the Ni-based binder as well as an increased carbide volume fraction were behind the high wear performance of the TiC–NiMo cermets.

ACKNOWLEDGEMENTS

This work was supported by the institutional research funding ‘Multi-scale structured ceramic-based composites for extreme applications’ (IUT 19-29) of the Estonian Research Council. The publication costs of this article were covered by the Estonian Academy of Sciences.

REFERENCES

1. Murr, L. E., Liu, G., and McClure, C. A TEM study of precipitation and related microstructures in friction-stir-welded 6061 aluminium. *J. Mater. Sci.*, 1998, **33**, 1243–1251.
2. Threadgrill, P. L., Leonard, A. J., Shercliff, H. R., and Withers, P. J. Friction stir welding of aluminium alloys. *Int. Mater. Rev.*, 2009, **54**, 49–93.
3. Schneider, J. A. Temperature distribution and resulting metal flow. In *Friction Stir Welding and Processing* (Misha, R. S. II and Mahoney, M. W., eds). ASM International, Materials Park, Ohio, 2007, 37–49.
4. Fuller, C. B. Friction stir tooling: tool materials and designs. In *Friction Stir Welding and Processing* (Misha, R. S. II and Mahoney, M. W., eds). ASM International, Materials Park, Ohio, 2007, 7–35.
5. Pirso, J., Juhani, K., Viljus, M., and Letunovič, S. Two-body abrasive wear of WC-Co hardmetals in wet and dry environments. In *Proceedings of the 8th International Conference of DAAAM Baltic Industrial Engineering*, 2012, 711–716.
6. Pirso, J., Viljus, M., Letunovič, S., Juhani, K., and Joost, R. Three-body abrasive wear of cermets. *Wear*, 2011, **271**, 2868–2878.
7. Kolnes, M., Kübarsepp, J., Sergejev, F., and Kolnes, M. Adhesive wear of WC- and TiC-based friction stir welding tool materials for aluminium alloy welding. In *Proceedings Euro PM2018*. EPMA, Bilbao, 2018.
8. Paerson, S. R., Shipway, P. H., Abere, J. O., and Hewitt, R. A. A. The effect of temperature on wear and friction of a high strength steel in fretting. *Wear*, 2013, **303**, 622–631.
9. Gåård, A., Hallbäck, N., Krakhmalev, P., and Bergström, J. Temperature effects on adhesive wear in dry sliding contacts. *Wear*, 2009, **268**, 968–975.
10. Tang, W., Guo, X., McClure, J. C., and Murr, L. E. Heat input and temperature distribution in friction stir welding. *J. Mater. Process. Manuf. Sci.*, 1998, **7**, 163–172.
11. Tarasov, S., Rubtsov, V. E., and Kolubaev, E. A. A proposed diffusion-controlled wear mechanism of alloy steel friction stir welding (FSW) tools used on an aluminum alloy. *Wear*, 2014, **318**, 130–134.
12. Alimadadi, H., Kjartansdottir, C., Burrows, A., Kasama, T., and Möller, P. Nickel-aluminum diffusion: a study of evolution of microstructure and phase. *Mater. Charact.*, 2017, **130**, 105–112.
13. Hirano, K. L., Agarwala, R. P., and Cohen, M. Diffusion of iron, nickel and cobalt in aluminum. *Acta Metall.*, 1962, **10**, 857–863.
14. Recktenwald, G. *Conversion of Thermocouple Voltage to Temperature*. Apostila, Portland, 2010.
15. De Backer, J. and Bolmsjö, G. Thermoelectric method for temperature measurement in friction stir welding. *Sci. Technol. Weld. Join.*, 2013, **18**:7, 558–565.
16. Santos, M. C. Jr., Araujo Filho, J. S., Barrozo, M. A. S., Jackson, M. J., and Macchado, A. R. Development and application of temperature measurement device using the tool-workpiece thermocouple method in turning at high cutting speeds. *Int. J. Adv. Manuf. Technol.*, 2017, **89**, 2287–2298.
17. Kübarsepp, J., Klaasen, H., and Pirso, J. Behaviour of TiC-base cermets in different wear conditions. *Wear*, 2001, **249**, 229–234.
18. Klaasen, H. and Kübarsepp, J. Abrasive wear performance of carbide composites. *Wear*, 2006, **261**, 520–526.
19. Klaasen, H., Kübarsepp, J., Roosaar, T., Viljus, M., and Traksmaa, R. Adhesive wear performance of hardmetals and cermets. *Wear*, 2010, **268**, 1122–1128.
20. Kolnes, M., Mere, A., Kübarsepp, J., Viljus, M., Maaten, M., and Tarraste, M. Microstructure evolution of TiC cermets with ferritic AISI 430L steel binder. *Powder Metall.*, 2018, **61**(3), 197–209.

Alumiiniumi otshõrdkeevituse tööriista potentsiaalsete materjalide kulumine keevitustemperatuuril

Mart Kolnes, Jakob Kübarsepp, Fjodor Sergejev ja Märt Kolnes

Otshõrdkeevitus on tardfaaskeevitus, kus materjalid liidetakse mehaanilise segamise teel neid sulatamata; hõrdkeevituse temperatuur on vahemikus 400–500 °C. Otshõrdkeevituse tööriista kulumist põhjustab peamiselt adhesioonkulumine. Adhesioonkulumise uuringud viidi läbi keevitusprotsessile ligilähedasel temperatuuril, et tagada võimalikult reaalne kulumise olukord. Selleks viidi läbi adhesioonkulumise katsed, treides alumiiniumsulamit AW6082-T6 kolme erinevast materjalist tööriistaga (WC–Co, TiC–NiMo ja TiC–FeCr) madalal (70 °C) ja kõrgel (400 °C) temperatuuril. Kõrgem temperatuur saavutati lõikekiiruse suurendamisega. Temperatuuri mõõtmiseks lõiketsoonis kasutati uutset meetodit, mis põhineb materjalide termoelektrilisel efektil. Kulumist hinnati kui lõikeriista lõike-servade geomeetria muutust, kasutades skaneerivat elektronmikroskoopiat. Katsete tulemusena selgus, et TiC baasil kermistel on WC–Co kõvasulamiga võrreldes eeliseid nii madalal kui ka kõrgel keevitusprotsessi temperatuuril. Parim kulumiskindlus madalatel temperatuuridel on raua baasil sideainega TiC–FeCr kermistel ja kõrgetel temperatuuridel nikli baasil sideainega TiC–NiMo kermistel.

Publication IV

Kolnes, M., Kübarsepp, J., Sergejev, F., Kolnes, M., Tarraste, M., Mikli, V. Wear behaviour of ceramic metal composites as tool materials for FSW of stainless steel. In: J. Padgurskas (Ed.). Proceedings of BALTRIB'2019 (107-112). Vytautas Magnus University, 2019.

WEAR BEHAVIOR OF CERAMIC-METAL COMPOSITES AS TOOL MATERIALS FOR FSW OF STAINLESS STEEL

M. Kolnes^{1*}, *J. Kübarsepp**, *F. Sergejev**, *M. Kolnes**, *M. Tarraste**, *V. Mikli***

*Department of Mechanical and Industrial Engineering, Tallinn University of Technology, Estonia

**Department of Material and Environmental Technology, Tallinn University of Technology, Estonia

Abstract: Friction stir welding (FSW) is a solid-state joining process that uses a non-consumable tool to join materials by mixing them mechanically in the weld area instead of melting the materials. The temperatures of the high-quality FSW process for stainless steels are above 1000°C. The main wear mechanism for a FSW tool in the case of stainless steels is diffusion controlled wear. In our study, wear and diffusion tests were performed at the temperature close to the welding process for better physical simulation of real-life FSW tool wear conditions by turning stainless steel AISI304 at high speed. Tool materials such as WC–Co cemented carbides and TiC–based cermets with different binder composition and fraction were used. The temperature required in the cutting zone was achieved by increasing the cutting speed. To measure the temperature at the interface of the cutting tool and the workpiece, the method based on the thermoelectric effect was used. The wear was determined as the change of the geometry of the cutting edges of the tool. Microscopic investigations were performed using scanning electron microscopy. The diffusion mechanism was studied using the energy dispersive X-ray spectroscopy (EDS). TiC–based cermets with nickel based binder TiC–NiMo demonstrated superiority over WC–Co cemented carbides and TiC–based Fe–alloys bonded cermets TiC–FeNi and TiC–FeCr.

Keywords: friction stir welding, stainless steel, cermet, cemented carbide, wear mechanism.

1. INTRODUCTION

The requirements for a friction stir welding (FSW) tool used for welding of high temperature materials are pronounced. A tool must maintain sufficient strength to constrain the weld material at softening temperatures in excess of 1000°C, which is the approximate temperature of FSW of stainless steels [1, 2]. The tool must be resistant to fatigue, fracture, mechanical and chemical wear. Therefore, it is necessary that the mechanical properties of the tool are sufficient at the high temperatures and that the tool is chemically inert to welded materials. According to the literature, currently used tool materials are expensive and difficult to machine; therefore, researchers also look for cost-effective FSW tool materials for stainless steel FSW. Several kinds of welding tools made of refractory materials or ceramic-based composites have been used [3–5].

To select proper FSW tool materials applicable for welding of different metallic materials, laboratory test methods are required. In our previous research, a simplified testing methodology for the wear behaviour of FSW tool materials at weld temperatures of aluminium alloy was proposed. The wear tests were performed using a cutting method, by turning aluminium alloy at low (70°C) and high (400°C) temperatures. Additionally, reaction diffusion between the tool material and the workpiece material at the welding temperature was addressed [6].

Our aim in this work was to study the behavior and reaction diffusion of ceramic-metal composites at the weld temperature characteristic of the FSW of stainless steel. The focus was on WC–Co cemented carbides with different binder fraction and TiC–based cermets with different composition (Ni– and Fe–based binder systems) and binder fraction.

¹ Author for contacts: Mart Kolnes
E-mail: mart.kolnes@taltech.ee

2. EXPERIMENTAL

To investigate the wear performance of different carbide composites during the FSW of stainless steel alloy, the wear tests were performed on a universal lathe. The stainless steel AISI 304 (18–20% Cr, 8–10,5% Ni, 2% Mn, max 1% Si, rest Fe) bar was machined at high speed, up to 280 m min⁻¹ to achieve high temperature approximately equal to the welding temperature (1000°C). To measure the cutting temperature in the cutting point, a tool–workpiece thermocouple method was used. Detailed calibration and temperature measurement parameters and tool geometry and cutting wear test parameters are described in [6]. The wear rate of the tool was determined as the shortening in the length of the cutting tool nose tip of the specimens. In our previous research (with aluminium alloy as workpiece material), shortening of the cutting nose tip was measured on the top surface of the tool but in the case of turning stainless steel, the height of the wear pattern was measured on the front surface of the tool because the tool wear rate was significantly more intensive.

The wear of WC– and TiC–based ceramic-based composites was studied. WC–Co cemented carbides and TiC–NiMo cermets with different binder fraction were analyzed. Because of high supply risk and toxicity of Co and Ni, TiC–based cermets with alternative binder systems (iron-based) were added in our research. The chemical composition and mechanical properties of the investigated tool materials are presented in Table 1. The carbide volume content was calculated taking into account the dissolution of Mo in TiC and the formation of secondary Cr–based carbides in cermets TiC–NiMo and TiC–FeCr, respectively.

Table 1. Composition and mechanical properties of carbide composites.

Designation	Initial composition, wt.%		Carbide content, vol.%	Hardness HV30	Fracture toughness, MPa·m ^{1/2}
	Carbide	Binder			
85WC–Co	85 WC	Co 15	76.4	1100±20	17.8±0.5
90WC–Co	90 WC	Co 10	83.7	1238±6	16.7±0.3
94WC–Co	94 WC	Co 6	90.0	1765±25	7.2±0.3
70TiC–NiMo	70 TiC	Ni 20, Mo 10	87.7	1492±16	10.3±0.4
75TiC–NiMo	75 TiC	Ni 16.7, Mo 8.3	89.9	1378±25	11.4±0.4
80TiC–NiMo	80 TiC	Ni 13.3, Mo 6.7	92.1	1340±21	12.4±0.3
70TiC–FeCr	70 TiC	Fe 24.9, Cr 5.1	84.0	1225±6	10.2±0.7
70TiC–FeNi	70 TiC	Fe 25.8, Ni 4.2	79.3	1323±21	18.0±0.5

Reaction diffusion tests were performed by heating the test samples up to 1000°C, followed by 4 hours dwelling at that temperature in vacuum furnace. Test samples were prepared using spark plasma consolidation of sintered carbide composite specimens and AISI 316 stainless steel powder (with Cr and Ni content similar to that in AISI 314 steel) to achieve a permanent bond between the tool material and steel. In order to understand the distribution of chemical elements in the microstructure in the tool–workpiece contact region, the energy-dispersive X–ray spectroscopy (EDS) system INCA was used.

3. RESULTS AND DISCUSSION

The results of our previous work focusing on the performance of carbide composites in the wear conditions with the prevalence of adhesion TiC–based cermets (TiC–NiMo, TiC–FeCr) demonstrated superiority over WC–Co cemented carbide both at low (70°C) and high (400°C) temperatures. The Ni–alloy bonded cermet TiC–NiMo showed the highest wear performance at high temperature [6]. The present research also proved that regardless of the binder fraction, TiC–NiMo cermets demonstrate superiority over other potential FSW tool materials. However, as different from previous research, TiC–FeCr cermet compares unfavourably both with WC–Co cemented carbides and TiC–NiMo cermets. This composite shows extremely high wear rate even at low cutting distances (see Figure 1 and Table 2). An alternative Fe–alloy bonded cermet TiC–FeNi exhibited better wear performance at the level of WC–Co cemented carbides.

Excellent wear performance of TiC–NiMo and good performance of TiC–FeNi cermets as compared to WC–Co cemented carbides indicate that the prevailing wear mechanisms in the wear testing

conditions used are diffusion and chemical wear and adhesion. Favourable conditions for diffusion and chemical wear are provided by very high localized temperature (1000°C) at the tool-workpiece contact zone.

Table 2. Shortening of the cutting nose tip of tested materials at the final cutting distance of 150 m.

	WC-Co			TiC-NiMo			TiC-FeCr*	TiC-FeNi*
Initial calculated carbide content, wt.%	85 WC	90 WC	94 WC	80 TiC	75 TiC	70 TiC	70 TiC	70 TiC
Shortening of the cutting tool, μm	1676	1132	958	328	270	704	1939	1044

*measured at the cutting distance of 100 m.

Figure 1 demonstrates the wear performance of the tested composites against their composition and carbide fraction. It can be seen that the increase in the volume fraction of the carbide phase in the composites causes improvement of the wear performance of both WC-Co cemented carbides and TiC-NiMo cermets. The best performance is demonstrated by the TiC-NiMo cermet with initial (calculated) carbide content at about 75...80 wt.% while the WC-Co cemented carbide with carbide content showed about 90...94 wt.%.

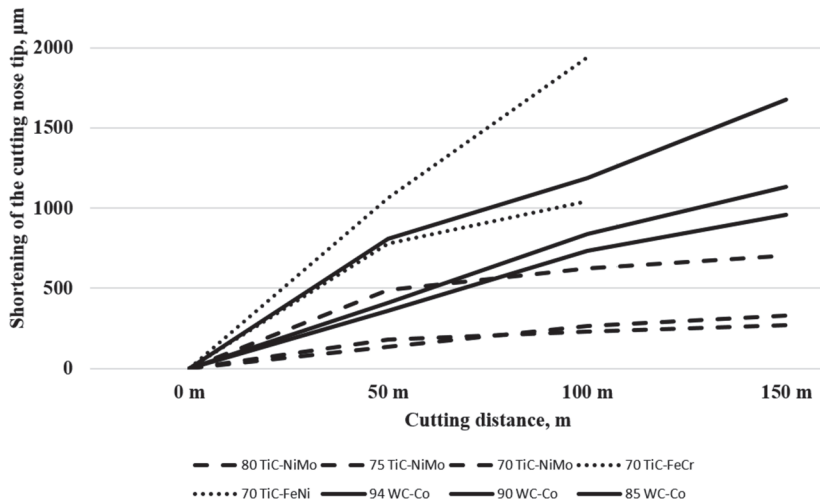


Figure 1. Wear of the carbide composites vs cutting distance at the welding temperature of 1000°C.

Figure 2 shows the SEM micrographs from the carbide composite tool – AISI 316 stainless steel contact zone and Table 3 presents the chemical composition of the tool and steel contact layers after heat treatment for 4 h at 1000°C. The results in Table 3 have been acquired from EDS line scan of tool- stainless steel contact region (see as an example WC-Co – stainless steel contact region in Figure 3). With regard to tool wear, special attention should be paid to the processes at the tool (cemented carbide, cermet) surface layers both during machining (wear tests) as well as during FSW as continuously new layers of steel are exposed to the reactions with the tool in the contact zone.

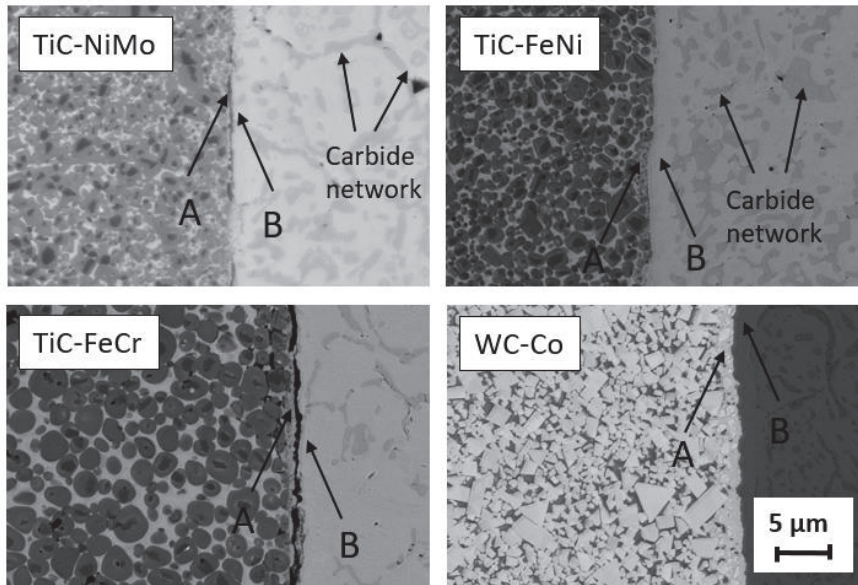


Figure 2. SEM micrographs of permanent bond between tool materials and stainless steel after heat treatment in vacuum during 4 h at 1000°C.

Table 3 and Figures 2 and 3 demonstrate intensive two-way diffusion of chemical elements of tool and stainless steel. As a result, Fe, Cr and Mo from steel are revealed at the surface layers of WC–Co cemented carbide and TiC–NiMo cermets. Similarly, W from cemented carbide and Ti from cermets are disclosed in the surface layers of stainless steel.

Table 3. Chemical composition of contact layers of tool materials and stainless steel AISI316 (EDS line scan).

Tool material	Location (on Figure 2)	Chemical composition , wt.%							
		W	Co	Ti	Cr	Ni	Mo	Fe	Others (C, Mn, Si)
85WC–Co	Tool surface (A)	60	10	–	7	2	3	13	5
	Steel surface (B)	6	25	–	6	10	1	50	2
70TiC–NiMo	Tool surface (A)	–	–	37	5	22	2	25	9
	Steel surface (B)	–	–	9	12	18	7	48	6
70TiC–FeCr	Tool surface (A)	2	–	16	46	–	7	23	3
	Steel surface (B)	–	5	4	20	8	8	50	5
70TiC–FeNi	Tool surface (A)	–	–	57	5	4	6	25	3
	Steel surface (B)	–	–	6	8	10	6	65	5

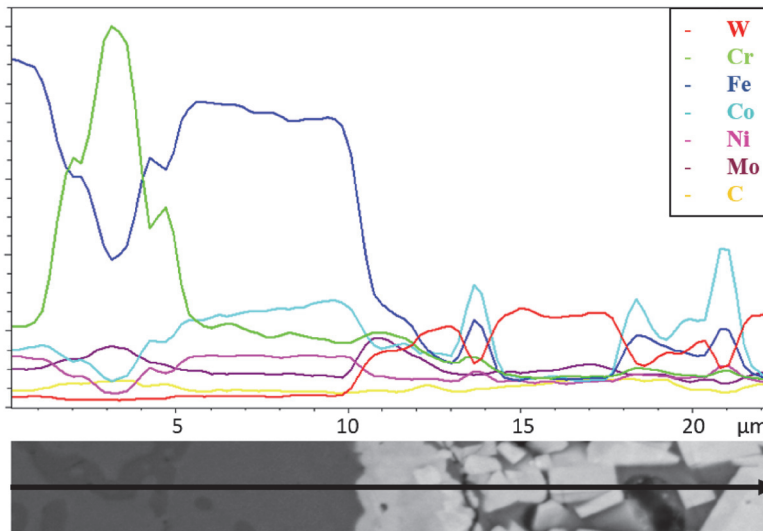


Figure 3. EDS line scan of the WC–Co tool bonded with stainless steel (AISI316) after heat treatment for four hours at 1000°C.

Carbon diffusion from carbide-based tools results in their carbon depletion and formation of Cr-containing carbides in the steel layer close to the tool – stainless steel interface (see Figure 2). Drastical decrease in Ti accompanied by marked increase in the Cr content is characteristic of TiC–FeCr cermets (see Table 3), demonstrating a high rate of wear (see Figure 1). It shows that high–Cr cermet has a great affinity to high–Cr stainless steel during the machining process, resulting in intensive diffusion and chemical wear of the tool.

4. CONCLUSIONS

The wear performance of carbide composites bonded with Ni, Co and Fe alloys, in particular of cermets TiC–NiMo, TiC–FeCr, TiC–FeNi and WC–Co cemented carbides, was investigated at 1000°C, approximately close to the FSW temperature of stainless steels. The following conclusions were drawn.

- TiC–NiMo cermets demonstrate superiority over the WC–Co cemented carbide as well as other TiC–based cermets (TiC–FeCr, TiC–FeNi). As a result of affinity to the high–chromium stainless steel, high–chromium TiC–FeCr cermets show extremely high wear rate as compared to other ceramic-based composites studied.
- Increase in the volume fraction of the carbide phase in the composites results in the improvement of the wear performance of both TiC–NiMo cermets and WC–Co cemented carbides. TiC–NiMo cermet with a starting (calculated) carbide content at about 75 wt.% and WC–Co cemented carbide with carbide content of about 90 wt.% show the best wear and mechanical performance combination (fracture toughness).

ACKNOWLEDGEMENTS

This work was supported by the institutional research funding ‘Multi-scale structured ceramic-based composites for extreme applications’ (IUT 19–29) of the Estonian Research Council.

REFERENCES

- [1] Prasanna P., Subba Rao B., Krishna Mohana Rao G. Finite element modeling for maximum temperature in friction stir welding and its validation, *Int J Adv Manuf Technol* 51, 2010, p. 925–933.

- [2] Armin Rahmati Darvazi, Mehdi Irnmanesh. Thermal modeling of friction stir welding of stainless steel 304L, *Int J Adv Manuf Technol* 75, 2014, p. 1299–1307.
- [3] Arshad Noor Siddiquee, Sunil Pandey. Experimental investigation on deformation and wear of WC tool during friction stir welding (FSW) of stainless steel, *Int J Adv Manuf Technol* 73, 2014, p. 479–486.
- [4] C. Meran, O.E.Canyurt. Friction Stir Welding of austenitic stainless steels, *Journal of Achievements in Materials and Manufacturing Engineering* 43, 2010, p. 432–439.
- [5] Yutaka S. Sato, Masahiro Muraguchi, Hiroyuki Kokawa. Tool Wear and Reactions in 304 Stainless Steel during Friction Stir Welding, *Materials Science Forum* 675–677, 2011, p. 731–734.
- [6] Kolnes M., Kübarsepp J., Sergejev F., Kolnes M. Wear of potential tool materials for aluminium alloys friction stir welding at weld temperatures, *Proceedings of the Estonian Academy of Sciences* 68, N2, 2019, p. 198–206.

Publication V

Kolnes, M., Kübarsepp, J., Sergejev, F., Kolnes, M., Tarraste, M., Viljus, M. Performance of ceramic-metal composites as potential tool materials for friction stir welding of aluminium, copper and stainless steel. *Materials*, 2020, 13 (8): 1994, 1-18.

Article

Performance of Ceramic-Metal Composites as Potential Tool Materials for Friction Stir Welding of Aluminium, Copper and Stainless Steel

Mart Kolnes ^{*}, Jakob Kübarsepp , Fjodor Sergejev, Märt Kolnes , Marek Tarraste  and Mart Viljus

Department of Mechanical and Industrial Engineering, Tallinn University of Technology, Ehitajate Tee 5, 19086 Tallinn, Estonia; jakob.kubarsepp@taltech.ee (J.K.); fjodor.sergejev@taltech.ee (F.S.); mart.kolnes1@taltech.ee (M.K.); marek.tarraste@taltech.ee (M.T.); mart.viljus@taltech.ee (M.V.)

* Correspondence: mart.kolnes@taltech.ee; Tel.: +372-620-3347

Received: 13 March 2020; Accepted: 21 April 2020; Published: 24 April 2020



Abstract: The aim of the research was to disclose the performance of ceramic-metal composites, in particular TiC-based cermets and WC-Co hardmetals, as tool materials for friction stir welding (FSW) of aluminium alloys, stainless steels and copper. The model tests were used to study the wear of tools during cutting of metallic workpiece materials. The primary focus was on the performance and degradation mechanism of tool materials during testing under conditions simulating the FSW process, in particular the welding process temperature. Carbide composites were produced using a common press-and-sinter powder metallurgy technique. The model tests were performed on a universal lathe at the cutting speeds enabling cutting temperatures comparable the temperatures of the FSW of aluminium alloys, stainless steels and pure copper. The wear rate of tools was evaluated as the shortening of the length of the cutting tool nose tip and reaction diffusion tests were performed for better understanding of the diffusion-controlled processes during tool degradation (wear). It was concluded that cermets, in particular TiC-NiMo with 75–80 wt.% TiC, show the highest performance in tests with counterparts from aluminium alloy and austenitic stainless steel. On the other hand, in the model tests with copper workpiece, WC-Co hardmetals, in particular composites with 90–94 wt.% WC, outperform most of TiC-based cermet, including TiC-NiMo. Tools from ceramic-metal composites wear most commonly by mechanisms based on adhesion and diffusion.

Keywords: cermet; hardmetal; friction stir welding; diffusion-controlled wear; adhesive wear

1. Introduction

Hardmetals (WC-based ceramic-metal composites) are extensively used under demanding wear resistance and high stiffness, e.g., in metal cutting and forming tools. The excellent wear resistance exhibited by the hardmetals is due to their combination of high hardness, wear resistance and moderate fracture toughness [1]. Cobalt is widely used as the binder metal because of its good wetting behavior and good mechanical properties. Hardmetals can be used as a tool material for friction stir welding (FSW), especially FSW of high melting point alloys [2,3] or metals with reinforcing particulates [4].

By their definition, cermets consist of ceramic particles bonded with a metal matrix, except for hardmetals that are WC-based [5]. Cermets exhibit high hardness and wear resistance at high cutting rates, as compared to WC-Co hardmetals. The most used metallic binder systems of TiC- and Ti(C, N)-based cermets are Ni alloys. However, Fe alloys have advantages over Ni and Co as metallic binders, such as potential to heat treatment, high strength and low cost. Therefore, research of completely or partially Ni- and Co-free metal composites has been intensified markedly during the last two decades.

In general, TiC cermets are applied where low density, high wear resistance or high temperature oxidation resistance is needed. In particular, TiC-cermets with a steel binder have demonstrated their superiority over ordinary WC-hardmetals in metalforming operations owing to their excellent adhesive wear resistance and low fatigue sensitivity [6].

Friction stir welding (FSW) was invented at The Welding Institute (TWI) of the United Kingdom in 1991 as a solid-state joining technique, initially applied to aluminum alloys [7]. FSW is a solid-state joining process that uses a non-consumable rotating tool with a specially designed geometry to join materials without melting them. Heating is created within the workpiece by friction between the rotating tool and welded material. The localized heating softens the material around the pin and while the tool is traversed along the joint line, it mechanically intermixes the two welded materials (see Figure 1). To avoid defects and welding tool fracture, the process temperature should not exceed 0.7 times of the melting workpiece material. The recommended temperatures range for aluminum alloys, stainless steel and copper 425–500 °C [8], 1000 °C [9] and 700–750 °C [10], respectively.

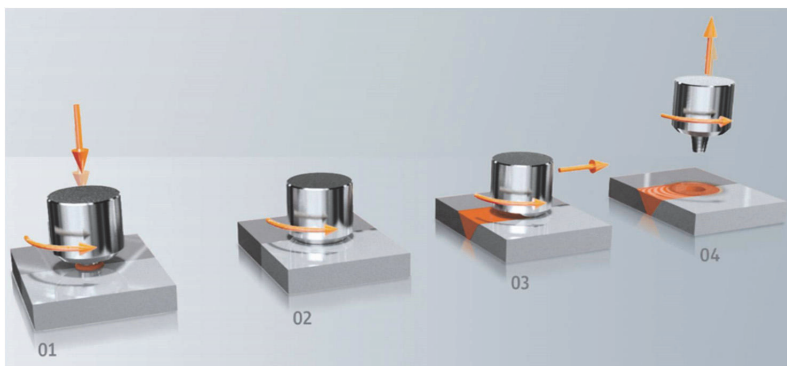


Figure 1. Process steps: (1) approach and plunge; (2) dwell for heating; (3) welding; (4) end of welding.

The solid-state nature of FSW leads to pronounced advantages over traditional fusion welding methods. One of them is the fully recrystallized, fine-grained microstructure created in the nugget by the deformation at elevated temperature. Secondly, there are no conduction problems associated with cooling from the liquid phase, such as solidification cracking, liquation cracking, porosity, and alloying element loss [11]. In addition, FSW is an emergent green technology due to its environmental friendliness and energy efficiency [12]. In comparison with other welding methods, FSW consumes considerably less energy, no shielded gas or filler materials are needed, and no toxic fumes are created during welding—FSW has low environmental impact.

Although originally FSW was invented for aluminium alloys, today it is possible to weld a wide range of metals including copper alloys, magnesium alloys, titanium alloys, stainless steels and even polymers [13]. In this work, we focused on aluminium, copper and stainless steel, because of their mediocre weldability if compared to the low-carbon steel fusion welding [14]. As a solid-state welding process, FSW can avoid the welding defects associated with fusion welding processes [4]. Each material to be welded requires a special approach for selecting the appropriate tool material. Weld quality and tool wear are two important considerations in the tool material selection. Rai et al. give the best understanding of the tool materials used for aluminium alloys and stainless steels FSW [15]. Chromium-molybdenum hot work air hardening tool steel X40CrMoV (AISI H13) and polycrystalline cubic boron nitride (pcBN) are the most widely used tool materials for aluminium alloys and stainless steels, respectively. Arulmoni et al. presents a good review of the tool materials used for friction stir processing (FSP) and FSW of copper [16]. Tool steel AISI H13 is the most common choice for the FSP/FSW of copper. Table 1 presents the tool materials widely used to weld aluminium alloys, copper and stainless steels.

Table 1. Common tool materials used for FSW of aluminium alloys, copper alloys and stainless steels [15,16].

Welded Material	Aluminium Alloy	Copper and Copper Alloy	Stainless Steel
Tool materials	AISI H13 steel, high carbon steel, HSS steel	AISI H13 steel, tungsten carbide, HSS steel	pcBN, W alloy

The tools have to withstand severe wear conditions during the FSW process. The degradation (wear) mechanism is complicated and depends on the interaction between the workpiece and the tool material, welding parameters and tool geometry. Studies on the tool wear mechanism in FSW are scarce; at the same time, adhesion, abrasion and diffusion-controlled wear are the expected wear mechanisms [15]. Wear through abrasion is substantial in the presence of a harder second phase in the workpiece material such as in aluminium matrix composites [4].

According to authors' knowledge, no comparative studies have been performed for revealing performance and degradation mechanism of ceramic-metal composites, as potential tool material, for FSW of different metals with substantially different welding temperatures. The present paper aims to demonstrate the feasibility of ceramic-metal composites use, in particular TiC-based cermets and WC-Co hardmetals, as tool materials for FSW of aluminium alloys, copper and stainless steels. The property requirements for cutting (machining) and FSW tools are quite similar [15]. Therefore, we used the model tests to study the wear of tools during workpiece material cutting. The main focus is on the performance and degradation mechanism of tool materials in the model tests simulating the wear of FSW tools.

2. Materials and Methods

2.1. Material Specifications

According to [17], the characteristics that have to be considered in selection of tool material for FSP/FSW include high compressive yield strength at elevated temperatures, no harmful reaction with workpiece material, resistance to wear (degradation), good strength and creep resistance, affordable cost etc. Ceramic-metal composites can be considered as significant FSW tool material candidates as they have high hardness, wear resistance and good mechanical properties at ambient and elevated temperatures [1].

The wear of tools made from carbide composites (WC-Co hardmetals and TiC-based cermets) during the model cutting tests of workpiece materials (Al alloy, Cu and austenitic stainless steel) was studied. The chemical composition and characteristics of starting powders for preparation of WC- and TiC- based ceramic-metal composites are shown in Table 2. The initial (starting) chemical composition, carbide content and average particle size in the sintered carbide composites and their mechanical properties are shown in Table 3. The content of tungsten carbide in the WC-Co hardmetals was 85–94 wt.% (76.4–90.0 vol.%).

In our study, TiC-based cermets were included taking into account raw materials supply, environmental safety as well as healthcare concerns related to the utilization of W and Co in hardmetals [18,19]. The most widely used metallic binder system of TiC- and Ti(C, N)- based cermets are NiMo alloys [5]. While Fe-alloys have additional advantages over Co and Ni such as low cost, potential to heat treatment and high strength, also Fe-alloy bonded TiC-FeCr and TiC-FeNi cermets were under investigation. The content of titanium carbide in TiC-based cermets was 70–80 wt.%, ensuring the fraction comparable that of the hardmetals carbide fraction of 79.3–92.1 vol.% (see Table 3).

Table 2. Characteristics of the starting powders.

Material	Chemical Composition (wt.%)	Powder Particle Size (μm)	Supplier
WC	W—base; C—6.13; oth. < 0.14	D50 = 0.86	Wolfram Bergbau und Hütten AG (Sankt Martin im Sulmtal, Austria)
TiC	Ti—base; C _{total} —19.12; C _{free} —0.15; oth. < 0.31	2.0–3.0	Pacific Particulate Materials Ltd. (New Westminster, BC, Canada)
Co	Co—99.5; oth.—0.5	5.0–6.0	Pacific Particulate Materials Ltd. (New Westminster, BC, Canada)
Fe	Fe—99.72; Si—0.01; P—0.07; Mn—0.02; oth—C	40–90	Rio Tinto (London, UK)
Ni	Ni—99.8; oth.—0.2	3.0–5.0	Pacific Particulate Materials Ltd. (New Westminster, BC, Canada)
Mo	Mo—99.8; oth.—0.2	1.0–3.0	Pacific Particulate Materials Ltd. (New Westminster, BC, Canada)
AISI430L	Fe—base; Fe—16.8; Mn—0.69; Si—0.64; oth < 0.05	10–45	Sandvik Osprey Ltd. (Neath, UK)

Table 3. Chemical compositions, average carbide particle size and mechanical properties of tool materials under investigation.

Designation	Initial Composition (wt.%)		Carbide Content after Sintering (vol.%)	Hardness HV30	Fracture Toughness, (MPa·m ^{1/2})	Average Carbide Particle Size, (μm)
	Carbide	Binder				
85WC-Co	85WC	15Co	76.4	1150 ± 20	17.8 ± 0.5	0.91
90WC-Co	90WC	10Co	83.7	1238 ± 6	16.7 ± 0.3	1.19
94WC-Co	94WC	6Co	90.0	1765 ± 25	7.2 ± 0.3	0.48
70TiC-NiMo	70TiC	20Ni; 10Mo	87.7	1340 ± 21	12.6 ± 0.3	1.21
75TiC-NiMo	75TiC	16.7Ni; 8.3Mo	89.9	1403 ± 25	11.4 ± 0.4	1.14
80TiC-NiMo	80TiC	13.3Ni; 6.7Mo	92.1	1492 ± 16	10.1 ± 0.4	1.60
70TiC-FeCr	70TiC	24.9Fe; 5.1Cr	84.0	1352 ± 6	9.1 ± 0.7	1.99
70TiC-FeNi	70TiC	25.8Fe; 4.2Ni	79.3	1379 ± 21	15.2 ± 0.5	1.60

The carbide volume content was calculated taking into account the dissolution of Mo in TiC and the formation of secondary Cr-based carbides in TiC-NiMo and TiC-FeCr cermets, respectively [20]. The microstructures of selected carbide composites are shown in Figure 2. All the composites were produced using conventional powder metallurgy technology routes for hardmetals and cermet. Powder mixtures for starting powders were prepared using conventional ball mill with WC-Co lining and balls for duration of 72 h at the ball to the powder weight ratio of 10:1. Isopropyl alcohol was used as a milling liquid. The WC-Co contamination from milling was approximately 5 wt.% in case of TiC-based cermet. Tungsten carbide dissolves in titanium carbide and cobalt in metallic binder. Milled powders were mixed with 3 wt.% paraffin, granulated, dried and compacted into green bodies with 100 MPa of uniaxial pressure. Pressureless liquid phase sintering in vacuum (0.1–0.5 mbar) during 30 min was carried out to obtain specimens for the mechanical and model (cutting) tests. The optimal sintering temperatures of 1450–1500 °C (depending on the composition) for achieving near-full densification (low porosity) and maximal mechanical characteristics were used. Heating rate up to the sintering temperature was 10 °C min⁻¹, followed by dwelling at the final temperature and cooling with furnace. The porosity of the consolidated ceramic-metallic composites was under 0.5 vol.%. The porosity was evaluated by measuring the surface area of pores on the optical image of the microstructure at the magnification of 200 times. Optical microscope Axiovert25 (Carl Zeiss AG, Oberkochen, Germany) and software Buehler Omnimet were used. The chemical composition of the counterpart materials for the model tests is shown in Table 4.

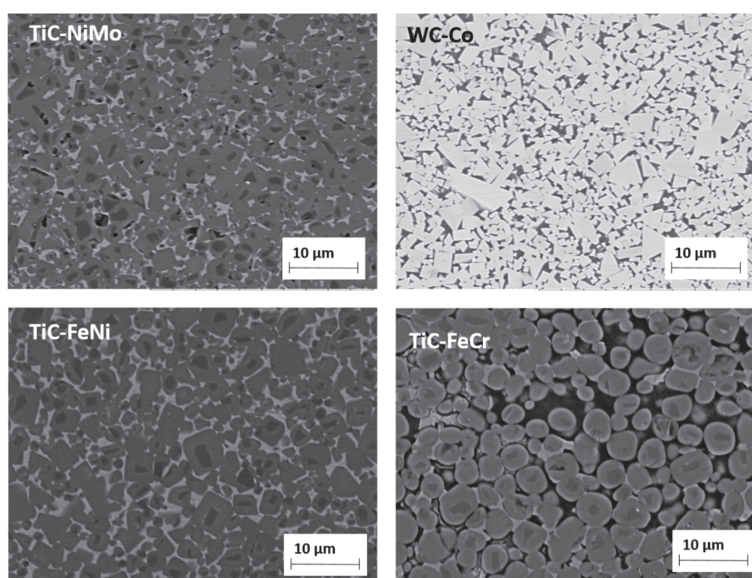


Figure 2. SEM micrographs of 75TiC-NiMo, 85WC-Co, 70TiC-FeNi and 70TiC-FeCr.

Table 4. Chemical composition of counterpart materials for model testing.

Workpiece Material	Chemical Composition (wt%)				
Aluminium alloy (AW6082-T6)	96.9 Al	1.1 Si	0.5 Mn	0.8 Mg	0.7 Other
Copper (Cu-ETP)			99.9 Cu		0.1 Other
Stainless steel (AISI 304)	70.7 Fe	1.6 Mn	18.0 Cr	8.1 Ni	0.3 Si 1.3 Other

2.2. Experimental Details

To evaluate the wear performance of different carbide composites during the FSW of aluminium alloy, copper and stainless steel, the model tests were performed on a universal lathe (see Figure 3a), using cutting tools from carbide composites with specific geometry (see Figure 3b). Tools were grounded to achieve a nose angle of 134° , side cutting edge angle of 23° and side relief angle of 8° . The set of three specimens were produced for every tested material, to assess the reliability and the reproducibility of experimental results. The investigated material bars were machined at high speed, up to 630 m/min, 470 m/min and 280 m/min to achieve the cutting zone temperature approximately similar to that of the welding temperature for aluminium alloy (400°C), copper (600°C) and stainless steel (1000°C), respectively. The feed rate and the depth of the cut were kept constant during testing at 0.39 mm/rev and 0.125 mm, respectively. Common FSW temperatures for Al-alloys ($\sim 400^\circ\text{C}$) and stainless steel ($\sim 1000^\circ\text{C}$) were achieved at described cutting speeds, while for copper temperature of 600°C , which is somewhat below regular FSW temperature ($700\text{--}750^\circ\text{C}$), was achieved as maximum.

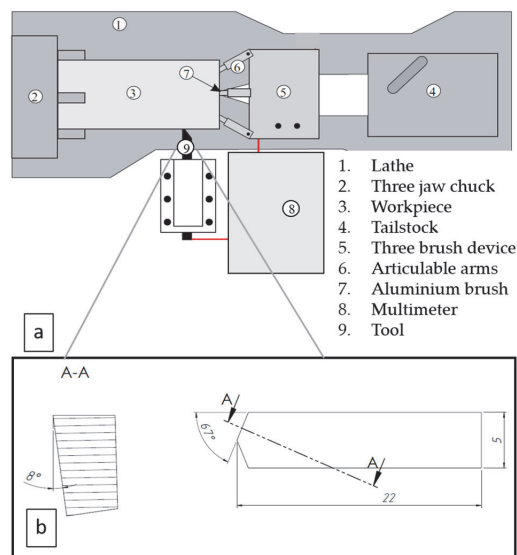


Figure 3. Schematic of the tool-workpiece thermocouple system (a) and cutting tool geometry (b).

To measure the cutting temperature in the cutting point, a tool-workpiece thermocouple method was used for all tested materials [21]. Detailed calibration, temperature measurement and cutting wear test parameters were described in [22]. The wear rate of the tool was determined as the shortening in the length of the cutting tool nose tip of the model test specimens. Shortening of the cutting nose tip was measured on the top surface of the tool in the case of aluminium alloy and copper as workpiece materials, using the images made from the top surface of the cutting tool by Hitachi TM 1000 Tabletop scanning electron microscope (Hitachi High-Tech, Krefeld, Germany) (see Figure 4). In the model tests with stainless steel, the height of the wear pattern was measured on the front surface of the tool because the tool wear rate was significantly more intensive. These measurement results were recalculated to the shortening of the cutting nose tip on the top surface for better comparison.

In the present research reaction diffusion tests were performed for better understanding of the diffusion controlled processes during tool degradation. The reaction diffusion of tool material is one of the important reasons of FSW tool degradation by intergrain fracture during working of aluminium alloys, especially if taking into account the acceleration of diffusion by temperature and contact stresses developed in the FSW. Fragments of the FSW tool material are deformed and detached from the FSW

tool by fracture along the embrittled grain boundaries under the shear stress developed on the surface of the tool during FSW [23]. Diffusion of workpiece material elements to tool is especial concern in FSW/FSP of high-melting point metals. As an example FSW tool wear by rapid-rate diffusion of elements from Ti- alloy into W-Re alloy tool causing degradation and wear by subsurface fracture has been reported [24]. Similar processes are significant considering FSW of steels and copper characterized by much higher working temperatures and contact stresses if compared to aluminium alloys.

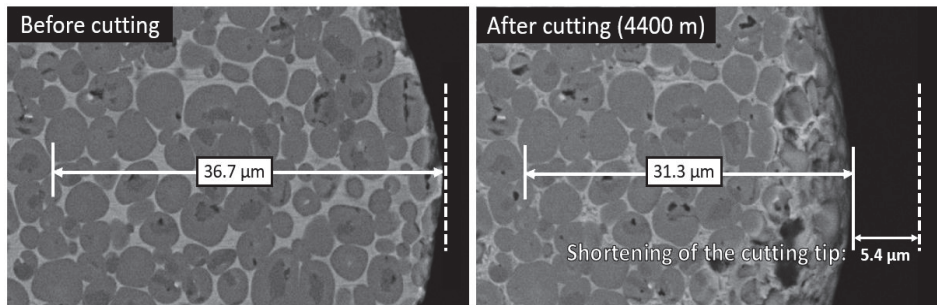


Figure 4. The measurement of the shortening of 70TiC-FeCr tool on the top surface of cutting nose tip after cutting aluminium alloy (cutting distance 4400 m).

It is known, that during the FSW of aluminium alloys FSW tool is covered by tribological deposits [23]. Similarly, during model cutting tests of aluminium alloy ceramic-metal tools were covered by strongly adhered layers of the workpiece material [22]. Such layers enable analysis of diffusion processes in the contact region of tool-workpiece. Unfortunately, the formation of such tribological layers was not evident during the model tests using stainless steel and copper as workpiece materials. Therefore, the special test samples were prepared for all tool and workpiece materials groups. Ceramic-metal composites with the highest binder fraction from each tested tool material group were selected (85WC-Co, 70TiC-NiMo, 70TiC-FeCr, 70TiC-FeNi) for achieving deeper diffusion of elements from workpiece materials into tool. The test samples for studying diffusion-controlled processes were prepared using spark plasma co-consolidation of sintered carbide composite specimens and workpiece material or material powder with similar chemical composition to obtain a permanent bond between the tool material and the metal (Al-alloy, copper, stainless steel). Reaction diffusion tests were performed by heating the test samples up to approximately the same temperature as in the model tests, followed by 4 h dwelling at that temperature in vacuum furnace. Such heating time is relatively short in comparison with FSW tool life during welding of aluminium alloys and copper. To understand the distribution of chemical elements in the microstructure in the tool-workpiece contact region, the scanning electron microscope (Zeiss EVO MA15, Oberkochen, Germany) equipped with energy-dispersive X-ray spectroscopy system INCA (Oxford Instruments, Wycombe, UK) was used.

Hardness and fracture toughness of sintered composites were determined using ground test specimens of 5 mm × 5 mm × 17 mm. Hardness (HV30) was measured with a hardness tester Indentec 5030KV (Indentec Hardness Testing Machines Limited, West Midlands, UK). Toughness was evaluated with the indentation method (Palmqvist method) using equation described in [25].

3. Results

Table 5 and Figure 5 presents tool materials wear rate (shortening of the cutting tool nose tip) in model tests with different workpiece materials. (Figures 5–7 for aluminium alloy, stainless steel and copper, respectively). Maximal cutting distances were 8800 m, 150 m and 920 m in case of aluminium alloy, stainless steel and copper, respectively. Although aluminium alloy is the softest of workpiece materials the cutting process proved to be unstable and tools were subjected to severe dynamic loads.

Therefore, the hardmetal and cermets with high binder fraction and fracture toughness were used in tests with workpiece material from aluminium alloy.

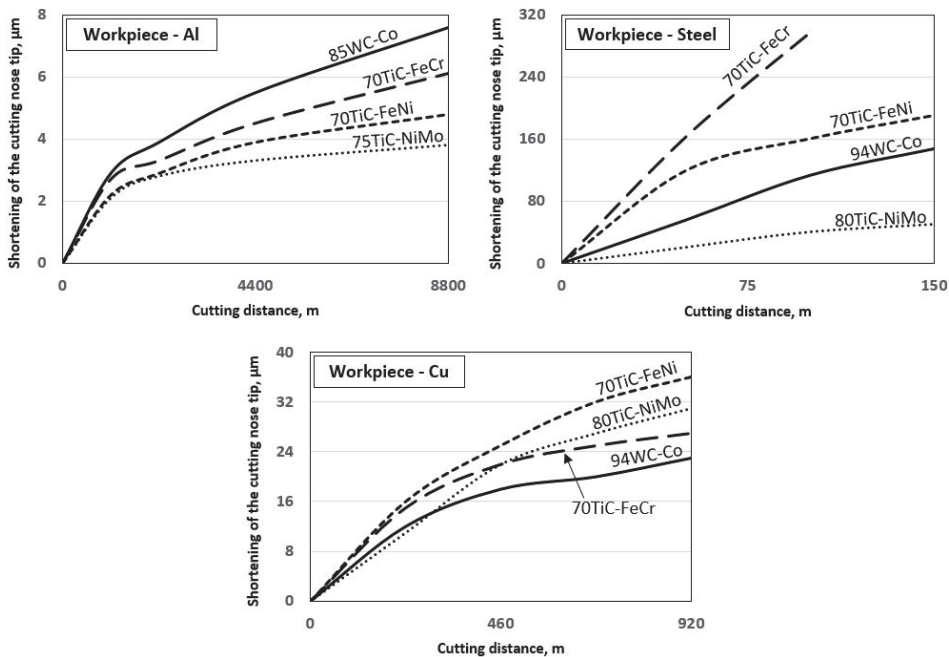


Figure 5. Wear of ceramic-metal composites vs. cutting distance in the case of all workpiece materials at work temperatures.

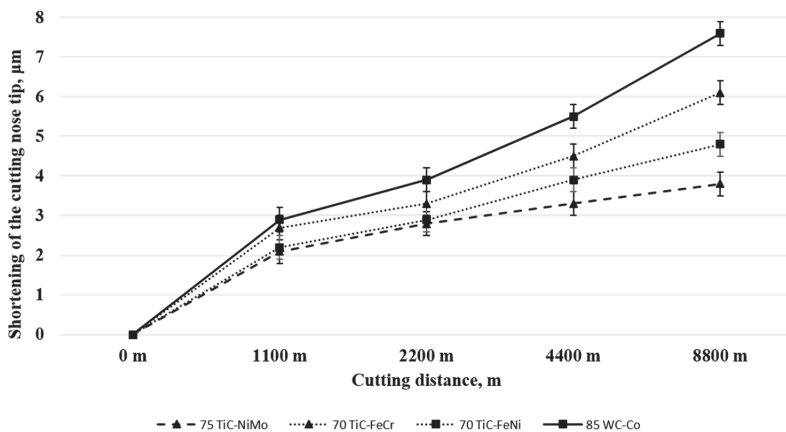


Figure 6. Wear of ceramic-metal composites vs. cutting distance in the case of aluminium alloy at 400 °C.

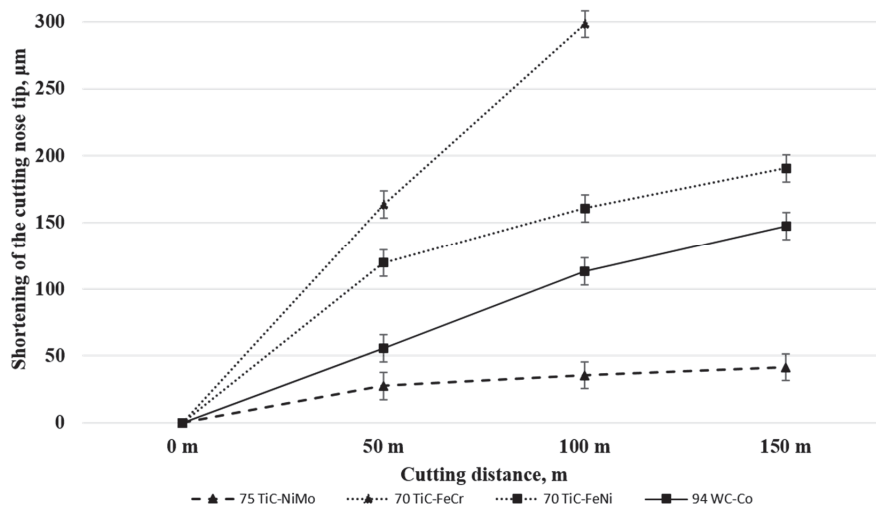


Figure 7. Wear of tested ceramic-metal composites vs. cutting distance in the case of stainless steel at 1000 °C.

Table 5. The selection of tool materials for model test.

Workpiece Material	Tool Materials Wear Rate at Maximal Cutting Distances (Shortening of the Cutting Tool Nose Tip, µm)							
	85WC-Co	90WC-Co	94WC-Co	70TiC-NiMo	75TiC-NiMo	80TiC-NiMo	70TiC-FeCr	70TiC-FeNi
Aluminium alloy (AW6082-T6)	7.6	-	fracture	-	3.8	-	6.1	4.8
Stainless steel (AISI 304)	258	174	147	108	42	50	298	191
Copper (Cu-ETP)	28	26	23	37	38	31	27	36

3.1. Working of Aluminium Alloy

Figure 6 and Table 5 demonstrate the wear performance plotted against the cutting distance of the WC-Co hardmetal and TiC-based cermets. Wear of ceramic-metal tools during model tests with workpiece from aluminium alloy at 400 °C is very small even at considerable cutting distances. For that reason, selected composites (5) from Table 3 were tested.

WC-Co hardmetal 85WC-Co demonstrated the highest wear rate during testing. This ceramic-metal composite showed also the highest wear gain during an increase of the cutting distance (compare wear rate increase angles of different composites in Figure 6). All TiC-based cermets showed an advantage over the hardmetal. However, cermets with NiMo binder are at advantage over composites with Fe-alloy binders (FeCr and FeNi).

3.2. Working of Stainless Steel

Figure 7 and Table 5 demonstrate wear (shortening of the cutting tool nose tip) plotted against the cutting distance of ceramic-based composites of different composition and carbide fraction. For clarity, Figure 7 shows testing results only for the most wear resistant grades of WC-Co hardmetals and TiC-NiMo cermets in Table 5. Unlike the model test results with aluminium alloy workpiece (at 400 °C), the wear of cermet and hardmetal tools was pronounced during cutting of stainless steel (at 1000 °C) even at comparatively short cutting distances (see Figure 5). Increase in the volume fraction of the carbide phase and hardness in the composites enhances wear performance of WC-Co hardmetals and TiC-NiMo cermets. Regardless of high chromium content, ensuring enhanced resistance to oxidation, FeCr alloy bonded cermet showed the highest wear rate as well as wear gain during the increase of the cutting distance. An alternative Fe-alloy bonded 70TiC-FeNi cermet exhibited better wear performance

at the level of WC-Co hardmetals. TiC-NiMo cermets with 75–80 wt.% TiC demonstrated superior wear performance in such conditions. Such results prove different wear mechanisms during testing of aluminium alloy workpiece and stainless steel at substantially different working temperatures.

3.3. Working of Copper

Figure 8 and Table 5 show wear performance plotted against the cutting distance of WC- and TiC- based ceramic-metal composites of different composition and fraction of carbides. For clarity, Figure 8 presents the testing results only for the most wear resistant grades of WC-Co hardmetals and TiC-NiMo cermets. Increase in the carbide (WC or TiC) fraction improves the wear performance of both WC-Co hardmetals and TiC-NiMo cermets (see Table 5). As different from the model tests with workpieces from aluminium alloy and stainless steel, WC-Co hardmetals with 90–94 wt.% WC demonstrated the best performance. It should be pointed out that 70TiC-FeCr cermet also showed high wear resistance, which, however, demonstrated the lowest performance during working of stainless steel (see Figure 5). Regardless of substantial performance of TiC-NiMo cermets in the model tests with Al alloy and stainless steel, NiMo-alloy bonded cermets compare unfavourably with WC-Co hardmetals when the counterpart is copper. These results demonstrate different wear mechanisms during testing (cutting) of workpieces from different metals at substantially different temperatures and contact stresses.

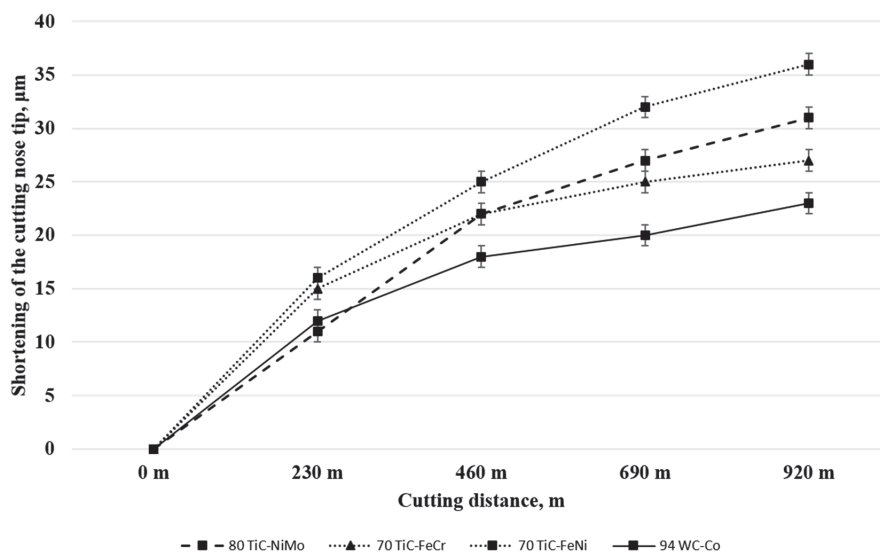


Figure 8. Wear of ceramic-metal composites vs. cutting distance in the case of copper at 600 °C.

4. Discussion

The tools have to bear severe wear during the FSW process and during the model cutting tests used in our research. Abrasion, adhesion as well as diffusion-controlled wear are the expected wear mechanisms. Previous research [26–28] has shown that at a similar volume fraction of carbides the TiC-based cermets, independent of their binder composition and structure in abrasive-erosion and in the abrasive wear conditions, are at a disadvantage in relation to the WC-based hardmetals. However, cermets with a steel binder are at an advantage over cermets with a NiMo-binder (at room temperature). The performance of carbide composites in abrasion conditions is controlled primarily by the stiffness of the composite—its resistance to elastic (evaluated by the modulus of elasticity) and plastic (evaluated by proof stress) straining and depends primarily on the properties of carbide phase (WC vs. TiC).

Prognosis of abrasive wear performance based on hardness may lead to pronounced mistakes when composites based on different ceramic phase are considered [26,27].

Adhesive wear performance (unlike performance in abrasion conditions) of cermets may be comparable to that of WC-based composites. It is controlled primarily by composite resistance to local plastic straining featured by the proof stress, depending both on the properties of metallic and ceramic phases. Similar to abrasion, inconclusive influence of hardness on the adhesive wear performance of ceramic-metal composites with substantially different composition must be highlighted. However, an increase in ceramic fraction and hardness in composites based on similar carbides and metallic binder results in the improvement of the wear performance [26,28].

Tool degradation under FSW conditions and during the model cutting tests is increased at elevated temperatures, by the reactions of the tools with the workpiece and with the oxygen-containing atmosphere. Therefore, reactivity of the tool material also accounts for severe wear during working at high temperatures. Diffusion controlled chemical reactions determine the nature of the interface formed between the tool and the workpiece. Tool material properties will alter at high temperatures, leading to a higher likelihood of tool degradation or even failure.

4.1. Working of Aluminium Alloy

Figure 6 and Table 5 demonstrate that TiC-based cermets with Ni- and Fe- alloy binders are at an advantage over WC-Co hardmetal. It may be explained to a considerable extent by the higher carbide fraction (see Table 3) as well as hardness of cermets. 94WC-Co hardmetal with substantially higher carbide fraction and hardness (and the lowest fracture toughness) suffered structural failure after comparatively short cutting distances.

During working (cutting) of plastic metals with the fractional content of hard second phases, tools fail most commonly by mechanisms based on adhesion and diffusion. Adhesion as the key wear mechanism is the reason why result of TiC-based cermets, in particular TiC-NiMo composites, demonstrate superiority over the WC-Co hardmetal during working of aluminium alloy. Adhesion as the wear mechanism is confirmed by strongly adherent workpiece metal deposits (layers) on the rake face of ceramic-metal tools. Other researchers addressing the wear mechanism of tools during FSW of Al- [23] and Ti- alloys [29] have made similar observations. Also, Al diffusion has been shown to be a degradation factor in the tools used for FSW of aluminium [23]. These diffusions-controlled reactions are possible due to the combinations of both local high thermal and high mechanical loading effects on the tool. It may lead to the formation of hard and brittle intermetallic compounds in heat affected zones of Co-, Ni- and Fe- based binders of ceramic-metal composite tools. The embrittlement created at the grain boundaries of a tool material may increase the likelihood of degradation under severe stresses that the tool surfaces are exposed to.

Figure 9 demonstrates the EDS mapping of Co-, Ni- and Fe- based binders in contact with Al-based workpiece material after heat treatment of 4 h at 400 °C. Diffusion of aluminium into ceramic-metal composites metallic phase is quite marginal as compared to the diffusion of stainless steel components and copper at 1000 °C and 600 °C (see Figures 10 and 11), respectively. Detailed study described in [22] based on the EDS line scan of the contact region “tool-aluminium alloy” has demonstrated that the diffusion of Al was the highest into the WC-Co hardmetal both in depth and intensity (content) while the lowest into the TiC-NiMo cermet. The highest wear gain during an increase of the cutting distance of the WC-Co hardmetal can be explained by the formation of hard and brittle intermetallic phases in the contact region of the tool-workpiece, whereas their amount increases with an increase in the aluminium content.

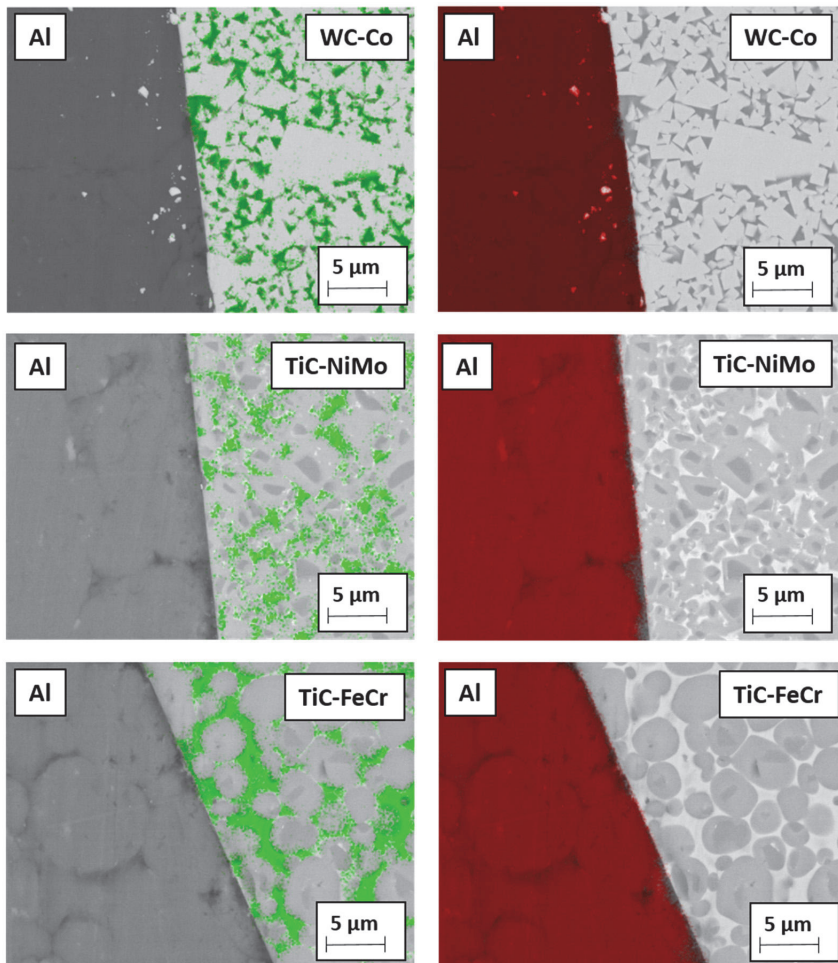


Figure 9. EDS mapping of permanent bond between tool materials and aluminium alloy heating in vacuum during 4 h at 400 °C: green—metallic binder (Co, Ni, Fe), red—aluminium.

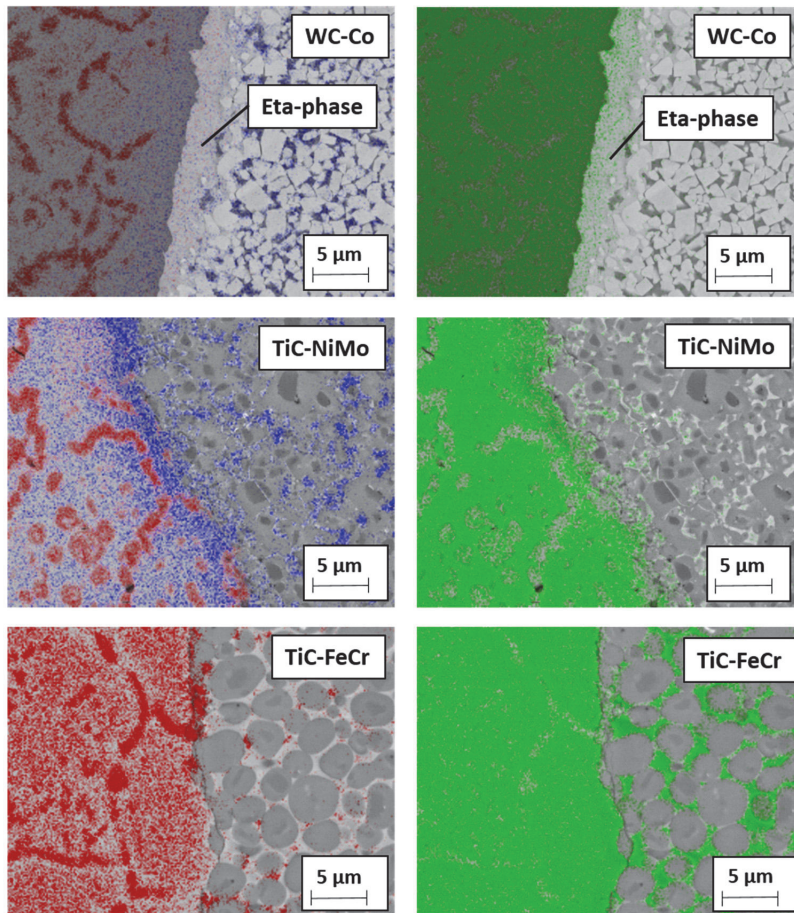


Figure 10. EDS mapping of permanent bond between tool materials and stainless steel after heating in vacuum during 4 h at 1000 °C: red—chromium, green—iron, blue—metallic binder (Co, Ni).

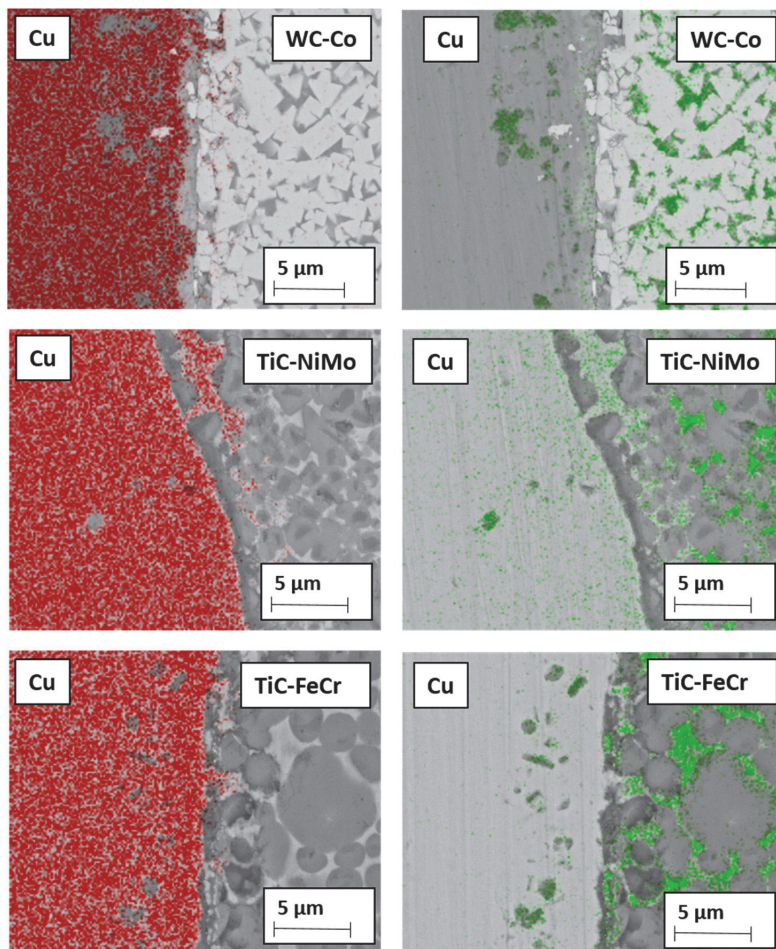


Figure 11. EDS mapping of permanent bond between tool materials and copper after heating in vacuum during 4 h at 600 °C: red—copper, green—metallic binder (Co, Fe, Ni).

4.2. Working of Stainless Steel

Figure 7 and Table 5 show that TiC-NiMo cermets with 75–80 wt.% TiC outperform 94WC-6Co hardmetal with the highest hardness (at room temperatures) among ceramic-metal composites considered. TiC-based cermets with Fe-alloy binders are at a disadvantage in relation to all ceramic-metal composites under investigation.

Ni-based alloys can withstand severe operating conditions involving high temperature and corrosion environments. Such alloys with excellent elevated temperature properties, in particular NiMo alloys, are used at the highest homologous temperature if compared to any common metallic alloy systems [30,31]. The Ni-based binders in cermets can decidedly handle the heat generated during FSW and the model cutting process better than cobalt in WC-Co hardmetal and Fe-based alloy in the TiC-FeNi and TiC-FeCr cermets.

Experimental investigation of WC-based tool materials wear during the FSW of stainless steel has shown that the wear at a pin root and at the bottom face of the pin is attributed mainly to diffusion, adhesion and attrition mechanisms [3]. Hot adhesion is one of the wear mechanisms behind the

result that TiC-NiMo cermets demonstrate superiority over abrasive wear resistant WC-Co hardmetals during working of stainless steel.

During cutting of stainless steel, tool materials are exposed to high temperatures affecting remarkably the mechanism of wear. The presence of Fe and Cr in stainless steel strongly influences the dissolution of carbide particles present in the WC-Co hardmetal as well as in TiC-based cermet tool materials. Dissolution of WC leads to the formation of carbon deficient forms of tungsten carbide W_2C , Co_xW_yC compounds (eta phase) and $M_{23}C_6$ phases [32]. During welding at high temperatures, the Fe present in the stainless steel also diffuses into the tool and forms a solid solution with cobalt [3]. The carbon liberated during the dissolution of WC dissolves in the Co-Fe solid solution and its solubility increases as the amount of Fe in the solid solution increases. Brittle metallic carbide compounds are easily removed by mechanical action, giving rise to craters on the surface of the tool [3]. These diffusion-controlled processes—formation of carbon deficient forms of tungsten carbide and metallic carbides in Co binder—remain relevant wear processes during FSW and during cutting in the model wear tests with the WC-Co tool.

Figure 10 demonstrates the EDS mapping of the WC-Co hardmetal and TiC-based cermets in contact with stainless steel after heat treatment 4 h at 1000 °C. The figure shows the formation of brittle carbon deficient tungsten carbide (eta phase) interaction layer at the interface between the cemented carbide and steel. High stresses acting on the tool at high temperature during the cutting process may lead to dislodging of this layer on the tool surface. This diffusion-controlled mechanism is probably behind the decreased wear performance of the WC-Co hardmetal as compared to the wear of TiC-NiMo cermets.

As different from tungsten carbide (WC), titanium carbide (TiC_x) exists as a homogeneous phase over a relatively wide range of carbon content. Dissolution of TiC leads to the formation of substoichiometric carbide particles, not special carbon deficient forms of carbide. As a result, no clear interaction layer at the interface cermet-steel was observed (see Figure 10), i.e., high-temperature diffusion-controlled wear mechanism of TiC-based cermets is different. At high temperatures of the model tests, the iron present in the stainless steel diffuses into the TiC-NiMo cermet tool, forming a solid solution with Ni (see Figure 10). The carbon liberated during the dissolution of TiC dissolves in Ni-based binder, favouring formation of additional metallic carbides. Also, diffusion of carbon to low-carbon austenitic stainless steel takes place during the reaction diffusion tests, favouring formation of the network of chromium carbides in steel (see Figure 9). During the working of stainless steel, this process is similar both to the WC- and TiC- based ceramic-metal composites.

TiC-FeCr cermet demonstrated the highest wear rate (the lowest wear performance) during the model testing. This composite showed also the highest wear gain rate during the increase of the cutting distance (see Figure 7). Diffusion-controlled processes play probably a secondary role in such a rapid degradation process of a cermet tool. The wear performance decrease may be explained by strong chromium steel-to-chromium steel adhesion and tool surface attrition in the contact region of a tool-workpiece.

4.3. Working of Copper

Figure 8 and Table 5 demonstrate that WC-Co hardmetals with 90–94 wt.% tungsten carbide outperform all cermets, in particular TiC-NiMo ones which showed the highest degradation resistance during working of the stainless steel (see Figure 7). WC-Co composites show better performance if compared to TiC-NiMo cermets even if they compare unfavourably with hardness (see Table 3 and Figure 5).

While tool wear during the FSW of aluminium and aluminium alloys, steels and titanium and its alloys has attracted interest of several researchers, only a few studies focused on copper alloys are available [10,33,34]. Investigation of the wear mechanism for the H13 steel tool during FSW of Cu-Cr-Zr alloy showed severe wear due to high stresses at elevated temperatures. The sticking of Cu over the tool material surface occurred due to diffusion bonding between copper and steel.

The analyses showed that diffusion of Fe from the tool and Cu from the workpiece takes place across the interface. Diffused Fe and Cu form a solid solution layer over the tool surface without any intermetallic formation as per the Fe-Cu phase diagram. High stresses on the tool surface at high temperature may result in dislodging of this layer on the tool surface [33]. Currently, no wear mechanism study is available for hardmetals or cermets during the FSW of copper or copper alloys.

Adhesion as one of the wear mechanisms is confirmed by adherent workpiece (copper) metal deposits on the rake face of tools during the model tests as a result of high stresses acting on the tool at high temperature. In addition to adhesion, diffusion is one of the factors for tool degradation. Figure 11 demonstrates the EDS mapping of the ceramic-metal composites with Co-, Ni- and Fe- based binders in contact with copper after heat treatment at 600 °C. The figure shows a comparatively high diffusion depth of Cu in Ni-alloy of the TiC-NiMo cermet as compared to Cu diffusion in WC-Co and TiC-FeCr composites. It is in agreement with the corresponding phase diagrams Cu-Ni, Cu-Fe and Cu-Co, demonstrating high mutual solubility of Cu and Ni and very low in Cu-Co and Cu-Fe systems even at the temperature of 600 °C. On the other hand, diffusion of Co, Ni and Fe takes place from tools across the interface into the copper workpiece. Intensive diffusion of Cu into the TiC-NiMo binder phase (Cu diffuses faster in Ni than vice-versa) results in a local increase of the binder fraction of the cermet and in a decrease of hardness. It may cause increased wear rate of TiC-NiMo cermets (and also TiC-FeNi cermet) as compared to WC-Co hardmetals and TiC-FeCr cermet. However, more detailed investigations are needed to comment the tool wear mechanism during working of Cu with higher confidence.

5. Conclusions

This paper addresses the feasibility of utilizing ceramic-metal composites, in particular TiC-based cermets and WC-Co hardmetals, as tool materials for friction stir welding (FSW) of different metals (aluminium alloy, austenitic stainless steel and copper). Model tests for the wear study of tools from TiC- and WC- based ceramic-metal composites during working of workpiece metals at the cutting temperatures approximately similar to the FSW temperatures and reaction-diffusion tests performed for better understanding of diffusion-controlled processes resulted in the following conclusions.

1. TiC-based cermets with Ni- and Fe- alloy binders show the highest performance in the model tests with workpiece from aluminium alloy.
2. TiC-NiMo cermets demonstrate the highest while cermets with Fe-alloy binders the lowest wear performance in the model tests using counterpart from austenitic stainless steel. An excellent elevated temperature performance is behind the high degradation resistance of TiC-NiMo cermets.
3. WC-Co hardmetals, in particular composites with 90–94 wt.% WC, outperform most of TiC-based cermet grades in the model tests with a workpiece from copper. Hardmetals show better performance if compared to cermets, in particular TiC-NiMo composites demonstrating high wear resistance during working of stainless steel, even if they compare unfavourably with hardness.
4. Irrespective of workpiece metal (aluminium alloy, stainless steel, copper), the most common wear mechanisms of tools from ceramic-metal composites in the model tests are adhesion and diffusion.

Author Contributions: Conceptualization, M.K. (Mart Kolnes), J.K. and F.S.; methodology, M.K. (Mart Kolnes) and J.K.; software, M.T. and M.V.; validation, J.K. and F.S.; formal analysis, M.K. (Mart Kolnes) and M.T.; investigation, M.K. (Mart Kolnes), M.T. and M.K. (Märt Kolnes); resources, M.K. (Mart Kolnes), J.K., M.T. and M.V.; data curation, J.K. and F.S.; writing—original draft preparation, M.K. (Mart Kolnes), J.K. and M.K. (Märt Kolnes); writing—review and editing, M.K. (Mart Kolnes), J.K., F.S., M.K. (Märt Kolnes) and M.T.; visualization, M.K. (Mart Kolnes), M.T. and M.V.; supervision, J.K. and F.S.; project administration, J.K.; funding acquisition, J.K. All authors have read and agreed to the published version of the manuscript.

Funding: This work was supported by the institutional research funding project ‘Multi-scale structured ceramic-based composites for extreme applications’ (IUT 19–29) and by the grant “Composites “ceramics-Fe alloy” for a wide range of application conditions” (PRG665) of the Estonian Research Council.

Acknowledgments: The research was supported by the Estonian Research Council projects IUT 19-29 and PRG 665.

Conflicts of Interest: The authors declare no conflict of interest.

References

1. Brookes, K.J. *World Directory and Handbook of Hardmetals and Hard Materials*; Metal Powder Industry: London, UK, 1996.
2. Choi, D.H.; Lee, C.W.; Ahn, B.W.; Choi, J.H.; Yeon, Y.M.; Song, K.; Park, H.S.; Kin, Y.J.; Yoo, C.D.; Jung, S.B. Frictional wear evaluation of WC-Co alloy tool in friction stir spot welding of low carbon steel plates. *Int. J. Refract. Met. Hard* **2009**, *27*, 931–936. [[CrossRef](#)]
3. Siddiquee, A.N.; Pandey, S. Experimental investigation of deformation and wear of WC tool during friction stir welding (FSW) of stainless steel. *Int. J. Adv. Manuf. Technol.* **2014**, *73*, 479–486. [[CrossRef](#)]
4. Liu, H.J.; Feng, J.C.; Fujii, H.; Nogi, K. Wear characteristics of a WC-Co tool in friction stir welding of AC4A + 30 vol% SiCp composite. *Int. J. Mach. Tool Manu.* **2005**, *45*, 1635–1639. [[CrossRef](#)]
5. Hardmetals. *Comprehensive Hard Materials*, 1st ed.; Sarin, V.K., Ed.; Elsevier: Amsterdam, The Netherlands, 2014.
6. Klaasen, J.; Kübarsepp, J. Wear of advanced cemented carbides for metalforming tool materials. *Wear* **2004**, *256*, 846–853. [[CrossRef](#)]
7. Thomas, W.M.; Nicholas, E.D.; Needham, J.C.; Murch, M.G.; Temple-Smith, P.; Dawes, C.J.G.B. Friction Welding. Patent 9,125,978.8, 6 December 1991.
8. Threadgill, P.L.; Leonard, A.J.; Shercliff, H.R.; Withers, P.J. Friction stir welding of aluminium alloys. *Int. Mater. Rev.* **2009**, *54*, 49–93. [[CrossRef](#)]
9. Prasanna, P.; Rao, B.S.; Rao, G.K.M. Finite element modeling for maximum temperature in friction stir welding and its validation. *Int. J. Adv. Manuf. Technol.* **2010**, *51*, 925–933. [[CrossRef](#)]
10. Nakata, K. Friction stir welding of copper and copper alloys. *Weld. Int.* **2005**, *19*, 929–933. [[CrossRef](#)]
11. Kah, R.; Tajan, R.; Matrikainen, J.; Suoranta, R. Investigation of weld defects in friction-stir welding and fusion welding of aluminium alloys. *Int. J. Mech. Mater. Eng.* **2015**, *10*, 26. [[CrossRef](#)]
12. Kumar, A.; Gautam, S.S.; Kumar, A. Heat input & joint efficiency of three welding processes TIG, MIG and FSW using AA6061. *Int. J. Mech. Eng. Rob. Res.* **2014**, *1*, 89–94.
13. Strand, S. Joining plastics-can friction stir welding compete. In Proceedings of the Electrical Insulation Conference and Electrical Manufacturing and Coil Winding Technology Conference, Indianapolis, IN, USA, 25–25 September 2003; pp. 321–326.
14. Olson, D.L.; Siewert, T.A.; Liu, S.; Edwards, G.R. Welding, brazing and soldering. In *ASM Handbook*; ASM International: Cleveland, OH, USA, 1993; Volume 6.
15. Rai, R.; De, A.; Bhadeshia, H.K.D.H.; DebRoy, T. Review: Friction stir welding tools. *Sci. Technol. Weld. Join.* **2011**, *16*, 325–342. [[CrossRef](#)]
16. Jeganathan Arulmoni, V.; Ranganath, M.S.; Mishra, R.S. Friction stir processed copper: A review. *Int. Res. J. Sustain. Sci. Eng.* **2015**, *3*, 1–11.
17. Mishra, R.; De, P.S.; Kumar, N. *Friction Stir Welding and Processing*; Springer: Berlin/Heidelberg, Germany, 2014.
18. Critical Raw Materials. Available online: https://europa.eu/growth/sectors/raw-materials/specificinterest/critical_et (accessed on 29 March 2020).
19. REACH (Registration, Evaluation, Authorization and Restriction of Chemical Substances). Available online: http://ec.europa.eu/environment/chemicals/reach/reach_intro.htm (accessed on 29 March 2020).
20. Kolnes, M.; Mere, A.; Kübarsepp, J.; Viljus, M.; Maaten, M.; Tarraste, M. Microstructure evolution of TiC cermets with ferritic AISI 430L steel binder. *Powder Metall.* **2018**, *61*, 197–209. [[CrossRef](#)]
21. Santos, M.C., Jr.; Araujo Filho, J.S.; Barrozo, M.A.S.; Jackson, M.J.; Macchado, A.R. Development and application of temperature measurement device using the tool-workpiece thermocouple method in turning at high cutting speeds. *Int. J. Adv. Manuf. Tech.* **2017**, *89*, 2287–2298. [[CrossRef](#)]
22. Kolnes, M.; Kübarsepp, J.; Sergejev, F.; Kolnes, M. Wear of potential tool materials for aluminium alloys friction stir welding at weld temperatures. *Proc. Est. Acad. Sci.* **2019**, *68*, 198–206. [[CrossRef](#)]

23. Tarasov, S.Y.; Rubtsov, V.E.; Kolubaev, E.A. A proposed diffusion-controlled wear mechanism of alloy steel friction stir welding (FSW) tools used on an aluminum alloy. *Wear* **2014**, *318*, 130–134. [[CrossRef](#)]
24. Thomson, B.T.; Babu, S.S.; Lolla, T. Application of diffusion models to predict FSW tool wear. In Proceedings of the Twenty-first International Offshore and Polar Engineering Conference, Maui, HI, USA, 19–24 June 2011; pp. 520–526.
25. Evans, A.G.; Charles, E.A. Fracture toughness determinations by indentation. *J. Am. Ceram. Soc.* **1976**, *59*, 371–372. [[CrossRef](#)]
26. Kübarsepp, J.; Klaasen, H.; Pirso, J. Behaviour of TiC-base cermets in different wear conditions. *Wear* **2001**, *249*, 229–234. [[CrossRef](#)]
27. Klaasen, H.; Kübarsepp, J. Abrasive wear performance of carbide composites. *Wear* **2006**, *261*, 520–526. [[CrossRef](#)]
28. Klaasen, H.; Kübarsepp, J.; Roosaar, T.; Viljus, M.; Traksmaa, R. Adhesive wear performance of hardmetals and cermets. *Wear* **2010**, *268*, 1122–1128. [[CrossRef](#)]
29. Nabhani, F. Wear mechanisms of ultra-hard cutting tools materials. *J. Mater. Process. Technol.* **2001**, *115*, 402–412. [[CrossRef](#)]
30. Lampman, S.; Zore, T.B. Properties and selection: Nonferrous alloys and special purpose materials. In *ASM Handbook*, 3rd ed.; ASM International: Cleveland, OH, USA, 1993; Volume 2, pp. 428–445.
31. Brooks, C.R.; Spruiell, J.E.; Stansbury, E.E. Physical metallurgy of nickel-molybdenum alloys. *Int. Met. Rev.* **1984**, *29*, 210–248. [[CrossRef](#)]
32. Lou, D.; Hellman, J.; Luhulima, D.; Liimatainen, J.; Lindroos, V.K. Interactions between tungsten carbide (WC) particulates and metal matrix in WC-reinforced composites. *Mater. Sci. Eng. A* **2003**, *340*, 155–162. [[CrossRef](#)]
33. Sahlot, P.; Jha, K.; Dey, G.K.; Arora, A. Quantitative wear analysis of H13 steel tool during friction stir welding of Cu-0.8%Cr-0.1%Zr alloy. *Wear* **2017**, *378–379*, 82–89. [[CrossRef](#)]
34. Sahlot, P.; Mishra, R.S.; Arora, A. Wear mechanism for H13 steel tool during friction stir welding of CuCrZr alloy. In *Friction Stir Welding and Processing X*; Springer: Cham, Switzerland, 2019; pp. 59–64.



© 2020 by the authors. Licensee MDPI, Basel, Switzerland. This article is an open access article distributed under the terms and conditions of the Creative Commons Attribution (CC BY) license (<http://creativecommons.org/licenses/by/4.0/>).

Publication VI

Kolnes, M., Kübarsepp, J., Sergejev, F., Kolnes, M., Tarraste, M., Viljus, M. Wear behaviour of ceramic-metal composites as tool material for FSW of copper. In: Materials Engineering 2020 Trans Tech Publications Ltd. (Solid State Phenomena). (accepted for publication: September, 2020).

Wear Behavior of Ceramic-Metal composites as Tool Material for FSW of Copper

Mart Kolnes^{1, a *}, Jakob Kübarsepp^{1, b}, Fjodor Sergejev^{1, c}, Märt kolnes^{1, d},
Marek Tarraste^{1, e} and Mart Viljus^{1, f}

¹Department of Mechanical and Industrial Engineering, Tallinn University of Technology, Ehitajate tee 5, 19086, Estonia

^amart.kolnes@taltech.ee, ^bjakob.kubarsepp@taltech.ee, ^cfjodor.sergejev@taltech.ee,
^dmart.kolnes1@taltech.ee, ^emarek.tarraste@taltech.ee, ^fmart.viljus@taltech.ee,

Keywords: Friction stir welding, Hardmetal, Cermet, Diffusion, Wear

Abstract. Friction stir welding (FSW) is employed primarily for metals characterized by poor weldability at fusion welding: aluminium, magnesium, titanium and copper alloys as well as stainless steels. The focus of the study was on the feasibility of application of WC-based hardmetal 85WC-Co and TiC-based cermet 80TiC-NiMo as potential tool materials for FSW of copper. The single-pass welding trials of Cu sheets were performed using a vertical milling machine. For better understanding of interactions between the tool and workpiece at welding temperature EDS line scans across the interfaces tool-workpiece after welding as well as after static diffusion tests were performed. It was concluded that both tested ceramic-metal composites did not failure during multiple plunges and during the total transverse welding distance of 10 m. Also, significant tool wear was not observed after such a welding distance. The possibility of producing visually defect-free welds using tools from WC- and TiC-based ceramic-metal composites was proved and also mutual diffusion of elements across the interface tool-workpiece was discussed.

Introduction

Copper has been widely used in many industrial areas for its high thermal and electrical conductivities, favorable mechanical properties and excellent resistance to corrosion. Therefore, there is an increasing demand for welding of copper and copper alloys. However, it is difficult to join pure Cu by fusion welding because of its high thermal conductivity and high oxidation rate at melting temperatures [1]. A relatively new solid state process, friction stir welding (FSW) can be appeared to produce defect-free joints from Cu and its alloys successfully [2-7]. However FSW of pure copper and its alloys has not been until present time investigated extensively if compared to FSW of low melting point metals such as aluminium and magnesium alloys. The primary attention has been paid to the study of the effect of welding regimes [2-7] and tool geometry [4, 8] on structure, mechanical properties and quality of FSW welds. Although FSW tool wear leads in addition to shorter tool life also to unexpected weld properties (structure, mechanical properties) only few studies have been addressed tool wear mechanism and tool materials selection [7, 9-11].

Sahlot et al. resents quantitative wear analysis of H13 hot work steel during FSW of CuCrZr (0.8 Cr, 0.1 Zr) alloy. Severe tool wear was observed for H13 steel tool due to high stresses at elevated welding temperatures. Macroscopic surface investigation showed that Cu alloy gets stuck at localized locations over the tool surface due to diffusion bonding. Scratches and grooves were also observed, proving also abrasive wear due to interaction of flowing workpiece material with a rotating tool. Higher tool wear was observed for faster tool rotational speeds and slower traverse speeds during initial stages of tool travel (~300 mm). With further tool travels the wear rate decreases significantly and is not much affected by the process parameters [10, 11].

Savolainen et al. [7] investigated the factors affecting friction stir weldability of pure copper and its alloys as well as addressed correct welding parameters and performance of tool materials. Studied tool materials were H13-type hot-work steel, Ni-based superalloy, TiC-NiMo and TiC-NiW cermets,

pure tungsten and poly-crystalline cubic boron nitride (PCBN). PCBN demonstrated the best performance as it was the only tool material able to produce welds in all the base materials – pure copper, aluminium bronze CuAl5Zn5Sn and copper-nickel CuNi25. The use of sintered TiC-NiW and TiC-NiMo cermets was not recommended as they demonstrated poor mechanical properties (were too brittle). However, authors comment that with optimal manufacturing parameters these composites may prove to be successful as FSW tool material [7].

Only few studies could be found in the literature addressing tool materials and wear mechanisms during FSW of Cu and Cu alloys. Therefore important task to be addressed includes the development of tool materials suitable for FSW of copper and its alloys. This work focuses on the feasibility of application of carbide composites, in particular WC-based hardmetal and TiC-based cermet as potential tool materials for FSW of pure copper.

Experimental details

Ceramic-metal composites can be considered as potential FSW tool materials candidates as they have high hardness, wear resistance and good strength at elevated temperatures [12]. In present research the wear and reaction diffusion behavior (one of reasons of FSW tools degradation) of tools made from WC-Co hardmetal and TiC-NiMo cermet were studied. Selection of these ceramic-metal composites grades bases on the results of our previous research demonstrating that WC-Co hardmetals, in particular composites with 85-94 wt.% WC outperform most of TiC-based cermet grades (70-80 wt.% TiC-NiMo, 70 wt.% TiC-FeCr and 70 wt.% TiC-FeNi) in model cutting tests (performed on a universal lathe) with a workpiece from pure copper (~99.9 % Cu) (see Fig 1a) [13]. WC-Co hardmetal grades showed better performance if compared to TiC-based cermets even if they compared unfavorably with hardness.

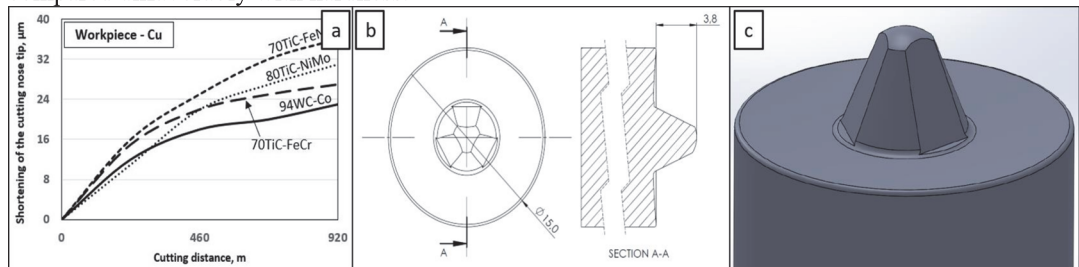


Fig. 1 Wear of ceramic-metal composites vs cutting distance in model tests in the case of copper at 600 °C (a) and geometry of used FSW tool in present research (b and c) [13].

The initial (starting) chemical composition, carbide fraction and average carbide particle size of the carbide composites sintered in vacuum and their mechanical properties are shown in Table 1.

Table 1. Chemical compositions, average carbide particle size and mechanical properties of FSW tool materials under investigation.

Designation	Initial composition, [wt.%]		Carbide fraction after sintering [vol.%]	Hardness HV30	Fracture toughness [MPa·m ^{1/2}]	Average carbide particle size [µm]
	Carbide	Binder				
85WC-Co	85WC	15Co	76.4	1150±20	17.8±0.5	0.91
80TiC-NiMo	80TiC	13.3Ni; 6.7Mo	92.1	1492±16	10.1±0.4	1.60

The welding trials consisted of one-sided butt welding of 4 mm sheets at ambient conditions (without gas shielding). Workpiece material was pure copper (Cu-ETP). A vertical milling machine was used in the FSW tests and single pass welding procedure was applied to fabricate the joints. FSW tools (see Fig. 1b and c) used in the experiments had 3.8 mm long conical tapered pin with a root diameter of Ø6.4 mm. The concave shoulder end surface with diameter of Ø15 mm was used to produce welds. A total of 10 m at welds were performed with both tool materials, during which the tool was at the process temperature more than an hour. As the length of the tested sheets was 125 mm, welding was

performed repeatedly for several times. The rotation speed of 1235 rpm and the traverse speed of 150 mm/min ensured a visually defect-free joint (see Fig. 2). After 10 m welds, the changes in the surface layer of the FSW tool were studied from polished cross sections (see Fig. 1b Section A-A).



Fig. 2 Image of the visually macroscopic defect-free weld of copper.

Also, the reaction-diffusion model test samples were prepared for both tool materials (80TiC-NiMo and 85WC-Co) and workpiece material to achieve better understanding of interaction between the tool and material to be worked. The test samples for studying diffusion-controlled processes were prepared using spark plasma co-consolidation of sintered carbide composite specimens and workpiece material (pure Cu powder with was used) to obtain a permanent bond between the tool material and the copper. Reaction diffusion tests were performed by heating the test samples up to approximately the welding temperature (~ 600 °C), followed by 4 h dwelling at that temperature in vacuum furnace. To understand the distribution of chemical elements in the microstructure in the tool-workpiece contact region, the energy-dispersive X-ray spectroscopy (EDS) system INCA was used.

Results and discussion

In the research of Savolainen et al. it was shown that despite of very little porosity FSW tools from TiC – NiMo and TiC – NiW cermets (50wt% TiC) showed low mechanical properties and, as a result, low reliability during welding of Cu and Cu alloys [7]. However, our research demonstrated feasibility of employing WC-Co hardmetals and TiC – NiMo cermets as tool materials for FSW of copper. Tools from these carbide composites (with a similar geometry as the Savolainen tools) did not failure during multiple plunges as well as traverse welding distances. Also, significant tool wear was not observed after total welding distance of 10 meters.

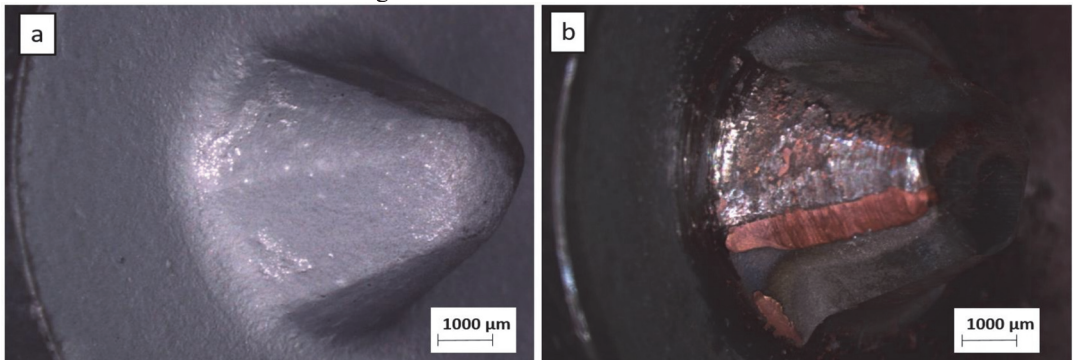


Fig. 3 Image of the FSW tool before (a) and after welding of copper (b).

Fig. 3 demonstrates FSW tool before welding (as sintered) (a) and after welding of 10 m (b). From the point of view of the geometry of FSW tool, special attention should be paid to the fact that cut-outs on the sides of the tool pin are most likely not necessary, as they were not filled with copper (see Fig. 3b) for both tool materials.

Adhesion as one of the wear mechanisms is confirmed by copper metal deposits at the tool surface during FSW (see Fig. 3 and Fig. 4) as well as during model cutting tests [13]. In addition to adhesion diffusion is one of the factors of tool degradation at high temperatures. Fig. 5 demonstrates the results of the EDS line scans of WC-Co and TiC-NiMo tools and workpiece interfaces after welding during

about 1 h (a, c) and 4 h of heat treatment at 600 °C (b, d). Fig. 5 shows a comparatively higher diffusion depth of Cu in TiC-NiMo cermet as compared to diffusion in WC-Co both during feasibility FSW trials (Fig. 5 a and c) and during prolonged heat treatment at 600 °C (Fig. 5 b, d). Results is in agreement with corresponding phase diagrams Cu-Ni and Cu-Co. Enhanced diffusion of copper into cermet Ni-based binder may result in a local increase of the binder fraction of a cermet and decrease in resistance to wear as compared to WC-Co hardmetal.

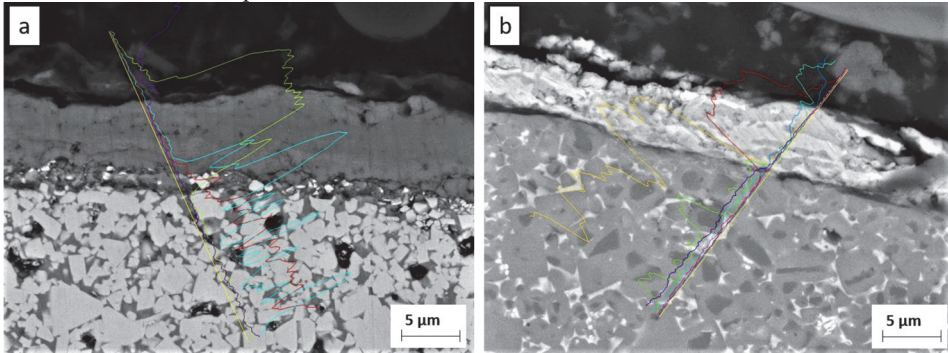


Fig. 4 Tool-workpiece interface images with EDS line scans after 10 m welding of copper: a) WC-Co tool, b) TiC-NiMo tool.

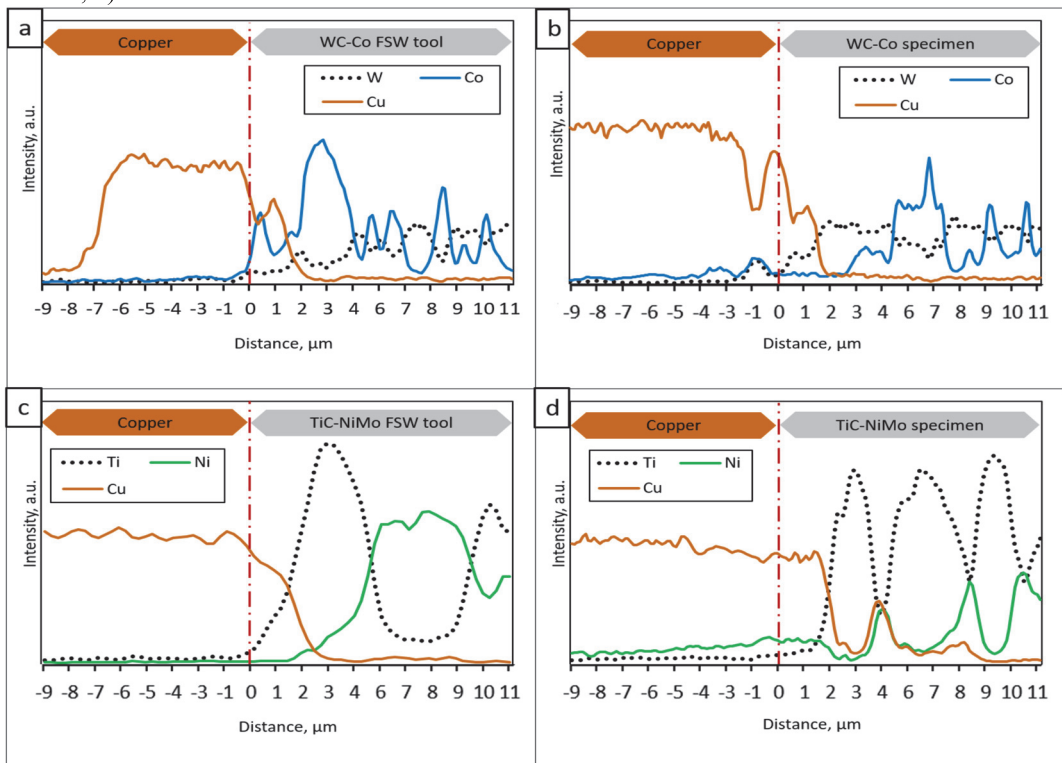


Fig. 5 EDS line scans of WC-Co (a) and TiC-NiMo (c) FSW tools surface in welding test after 10 m welds (1 h), and WC-Co (b) and TiC-NiMo (d) diffusion model test specimens in contact with copper after heat treatment for 4 h at 600 °C.

Apparently almost no diffusion of components of carbide composite tools in particular Co and Ni to workpiece during FSW process can be observed (Fig. 5a and c). Continuous movement and replacement of Cu layer on the tool surface during welding, unlike during prolonged diffusion tests (Fig. 5b and d) is behind such a conclusion. Loss of nickel due to diffusion to workpiece seems to exceed somewhat that of cobalt.

Conclusions

Feasibility study of applicability of carbide composites, in particular WC-Co hardmetal and TiC-NiMo cermet as tool materials for FSW of copper was performed. The following conclusions can be drawn.

- Both tested ceramic-metal composites did not failure during multiple plunges and during the total transverse welding distance of 10m. Also, significant wear of tools was not observed.
- It is possible to produce visually defect-free welds using tools from WC- and TiC-based ceramic-metal composites.
- Mutual diffusion of elements across the interface tool – workpiece both during welding as well as during static diffusion tests takes place. Diffusion of Cu to Ni and Ni to Cu exceeds somewhat diffusion of Cu to Co and vice-versa. It may be one of preconditions for enhanced wear rate of TiC-NiMo cermets as compared to WC-Co hardmetals.

Acknowledgements

This work was supported by the institutional research funding project ‘Multi-scale structured ceramic-based composites for extreme applications’ (IUT 19–29) and by the grant “Composites “ceramics-Fe alloy” for a wide range of application conditions” (PRG665) of the Estonian Research Council.

References

- [1] Welding Handbook. Vol. 5 Materials and Applications. (9th edition) Miami, American Welding Society (2015) 255-226.
- [2] J.J. Shen, H.J. Liu, F. Cui, Effect of welding speed on microstructure and mechanical properties of friction stir welded copper. *Materials & Design*, 31 (2010) 3937-3942.
- [3] Y.M. Hwang, P.L. Fan, C.H. Lin, Experimental study on friction stir welding of copper metals. *J. Mater. Process. Technol.*, 210 (2010) 1667-1672.
- [4] M. Miličić, P. Gladović, R. Bojanić, T. Savković, N. Stojić, Friction stir welding (FSW) process of copper alloys. *Metalurgija*, 55 (2016) 1, 107-110.
- [5] H.S. Park, B.W. Lee, T. Murakami, K. Nakata, M. Ushio, Friction stir welding of oxygen free copper and 60%Cu-40%Zn copper alloy. *Materials Science Forum*, 580-582 (2008) 447-450.
- [6] Y.F. Sun, H. Fujii, Investigation of the welding parameter dependent microstructure and mechanical properties of friction stir welded pure copper. *Mater. Sci. Eng. A*, 527 (2010) 6879-6886.
- [7] K. Savolainen, J. Mononen, T. Saukkonen, H. Hänninen, J. Koivula, Friction stir weldability of copper alloys. 5th International Friction Stir Welding Conference, September 14-16 (2004), Metz, France.
- [8] H. Khodaverdizadeh, A. Heidarzadeh, T. Saeid, Effect of tool pin profile on microstructure and mechanical properties of friction stir welded pure copper joints. *Materials & Design*, 45 (2013) 265-270.
- [9] K. Nakata, Friction stir welding of copper and copper alloys. *Weld. Int.* 19:12 (2005) 929-933.
- [10] P. Sahlot, K. Jha, G.K. Dey, A. Arora, Quantitative wear analysis of H13 steel tool during friction stir welding of Cu-0.8%Cr-0.1%Zr alloy. *Wear*, 378-379 (2017) 82-89.
- [11] P. Sahlot, R.S. Mishra, A. Arora, Wear mechanism for H13 steel tool during friction stir welding of CuCrZr alloy. *Int. J. Min. Met. Mater.* (2019), 59-64
- [12] K.J. Brooks, *World Directory and Handbook of Hardmetals and Hard Materials*, Metal Powder Industry, London, UK, 1996.
- [13] M. Kolnes, J. Kübarsepp, F. Sergejev, M. Kolnes, M. Tarraste, M. Viljus, Performance of ceramic-metal composites as potential tool materials for friction stir welding of aluminium, copper and stainless steel. *Materials*, 13(8) (2020)

Curriculum vitae

Personal data

Name: Mart Kolnes
Date of birth: 18/11/1987
Place of birth: Pärnu, Estonia
Citizenship: Estonian

Contact data

E-mail: mart.kolnes@taltech.ee

Education

2016–2020 Tallinn University of Technology – PhD
2011–2013 Tallinn University of Technology – MSc
2007–2011 Tallinn University of Technology – BSc
1995–2007 Pärnu Koidula Gymnasium – High school

Language competence

Estonian Mother Tongue
English Fluent

Professional employment

2016– Early Stage Researcher, Tallinn University of Technology

Projects

IUT 19-29 – Multi-scale structured ceramic-based composites for extreme applications (Estonian Research Council, 01.01.2014-31.12.2019). Principal investigator: Jakob Kübarsepp, Department of Mechanical and Industrial engineering, Tallinn University of Technology.

PRG665 – Composites “ceramics-Fe alloy” for a wide range of application conditions (Estonian Research Council, 01.01.2020-31.12.2020). Principal investigator: Kristjan Juhani, Department of Mechanical and Industrial engineering, Tallinn University of Technology.

Elulookirjeldus

Isikuandmed

Nimi: Mart Kolnes
Sünniaeg: 18/11/1987
Sünnikoht: Pärnu, Eesti
Kodakondsus: Eesti

Kontaktandmed

E-post: mart.kolnes@taltech.ee

Hariduskäik

2016–2020 Tallinna Tehnikaülikool – PhD
2011–2013 Tallinna Tehnikaülikool – MSc
2007–2011 Tallinna Tehnikaülikool – BSc
1995–2007 Pärnu Koidula Gümnaasium – Keskkharidus

Keelteoskus

Eesti keel emakeel
Inglise keel kõrgtase

Teenistuskäik

2016– Nooremteadur, Tallinna Tehnikaülikool

Osalus projektides

IUT 19-29 – Mitmeastmeliselt struktureeritud keraamika-baasil komposiitmaterjalid kasutamiseks ekstreemtingimustes (1.01.2014–31.12.2019), Jakob Kübarsepp, Mehaanika ja tööstustehnika instituut, Tallinna Tehnikaülikool.

PRG665 – Komposiitmaterjalid “keraamika-Fe sulam” kasutamiseks tingimuste laias diapasoonis (1.01.2020–31.12.2020), Kristjan Juhani, Mehaanika ja tööstustehnika instituut, Tallinna Tehnikaülikool.